

UC Santa Barbara

UC Santa Barbara Electronic Theses and Dissertations

Title

A categorical perspective on symmetry, topological order, and quantum information

Permalink

<https://escholarship.org/uc/item/5z384290>

Author

Delaney, Colleen

Publication Date

2019

Peer reviewed|Thesis/dissertation

University of California
Santa Barbara

**A categorical perspective on symmetry, topological
order, and quantum information**

A dissertation submitted in partial satisfaction
of the requirements for the degree

Doctor of Philosophy
in
Mathematics

by

Colleen Delaney

Committee in charge:

Professor Zhenghan Wang, Chair
Professor Michael Freedman
Professor Stephen Bigelow
Professor Dave Morrison

June 2019

The Dissertation of Colleen Delaney is approved.

Professor Michael Freedman

Professor Stephen Bigelow

Professor Dave Morrison

Professor Zhenghan Wang, Committee Chair

May 2019

A categorical perspective on symmetry, topological order, and quantum information

Copyright © 2019

by

Colleen Delaney

Colleen Delaney

Education

PhD, Mathematics, UCSB	2019
Certification in College and University Teaching, UCSB	2019
MA, Mathematics, UCSB	2016
BS, Physics, California Institute of Technology	2013

Research Experience

Microsoft Station Q Graduate Student Fellow	2016-2017, 2018-2019
HRL Laboratories Intern in Computational Physics	Summer 2017
National Science Foundation Graduate Research Fellow	2013-2016
Caltech Summer Undergraduate Research Fellow	2010, 2011, 2012

Writing

Symmetry defects and their application to topological quantum computing. C. Delaney, Zhenghan Wang. Accepted to AMS Contemporary Mathematics Series. (2018). arXiv:1811.02143

A systematic search of knot and link invariants beyond modular data. C. Delaney, Alan Tran. (2018). arXiv:1806.02843

On invariants of modular categories beyond modular data. Parsa Bonderson, C. Delaney, César Galindo, Eric C. Rowell, Alan Tran, Zhenghan Wang. Accepted to Journal of Pure and Applied Algebra. (2018). arXiv:1805.05736

Local unitary representations of the braid group and their application to quantum computing. Revista Colombiana de Matemáticas. Vol. 50, No. 2. (2016). C. Delaney, Eric C. Rowell, Zhenghan Wang. arXiv:1604.06429

Dyson-Schwinger equations and the theory of computation. C. Delaney, Matilde Marcolli. "Feynman Amplitudes, Periods and Motives." Clay Math Institute and AMS. (2015). arXiv:1302.5040

Generalizing the Connes-Moscovici Hopf algebra to contain all rooted trees. Susama Agarwala, C. Delaney. Journal of Mathematical Physics, Vol. 56, No. 4. (2015). arXiv: 1302.4004

Organization and Outreach

Co-organizer, Session on Braid Groups and Quantum Computing at AWM Symposium	2019
Co-organizer/co-founder, UCSB Quantum Algebra and Topology Seminar	2015-2019
Co-organizer/co-founder UCSB Mathematical Physics Seminar	2018-2019
• Mentor for Scholarships for Transfer Students to Engage and Excel (STEEM)	2014-2016
• Mentor for UCSB Women in STEM Undergraduate Mentorship Program	2016-2019

Abstract

A categorical perspective on symmetry, topological order, and quantum information

by

Colleen Delaney

We investigate the algebraic theory of symmetry-enriched topological (SET) order in (2+1)D bosonic topological phases of matter and its applications to topological quantum computing. Our goal is twofold: first, to demonstrate how an abstract categorical approach can be applied to understand phenomena in (2+1)D topological phases of matter, and second, to show how ideas from physics can be useful for categorification.

After reviewing modular tensor categories (MTCs) and their role as algebraic theories of anyons in topological phases of matter, we recall their associated quantum representations and their interpretation as quantum gates for a topological quantum computer. Next we recall the characterization of SET order in terms of G -crossed braided extensions of MTCs and the mathematical formalism of topological quantum computing (TQC) with anyons and symmetry defects.

We then apply modular tensor category theory to construct algebraic models of symmetry defects in multi-layer (2+1)D topological order with layer-exchange permutation symmetry. Our main result frames a correspondence between bilayer symmetry enriched topological order and monolayer topological order on surfaces with genus, illuminating a connection between quantum symmetry and topological order that first appeared in the work of condensed matter theorists Barkeshi, Jian, and Qi.

Contents

Abstract	v
Introduction	2
Part I Modular tensor categories, (2+1)D topological phases, and topological quantum computing	3
1 MTCs and (2+1)D TPM	4
1.1 Overview of modular tensor category theory	4
1.1.1 MTCs and tensor category theory	4
1.1.2 MTCs and topological quantum field theory	8
1.1.3 MTCs and condensed matter physics	11
1.1.4 MTCs and anyon models	15
1.1.5 MTCs and topological quantum computing	17
1.2 Topological order and the definition of an MTC	18
1.2.1 Fusion rules for anyons and the fusion ring of a UMTC	21
1.2.2 Quantum states of anyonic systems and the structure of a UMTC	22
1.2.3 The monoidal structure, anyon fusion, and $6j$ symbols	25
1.2.4 Rigidity and quasiparticle generation/annihilation	30
1.2.5 Rigidity in a skeletal UMTC	32
1.2.6 Unitarity	34
1.2.7 Pivotal fusion categories	35
1.2.8 Braided fusion categories	37
1.3 Invariants and classification of MTCs	42
1.3.1 Quantum dimensions, twists, and Frobenius-Schur indicators	43
1.3.2 The modular data and modular representation	45
1.3.3 Knot and link invariants from MTCs	47
1.3.4 Classification and structure theory of MTCs	48
1.4 Examples	50
1.4.1 Semion UMTC	50

1.4.2	Fibonacci UMTC	50
1.4.3	Ising UMTCs	51
1.4.4	Quantum doubles of finite groups and Dijkgraaff-Witten TQFT	52
2	Quantum representations from MTCs and topological quantum computing	54
2.1	Quantum computation	55
2.1.1	Encoding quantum information	55
2.1.2	Processing quantum information	59
2.1.3	Measurement and readout	61
2.1.4	Towards quantum computers	62
2.2	Topological quantum computing with anyons	62
2.2.1	Topological qubits	64
2.2.2	Fault-tolerant gates from anyon exchange	64
2.3	Braid group representations from MTCs	65
2.3.1	The n -strand braid group	65
2.3.2	Action of \mathcal{B}_n on $\text{Hom}(i, a^{\otimes n})$	67
2.3.3	The action of \mathcal{B}_3 on state spaces of three anyons	68
2.3.4	Measurement	72
2.4	Examples	74
2.4.1	TQC with metaplectic anyons	74
2.4.2	TQC with Fibonacci anyons	76
2.4.3	TQC with twisted doubles of finite groups	76
2.5	Topological quantum computing beyond anyons	77
2.5.1	TQC with domain walls and defects in (2+1)D	78
	 Part II G-crossed braided fusion categories, SET phases, and TQC	 82
3	Symmetry, gauging, and condensation in topological order	83
3.1	Symmetries of MTCs	83
3.1.1	Braided tensor autoequivalences and topological symmetry	84
3.1.2	Skeletal autoequivalences and gauge symmetry	86
3.1.3	Categorical group symmetry and global symmetry in TPM	88
3.2	From global symmetries to defects	89
3.2.1	Examples of categorical symmetries	93
3.3	Gauging topological order: local symmetry from global symmetry	95
3.4	Anyon condensation and generalized symmetry breaking	97
3.4.1	$D(S_3)$ defect fusion rules from boson condensation	100
3.4.2	Example: non-boson condensation in $D(S_3)$	101

4	(2+1)D Symmetry-enriched topological order and TQC	103
4.1	Algebraic theory of symmetry defects	104
4.1.1	Symmetry defects in SET phases and TQC	107
4.1.2	Skeletal G -crossed braided extensions of MTCs	111
4.1.3	The graphical calculus for G -crossed braided fusion categories	113
4.2	Examples of defects in SET order and applications to TQC	116
4.2.1	Non-abelian defects from abelian topological order	116
4.3	Example: T -gate from bilayer Ising defects and measurement	121
4.3.1	Defect qudit and T -protocol encoding	122
4.3.2	Calculation of $\langle 1 T 1 \rangle$	124
4.3.3	Calculation of $\langle \psi T \psi \rangle$	128

Part III Permutation extensions of MTCs, bilayer symmetry defects, and TQC **132**

5	Fusion rules for permutation defects	136
5.1	Introduction	136
5.1.1	Preliminaries	137
5.1.2	Categorical S_n -symmetry of $\mathcal{C}^{\boxtimes n}$ and multilayer topological order	138
5.1.3	Bilayer SET order and S_2 -extensions of $\mathcal{C} \boxtimes \mathcal{C}$	140
5.2	Combinatorial model of multilayer anyon and permutation defects	141
5.2.1	Confinement, deconfinement, and anyon-defect fusion	142
5.2.2	Permutation defect fusion ring	146
5.2.3	Fusion rules for inequivalent permutation extensions	149
5.3	Example: bilayer Fibonacci defect fusion	151
5.4	Example: trilayer Fibonacci with S_3 permutation symmetry	152
6	On the algebraic theory of bilayer symmetry defects	154
6.1	Introduction	154
6.2	Bilayer topological order $\mathcal{C} \boxtimes \mathcal{C}$ and layer-exchange symmetry	155
6.2.1	Categorical layer-exchange symmetry	156
6.3	Single defect associators	156
6.3.1	Single-defect F -symbols	161
6.4	S_2 -crossed braiding of anyons and defects	162
6.4.1	The S_2 -action on the defects	165
6.4.2	Braiding and associators for bare defects	165
6.4.3	Coherences	167
6.5	Topological quantum computing with bare defects and the modular representation	168
6.5.1	Bare defect qudit gates	169
6.6	Conclusions	170

Introduction

The main result we wish to present uses modular tensor category theory to frame a correspondence between quantum systems of certain defects in bilayer topological phases of matter and monolayer topological phases on surfaces with genus which first appeared in the work of Barkeshli, Jian, and Qi [4]. We also examine the implications for topological quantum computation and applications.

While motivated by physics and owing a great debt to several papers in physics literature, the methods we use to investigate the algebraic theory of SET phases are primarily mathematical - tensor categories, linear algebra, and representation theory. While we present our results as proofs whenever possible, our approach emphasizes first principles and the reader will note that we do not use any heavy machinery to prove results.

The following chapters are broken into three parts: [Part I](#) covers modular tensor categories, topological order of (2+1)D topological phases of matter, and the mathematical theory of anyonic quantum computing.

Building on Part I, the characterization of symmetry-enriched topological order in terms of G -crossed braided extensions of modular tensor categories and the theory of quantum computing with their symmetry defects are examined in [Part II](#).

In [Part III](#), we describe aspects of the algebraic theory of multi-layer topological order and permutation defects and apply it to derive an understanding of the mathematical

CONTENTS

relationship between symmetry, topological order, and quantum information.

Part I

Modular tensor categories, (2+1)D
topological phases, and topological
quantum computing

Chapter 1

MTCs and (2+1)D TPM

1.1 Overview of modular tensor category theory

Modular tensor categories have many facets, and it will be useful to appreciate them from several perspectives: as a kind of “quantum” categorification of a finite abelian group, as algebraic objects that encode the axioms of a topological quantum field theory, and as models for anyons in topological phases of matter. Each of these settings have their own language and tools that we will use interchangeably.

1.1.1 MTCs and tensor category theory

To specify a category \mathcal{C} one must define its *objects* $\text{Obj}(\mathcal{C})$ and maps between them, or *morphisms*.

$$\begin{array}{ccc} & f \in \text{Hom}(X, Y) & \\ & \curvearrowright & \\ X & & Y \end{array}$$

Preliminaries

Structure preserving morphisms, or isomorphisms, separate objects into *isomorphism classes*. All categories considered here are *small* in the sense that their isomorphism classes form a set, and the morphisms between any two objects $X, Y \in \text{Obj}(\mathcal{C})$ also form a set $\text{Hom}(X, Y)$.

They will also be *locally finite*, *k-linear* and *abelian*¹, which means that the Hom spaces are equipped with the structure of finite-dimensional *k*-vector spaces in such a way that all of the usual tools of linear algebra are available to use. In particular, there is a way to take the direct sum of objects X and Y produces another object $X \oplus Y$. Detailed definitions can be found in Chapter 1 of [38], which is our reference for tensor category theory throughout. Basic definitions are stated as in [38] with a few exceptions.

An object is called *simple* if it cannot be written nontrivially as a direct sum, and the *rank* of a category $\text{Rank}(\mathcal{C})$ is the cardinality of a set of representatives of isomorphism classes of simple objects, denoted $\text{Irr}(\mathcal{C})$.

A functor F between categories \mathcal{C} and \mathcal{D} is an assignment of an object $F(X) \in \text{Obj}(\mathcal{D})$ for each $X \in \text{Obj}(\mathcal{C})$, and a morphism $F(f) \in \text{Hom}_{\mathcal{D}}(F(X), F(Y))$ for every $f \in \text{Hom}_{\mathcal{C}}(X, Y)$ satisfying

- $F(\text{id}_X) = \text{id}_{F(X)}$ for every $X \in \text{Obj}(\mathcal{C})$
- $F(g \circ f) = F(g) \circ F(f)$ for all $f \in \text{Hom}_{\mathcal{C}}(X, Y), g \in \text{Hom}_{\mathcal{C}}(Y, Z)$.

It will also help to establish some basic examples that will recur throughout the text.

Example 1.1 (*Vec*). *Let k be a field. The category Vec has objects given by finite-dimensional k -vector spaces, and morphisms between objects are given by k -linear transformations.*

¹Not to be confused with the notion of an *abelian* MTC, see Section 1.3.

We will see that when $k = \mathbb{C}$, \mathbf{Vec} can be thought of as a trivial MTC.

Example 1.2 ($\text{Rep}(G)$). *Let G be a finite group. The objects of the category $\text{Rep}(G)$ are finite-dimensional representations of G , and morphisms are given by intertwiners.*

$\mathbf{Rep}(G)$ is an example of a braided fusion category which is not modular.

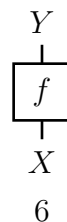
Fundamentally a modular tensor category (MTC) (\mathcal{C}, \oplus) is an abelian category with three structures. There is a monoidal structure $(\mathcal{C}, 1, \otimes, \alpha)$, a braiding (\mathcal{C}, c) , and a pivotal structure (\mathcal{C}, ϕ) , and they must satisfy compatibility conditions in the form of commutative diagrams of certain morphisms between objects in the category.

Definition 1.1. *A modular tensor category $(\mathcal{C}, \oplus, 1, \otimes, \alpha, c)$ is a nondegenerate ribbon fusion category.*

The next section is devoted to a physically motivated unpacking of each detail of this definition. For now we take a holistic approach to understanding the structures through pictures.

String Diagrams

Using string diagrams to represent morphisms in a monoidal category dates back to at least the mid 1960s [55, 69] and became a standard tool for algebraists following their popularization in the 1980s [58, 59]. In a string diagram, a morphism between two objects $f \in \text{Hom}(X, Y)$ is drawn as a box, sometimes called a coupon, with an input strand labeled by X and an output strand labeled by Y . We take the convention that diagrams are read from the bottom up.



The composition of morphisms is given by vertical stacking and tensor product by horizontal juxtaposition.

$$\begin{array}{c}
 Z \\
 | \\
 \boxed{g} \\
 | \\
 \boxed{f} \\
 | \\
 X
 \end{array}
 = g \circ f
 \quad
 \begin{array}{c}
 Y_1 \quad Y_2 \\
 | \quad | \\
 \boxed{f_1} \otimes \boxed{f_2} \\
 | \quad | \\
 X_1 \quad X_2
 \end{array}
 = f_1 \otimes f_2
 \quad
 \begin{array}{c}
 Y_1 \quad Y_2 \\
 | \quad | \\
 \boxed{f_1 \otimes f_2} \\
 | \quad | \\
 X_1 \quad X_2
 \end{array}
 \quad (1.1)$$

where $f \in \text{Hom}(X, Y)$, $g \in \text{Hom}(Y, Z)$, $f_i \in \text{Hom}(X_i, Y_i)$.

In *braided* monoidal categories, the braiding isomorphisms and their inverses are represented by crossings.

Categorification and the idea of an MTC

An MTC can be thought of as a “quantum” analogue of a finite abelian group: while group multiplication is associative and commutative, the tensor product of objects in an MTC is only associative and commutative up to isomorphism.

This analogy is made precise by the idea of *categorification*.

To categorify a mathematical object is to find a category such that the its original structure is recovered in the “classical”, de-categorified part of the category, the set of objects. In the case of fusion categories this is the ring $(\text{Irr}(\mathcal{C}), \oplus, \otimes)$, see Definition 5.3 for a precise definition of fusion ring.

The program of categorification is an active area of modern mathematics and part of the “quantum” frontier of abstract algebra. From this perspective, asking for a classification and structure theory of MTCs is then as natural as asking for the classification of finite simple groups.

1.1.2 MTCs and topological quantum field theory

Modular tensor categories (MTCs) arise in physics as an equivalent notion of a (2+1)D topological quantum field theory (TQFT). When *unitary*, both can be thought of as a way to describe 2-dimensional quantum systems whose evolution depends only on the topology, as opposed to the geometry, of its underlying space manifold.

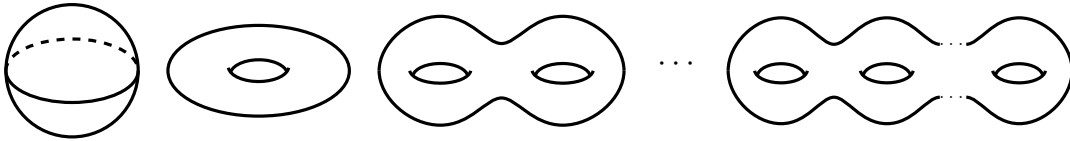


Figure 1.1: The classification of oriented surfaces, shown here without boundary, gives the possible space manifolds where the 2-dimensional quantum systems are governed by a TQFT. When there is boundary the physics is described by a (1+1)D CFT, see Section 1.1.2.

Roughly then a (2+1)D TQFT is a way to consistently assign spaces of quantum states to surfaces and evolution operators to cobordisms between such surfaces. Mathematically, the right way to describe such a thing is a functor from a category of cobordisms to a category of vector spaces.

In particular, the evolution of an isolated quantum system on a closed genus g surface is given by a unitary representation of the *mapping class group* of the surface.

To be absolutely precise, there is additional structure required on the categories to keep track of the boundary components of surfaces - their orientations and relative positions. One considers a category of *extended* cobordisms and category of vector spaces where maps are only linear up to powers of a root of unity called the *framing anomaly* [81], which we denote by $\Theta \in \mathbb{C}$.

In particular, the quantum representations of mapping class groups coming from

TQFTs are only projective, i.e. there are homomorphisms

$$\rho : MCG(\Sigma_{g,n,a}) \longrightarrow U(d)/U(1) \quad (1.2)$$

and their failure to be linear is controlled by the framing anomaly. We explain projective quantum representations in detail in Chapter 2, where they are interpreted as quantum operations for a topological quantum computer.

These considerations make the axiomatic definition of a TQFT somewhat lengthy and intricate, and hence we refer the reader to [81] for details.

However, the projectivity of representations is something fundamental: in quantum mechanics states can only be measured up to an overall $U(1)$ phase. While difficult to appreciate from first principles in the TQFT setting, the framing anomaly Θ exhibits a fascinating connection between quantum symmetry and topology, the description of which is the culmination of this work in Theorem 6.1.

While the mathematical definition of a (2+1)D TQFT already uses the language of categories and functors, the information contained in a (2+1)D TQFT is encoded in yet a different category, one with the structure of a modular tensor category (MTC).

Theorem ([8]). *A modular tensor category is equivalent to a 3-2-1 topological quantum field theory.*

We include some examples of the dictionary provided by the equivalence of (2+1)D TQFTs and MTCs so that we can put our examples in context for mathematicians and physicists alike.

It is through MTCs that we will explore the interplay between quantum symmetry and topology. There the framing anomaly Θ is given by an invariant quantity of an MTC and determines a related quantity called the *chiral central charge*, which in turn is related to the (1+1)D physics on the boundary components of the space manifolds.

(2+1)D TQFTs	MTCs
Reshetikhin-Turaev/ Witten-Chern-Simons TQFT at level k	Deformations of the universal enveloping algebra of the Lie algebra $\mathfrak{su}(2)$ at certain roots of unity
Jones-Kauffman TQFTs	Temperley-Lieb-Jones categories at certain roots of unity
Turaev-Viro TQFT	Drinfeld centers $\mathcal{Z}(\mathcal{C})$ of spherical fusion categories
Twisted Dijkgraaf- Witten TQFT with finite gauge group G	Twisted quantum doubles of finite groups $D^\omega(G)$, (equivalent to Drinfeld centers of the form $\mathcal{Z}(\text{Vec}_G^\omega)$)

Table 1.1: Names of some familiar TQFTs from physics and the description of their corresponding MTC.

MTCs and rational conformal field theory

For the surfaces with boundary, the boundary physics is described by a different quantum field theory, namely a *conformal* field theory one dimension down.

This relationship between (2+1)D TQFTs and (1+1)D conformal field theories (CFTs) is referred to as a *bulk-boundary* or *bulk-edge correspondence* in physics.

Like (2+1)D TQFTs are equivalent to MTCs, (1+1)D CFTs have algebraic, now also analytic, equivalents, for example vertex operator algebras (VOAs) and conformal nets [20].

An algebraic formulation of one side of the bulk-boundary correspondence then says that the representation theory of certain CFTs, i.e. the *representation category* of a VOA/conformal net, is given by an MTC.

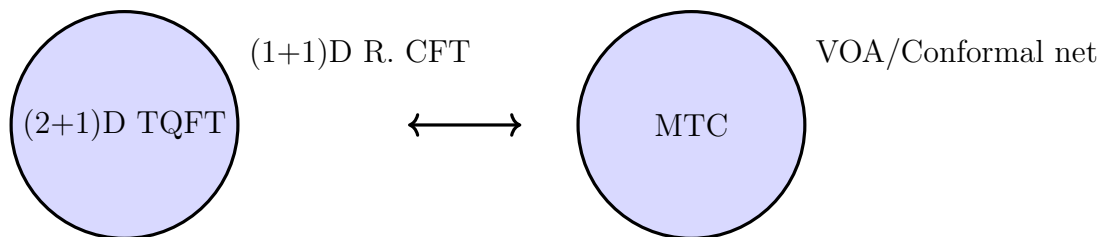


Figure 1.2: Schematic illustration of the “bulk-boundary correspondence” between (2+1)D topological quantum field theories and (1+1)D rational conformal field theories. More general formulations of the correspondence are studied, for example via the representation theory of logarithmic CFTs [74].

That MTCs are related to TQFTs and CFTs in this manner exerts a great influence on the efforts to classify MTCs as purely mathematical objects, see Section 1.4.

1.1.3 MTCs and condensed matter physics

In condensed matter physics, which is concerned with large numbers of strongly interacting particles, the physics of certain effectively 2-dimensional materials are governed by (2+1)D TQFTs. When physical bosons are confined to 2 spatial dimensions, the ideal, zero-temperature physics is described by the low-energy effective theory of a (2+1)D unitary TQFT and the collective quantum system is said to be in a bosonic (2+1)D *topological phase of matter* (TPM).

For 2D systems whose constituent particles are fermions, there is an analogous story but the TQFTs must be equipped with a spin structure [44]. Like with the algebraic equivalence of (2+1)D TQFTs and MTCs, (2+1)D spin TQFTs are related to generalizations of MTC called *supermodular categories*, although this correspondence is still being developed on both sides of the aisle: for example via super-modular categories [16, 13], under the name of super-pivotal categories in [1]. Hereafter when referring to topological phases we assume bosonic. While aspects of fermionic topological phases can be studied through “bosonization” [16], it would be interesting to generalize the

considerations we make in the later chapters to super-modular tensor categories.

Often materials which are believed to exist in a topological phase are modeled by a lattice of strongly interacting particles, so that the quantum system is comprised of interactions between local degrees of freedom. As we will see in the next section, the space of states of such a quantum system is then given by a Hilbert space, in this case one of the form

$$\mathcal{H} = \otimes_i \mathcal{H}_i$$

where i sums over the sites on a lattice, for example. The interactions between the local degrees of freedom is encoded in a *Hamiltonian* operator, which in turn dictates the time evolution of the quantum system as a whole.

Prior to measurement the system exists in a quantum superposition of eigenstates $\{|\psi_\alpha\rangle\}$ of the Hamiltonian

$$H|\psi_\alpha\rangle = \lambda_\alpha|\psi_\alpha\rangle,$$

where λ_α is the energy of the state $|\psi_\alpha\rangle$. An eigenstate with smallest energy is called the *ground state*, and all other states *excited states*.

While the Hamiltonian of a TPM is trivial in the sense that it is equivalent to $H \equiv 0$, (2+1)D topological phases have a rich physical theory that can involve hosting quasi-particle excitations called *anyons*. These point-like quasiparticles are called *emergent* to distinguish from the *physical* or *constituent* particles underlying the system.

Topological phases of matter and their anyons exhibit many phenomena which are interesting for physics and applications: namely nonabelian statistics, ground state degeneracy, and energy gaps.

Nonabelian anyon statistics

Physical bosons have trivial *self-exchange statistics*, meaning that for indistinguishable particles b_i a wavefunction ψ depending on their position is unchanged by the exchange of any pair:

$$\psi(\dots, b_i, \dots, b_j, \dots) = \psi(\dots, b_j, \dots, b_i, \dots) \quad \text{bosonic statistics,} \quad (1.3)$$

while for fermions exchange results in a sign change

$$\psi(\dots, f_i, \dots, f_j, \dots) = -\psi(\dots, f_j, \dots, f_i, \dots) \quad \text{fermionic statistics.} \quad (1.4)$$

All (3+1)D point-like particles are either bosons or fermions, but anyons are effectively (2+1)D, and their exchange statistics are more interesting. For *abelian* anyons of a fixed type, which we give a precise definition of in Section 1.3, exchange can change the wavefunction by *any* phase $e^{i\theta}$, hence the name anyon.

$$\psi(\dots, a_i, \dots, a_j, \dots) = e^{i\theta} \psi(\dots, a_j, \dots, a_i, \dots) \quad \text{abelian anyonic statistics} \quad (1.5)$$

We will see in the next chapter that the mathematical notion of *self-exchange statistics* is given by a unitary representation of *braid groups*. Then physical boson and fermion statistics can be restated as saying that their quantum braid group representations factor through the trivial and sign representation of the symmetric group, respectively. The braid group representations of abelian anyons are one-dimensional, and for nonabelian

anyons,

$$\psi(\dots, a_i, \dots, a_j, \dots) = U \psi(\dots, a_j, \dots, a_i, \dots) \quad (1.6)$$

for some unitary transformation U .

Nonabelian statistics enable quantum information to be stored the fusion space of collections of anyons, one aspect of their application to quantum computing [64].

Ground state degeneracy and gapped Hamiltonians

Topological phases of matter can exhibit *ground state degeneracy*, where there are multiple distinct ground states.

When the next excited states above the degenerate ground states are separated by a finite amount of energy ΔE , the system is said to be *gapped*. Otherwise, there exist states with arbitrarily small energy above the ground state, and it is *gapless*.

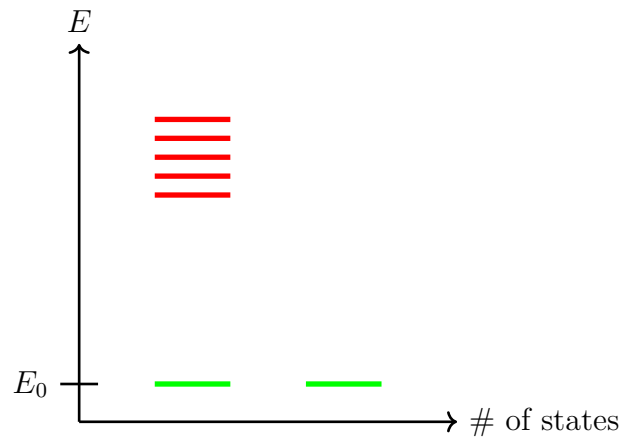


Figure 1.3: Illustration of a gapped quantum system with ground state degeneracy.

Armed with these concepts, we can be a bit more precise about what we mean by topological phases of matter. The following definition is due to [83].

Definition 1.2. A (bosonic) **topological phase of matter** is an equivalence class of local Hamiltonians whose low energy effective theory is given by a unitary TQFT where the ground state space cannot be changed by local operators.

The physical theory of anyons in a gapped TPM at absolute zero is then described by a unitary modular tensor category (UMTC) - objects are collections of anyons and morphisms are anyon processes.

Definition 1.3. The **topological order** of a gapped (2+1)D bosonic topological phase of matter is the UMTC realizing its effective unitary TQFT.

Definition 1.4. An **anyon** is a simple object in a UMTC.

Recalling that internal to any category is a notion of isomorphism that dictates when two objects are equivalent, it is necessary to differentiate between an anyon and its type.

Definition 1.5. An **anyon type** or **topological charge** is an isomorphism class of simple objects in a UMTC.

1.1.4 MTCs and anyon models

Thinking of an abstract UMTC as the algebraic theory of anyons, a *skeletal UMTC* will be precisely what is required to do topological quantum mechanics on Hilbert spaces *with bases*.

Every category is equivalent to a *skeletal* category, which has only one object per isomorphism class [38]. Passing from a category to its equivalent skeleton, or working with the skeletonization of the category, is morally like choosing a basis of a vector space. In the case of vector spaces, choosing a basis is what allows one to write down abstract linear transformations as matrices. For MTCs, it is what allows for a finite description

of the category and its structures indexed by simple objects.

$$\{N_c^{ab}, [R_c^{ab}], [F_d^{abc}]_{ef}\} \quad \text{algebraic data of a UMTC } \mathcal{C} \quad (1.7)$$

Thus we will make one further distinction - while every UMTC is a topological order, we try to reserve the word anyon model for *skeletal* UMTCs, in keeping with [3].

Definition 1.6. *An **anyon model** is a skeletal UMTC.*

While one typically one needs to pass to a skeletonization of a UMTC to make concrete numerical predictions about the physics of anyons in the corresponding topological phase, the abstract theory of UMTCs is necessary for understanding the general mathematical formalism of topological phases and their applications to quantum computing.

The graphical calculus for anyon models

When an MTC is identified with the algebraic theory of anyons, the diagram of a morphism has the interpretation as a quasiparticle process, and can be thought of as a kind of topological Feynman diagram.

Happily the intuitive pictures one can draw of the spacetime trajectories and interactions of anyons then become rigorous mathematical equations that describe quantum states of anyonic systems and their evolution, where the bottom-up orientation of string diagrams corresponds to the time direction. When drawing ribbon fusion graphs we assume they inherit this orientation unless otherwise indicated.

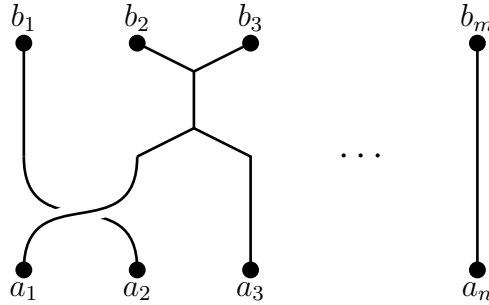


Figure 1.4: The algebraic theory of anyons is given by a unitary modular tensor category (UMTC), whose objects model collections of anyons and morphisms between objects model anyon processes like fusion, exchange, and measurement.

This is the *graphical calculus* of an anyon model, in which braided trivalent graphs depicting anyon processes correspond to morphisms in a skeletal UMTC.

1.1.5 MTCs and topological quantum computing

One thing that makes topological phases of matter *topological* is that they can support gaps which are large, in the sense that the separation between ground states and excited states decays exponentially slowly in the size of the system.

In this case it is said that the ground states are *topologically protected* from the excited states. Kitaev was the first to observe that such systems would support a kind of inherently error-resistant quantum memory, as the encoded quantum information is protected from decoherence by the gap [64].

This led to the advent of *topological quantum computing*, the idea to use materials in topological phases of matter as the hardware for quantum computers. The idea of a quantum computer - precise control the evolution of a quantum system - dates back to Feynman [41].

The seminal idea behind topological quantum computation is to store quantum in-

formation in the degenerate ground state spaces of collections of anyons and then either physically or effectively manipulate the motions of the quasiparticles to evolve the system to perform a desired computation.

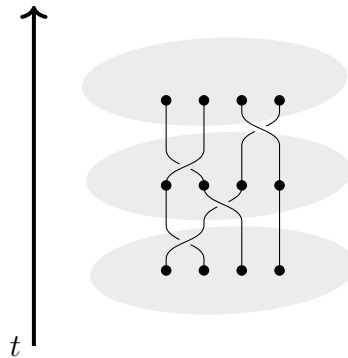


Figure 1.5: Schematic illustration of topological quantum computing with anyons.

In addition to anyons, the physics of defects and domain walls can also be used to store and process quantum information, and there is a general program beyond the (2+1)D realm to understand how quantum information can be stored using excitations in higher dimensional phases and transformed under their motions [82].

We review the theory of general quantum computation later in Section 2.1 and the mathematical formalism of topological quantum computing with anyons in Section 2.2, which entails studying unitary representations of braid and mapping class groups. The more general mathematical formalism of topological quantum computing that we will use to analyze symmetry-enriched topological order is discussed in Section 2.5 and Part II.

1.2 Topological order and the definition of an MTC

In this section we motivate the abstract definition of a MTC as a nondegenerate BFC by describing how each structure and coherence in the category in the unitary case relates

to the physics of anyons in gapped topological phases of matter.

We will see that the structure of a unitary modular tensor category (UMTC) is precisely what is required to do topological quantum mechanics on the Hilbert spaces of states of collections of anyons.

It is quite possible to study topological order without using category theory at all, as working with skeletal MTCs can be done combinatorially and diagrammatically using 6j braided fusion systems (6j-BFS) and their graphical calculus. And in the physics literature, this is typically what is meant by the algebraic theory of anyons [3]. But in no sense is the abstract definition of a UMTC devoid of meaningful physical interpretation or utility: in [Part III](#) where we develop the theory of symmetry-enriched bilayer topological order, we see an instance where an understanding of the category theory and concrete algebraic data/diagrams are more powerful for building both physical theory and concrete examples than either on their own.

Therefore we choose to present the theory of topological order in a unified way using modular tensor category theory, anyon models, and the graphical calculus simultaneously. The intended result is a dictionary between the math and physics treatments of the subject that can serve as a guide for readers of different backgrounds, and overview of which is contained in [Table 1.2](#).

One would be remiss not to point out that there are already many excellent references containing introductions to MTCs and TQC, see for example [[12](#), [76](#), [81](#)].

First we will understand the fusion algebra obeyed by the topological charges of the anyons, which corresponds to the “de-categorified” part of a UMTC \mathcal{C} , its fusion ring.²

²A \mathbb{Z}_+ -based ring [[38](#)], see [Definition 5.3](#).

(2+1)D TO	UMTC	6j-BFS	Diagrams
Algebraic theory of anyons in a (2+1)D TPM	nondegenerate ribbon fusion category $(\mathcal{C}, \oplus, \otimes, \mathbb{1}, \alpha, c, \phi)$	Complex numbers $\{N_c^{ab}, R_c^{ab}, [F_d^{abc}]_{nm}\}$ satisfying equations	Admissibly labeled trivalent graphs satisfying local relations
Anyon types	Isomorphism classes of simple objects	Label set \mathcal{L}	edge labels
Quasiparticle processes	Morphisms		Admissibly labeled trivalent graphs
Fusion and recoupling	Monoidal structure	F -symbols	vertex labels
Exchange	Braiding	R -symbols	resolve crossings
Measurement	Pivotal structure	t -symbols (determined by R - and F - symbols)	rotation*

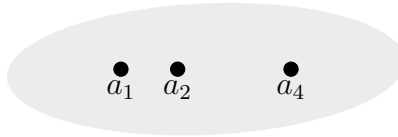
Table 1.2: Passing from column 1 to column 2 relates the physics terminology and concepts with the language of a modular tensor category. Passing from a modular tensor category in column 2 to column 3 is passing to a skeletal representative of its braided tensor autoequivalence class, which can be independently defined in a purely combinatorial way as a 6j-braided fusion system (6j-BFS). Column 4 gives the diagrams and operations in the graphical calculus of the skeletonization in column 3.

Then we will make quantum considerations and categorify.

1.2.1 Fusion rules for anyons and the fusion ring of a UMTC

Anyons are point-like quasiparticle excitations in a gapped (2+1)D topological phases of matter. While their physical size can be changed by local operators [81], they still behave in the same way as if they were localized at a single point in space.

For this reason, when we draw an anyon in space we draw a point³. This point comes with a label, the *topological charge* or *anyon type*. The set of topological charge labels is called the label set and denoted by \mathcal{L} .



Topological charges can be fused together, which in general results in a superposition of topological charges, written

$$a \otimes b = \bigoplus_c N_c^{ab} c \quad (1.8)$$

The N_c^{ab} are called *fusion coefficients* and are always nonnegative integers.

The vacuum charge label 1 is always an element of \mathcal{L} , and satisfies $1 \otimes a = a \otimes 1 = a$ for all $a \in \mathcal{L}$. For every $a \in \mathcal{L}$, there exists $a^* \in \mathcal{L}$ such that $N_1^{aa^*} = 1$. That is, every topological charge has a unique dual charge with which it can fuse to the vacuum charge label.

³To be completely precise, we want to specify an orientation of each anyon, and so they are really modeled by framed points. However, we will suppress this in pictures and point out when the framing needs to be taken into account.

1.2.2 Quantum states of anyonic systems and the structure of a UMTC

For the reader unfamiliar with either of tensor category theory or quantum mechanics, we now recall the postulates of quantum mechanics following [68] and motivate each detail of the abstract categorical definition of a UMTC in terms of the physics of anyons in quantum phases of matter.

Postulates of quantum mechanics

1. A quantum state $|\psi\rangle$ of an isolated quantum system is a unit vector in a complex Hilbert space \mathcal{H} .
2. The evolution of a closed quantum system is given by a unitary transformation on Hilbert space $U : \mathcal{H} \rightarrow \mathcal{H}$.
3. Measurement of a quantum system is described by the action of a set of projection operators $\{P_\lambda\}$ on \mathcal{H} whose projections form a basis of \mathcal{H} .
4. The Hilbert space of states of a composite quantum system is given by the tensor product of the Hilbert spaces of its components.

Fundamentally a UMTC is a category whose objects can be interpreted as collections of anyons and morphisms as anyon processes, together with three coherent structures with precisely the right properties to enforce the laws of quantum mechanics: the monoidal structure to define quantum states with properties that allow these states to be superposed and entangled (Postulate 1), the pivotal structure to define measurement (Postulate 3), and the structure of a braiding to describe evolution of states. (Postulate 2).

1. The **monoidal structure** is needed to consistently define vector spaces of states associated to collections of anyons. As a monoidal category an MTC must also
 - be *rigid*, which ensures that all objects have duals and thus formalizes the notion of anti-quasiparticle.
 - be \mathbb{C} -linear, so that Hom spaces are equipped with the interpretation as complex vector spaces of systems of anyons.
 - be *locally finite*, so that these state spaces are finite dimensional
 - have *simple monoidal unit* 1, so that the ground state of topological phase on a sphere (or disk with vacuum total charge) is the vacuum in the absence of excitations.

Definition 1.7. *A tensor category is a locally finite \mathbb{C} -linear monoidal category $(\mathcal{C}, \otimes, \alpha, 1, \iota)$ with simple unit 1.*

- be finitely semisimple, to enforce that there are only finitely many anyon types in a given model and that their fusion results in a finite quantum superposition of anyon types.
- as a fusion category \mathcal{C} must be *unitary*⁴, so that there is a notion of conjugation on Hom spaces which corresponds to consistency between reversal of quasiparticle processes being and anti-quasiparticle processes.

Definition 1.8. *A fusion category is a finitely semisimple tensor category.*

See Definition 1.19 for the precise statement of the definition of a unitary fusion category.

⁴We use the notion of unitary fusion category from [3]

2. The pivotal structure of a unitary fusion category uses the conjugation on Hom spaces to build positive-definite inner products, which are necessary ingredients for our spaces of states to be Hilbert space and for measurement to make sense, per the laws of quantum mechanics.

- The **pivotal** structure on an MTC is required to be *spherical*, which means that there is a unique inner product on Hom spaces and hence a consistent way to define probability amplitudes of quasiparticle processes that depend only on topology.

Definition 1.9. *A spherical fusion category is a fusion category with a pivotal structure which is spherical.*

3. Lastly, a UMTC needs the structure of a **braiding** to describe how anyonic systems evolve under quasiparticle exchange.

Definition 1.10. *A ribbon fusion category is a braided spherical fusion category.*

- the braiding must be *nondegenerate* - roughly the braiding isomorphisms between any two objects is unique and nontrivial

Definition 1.11. *A modular tensor category is a nondegenerate ribbon fusion category.*

In the absence of unitarity on the level of a fusion category, a braided fusion category is said to be a modular tensor category, or modular category, if the braiding is nondegenerate.

Requiring unitary as one would for most applications, we have that a UMTC is a unitary ribbon fusion category, which extends the notion of unitarity given above

so that anyonic systems evolve unitarily under exchange (in addition to fusion) processes. nondegeneracy of the braiding is then a consequence of unitarity.

Definition 1.12. *A unitary modular tensor category is a unitary ribbon fusion category.*

Having motivated each component of the abstract definition of a UMTC we turn to the details of its structures, their coherences, and properties. For each structure we start with abstract definitions, record them in the skeletal case, and then illustrate the local moves they define in the graphical calculus.

1.2.3 The monoidal structure, anyon fusion, and 6j symbols

The tensor product bifunctor categorifies the fusion product of topological charges introduced in Section 1.2.1 and the monoidal structure categorifies the associativity of multiplication of topological charge types.

Definition 1.13. *A monoidal category is the data $(\mathcal{C}, \otimes, \alpha, 1, l, r)$: a category \mathcal{C} with a bifunctor $\otimes : \mathcal{C} \times \mathcal{C} \rightarrow \mathcal{C}$, a natural isomorphism*

$$\alpha : (- \otimes -) \otimes - \longrightarrow - \otimes (- \otimes -) \quad (1.9)$$

$$\alpha_{X,Y,Z} : (X \otimes Y) \otimes Z \longrightarrow X \otimes (Y \otimes Z) \quad (1.10)$$

for $X, Y, Z \in \text{Obj}(\mathcal{C})$, an object $1 \in \text{Obj}(\mathcal{C})$, and natural isomorphisms $l_X : 1 \otimes X \rightarrow X$ and $r_X : X \otimes 1 \rightarrow X$ satisfying

(i) the pentagon axiom

$$\begin{array}{ccc}
 & ((W \otimes X) \otimes Y) \otimes Z & \\
 \alpha_{W,X,Y} \otimes \text{id}_Z \swarrow & & \searrow \alpha_{W \otimes X, Y, Z} \\
 (W \otimes (X \otimes Y)) \otimes Z & & (W \otimes X) \otimes (Y \otimes Z) \\
 \alpha_{W, X \otimes Y, Z} \downarrow & & \downarrow \alpha_{W, X, Y \otimes Z} \\
 W \otimes ((X \otimes Y) \otimes Z) & \xrightarrow{\text{id}_W \otimes \alpha_{X, Y, Z}} & W \otimes (X \otimes (Y \otimes Z))
 \end{array}$$

and

(ii) the triangle axiom

$$\begin{array}{ccc}
 (X \otimes 1) \otimes Y & \xrightarrow{\alpha_{X, 1, Y}} & X \otimes (1 \otimes Y) \\
 \downarrow r_X \otimes \text{id}_Y & & \downarrow \text{id}_X \otimes l_Y \\
 & X \otimes Y &
 \end{array}$$

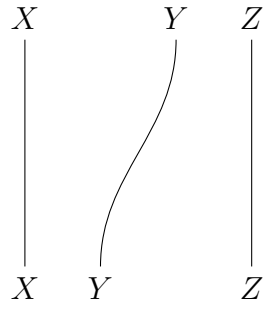
The isomorphisms α are called *associators* or associativity constraints, and the isomorphisms l and r the left and right *unitors* or unit constraints, respectively.

When the unit constraints are trivial in the sense that they are given by the identity isomorphisms, which will be the case we are interested in here, we can specify a monoidal category by the data $(\mathcal{C}, \otimes, 1, \alpha)$. Hence in all definitions involving the monoidal structure we will suppress the dependency on the unitors, as in [38]. In terms of string diagrams, this means that we do not have to draw the identity morphism on the monoidal unit.

Definition 1.14. A monoidal category $(\mathcal{C}, \otimes, 1, \alpha)$ is strict if the unit constraints and associators α are identity isomorphisms.

Theorem 1.1 (MacLane’s strictness theorem). *Every monoidal category is monoidally equivalent to a strict monoidal category.*

In a strict monoidal category, the string diagrams for an associator can be represented as a regrouping of strands



$$(1.11)$$

While it is possible to trivialize the monoidal structure, it is not possible in general to simultaneously skeletalize. Working with strict categories can be a useful technique but for our purposes skeletality cannot be compromised, and so the monoidal structure must be carefully kept track of when using string diagrams.

Skeletal monoidal categories

With the additional stipulations that \mathcal{C} is finite and semisimple, i.e. each $X \in \text{Obj}(\mathcal{C})$ can be written as a direct sum of simple objects, and that the monoidal unit 1 is simple, a skeletonization of a monoidal category \mathcal{C} admits a finite description by fusion coefficients and F -symbols $\{N_c^{ab}, [F_d^{abc}]_{(e,\alpha,\beta);(f,\mu,\nu)}\}$.

The skeletal data of the bifunctor \otimes is encoded in the *fusion coefficients* N_c^{ab} , which in turn determine the admissibly labeled trivalent fusion trees underlying the graphical calculus. For every fusion product of simple objects

$$a \otimes b = \bigoplus_c N_c^{ab} c \quad (1.12)$$

there are corresponding admissibly labeled fusion trees

$$\begin{array}{c} a & & b \\ & \diagdown & / \\ & \mu & \\ & | & \\ & c & \end{array} \quad 1 \leq \mu \leq N_c^{ab} \tag{1.13}$$

which are to be interpreted as basis vectors of $\text{Hom}(c, a \otimes b)$. We sometimes use the notation $|a, b; c, \mu\rangle$ for basis vectors and denote the vector space formed by their span by

$$V_c^{ab} = \text{Span}_{\mathbb{C}} \{|a, b; c, \mu\rangle\}_{1 \leq \mu \leq N_c^{ab}}. \tag{1.14}$$

The monoidal structure skeletalizes to the F -symbols, i.e. the matrix entries of the associator α with respect to some basis.

$$\begin{array}{c} a & & b & & c \\ & \diagdown & / & & / \\ & \mu & & & \\ & & m & & \nu \\ & & | & & \\ & & d & & \end{array} = \sum_n [F_d^{abc}]_{(n, \alpha, \beta); (m, \mu, \nu)} \begin{array}{c} a & & b & & c \\ & \diagdown & / & & / \\ & & & & \beta \\ & & \alpha & & n \\ & & | & & \\ & & d & & \end{array} \tag{1.15}$$

The unit isomorphism ι is a morphism in $\text{Hom}(1, 1) \cong \mathbb{C}$, and hence is given by a scalar. The left and right unitor data are determined by the scalar ι and F -symbols of the form $[F_a^{11a}]_{a1}, [F_a^{a11}]_{1a}$ according to

$$l_a = \iota [F_a^{11a}]_{1a}^{-1} \tag{1.16}$$

$$r_b = \iota [F_a^{a11}]_{1a} \tag{1.17}$$

Inspecting the triangle axiom, we get the equation

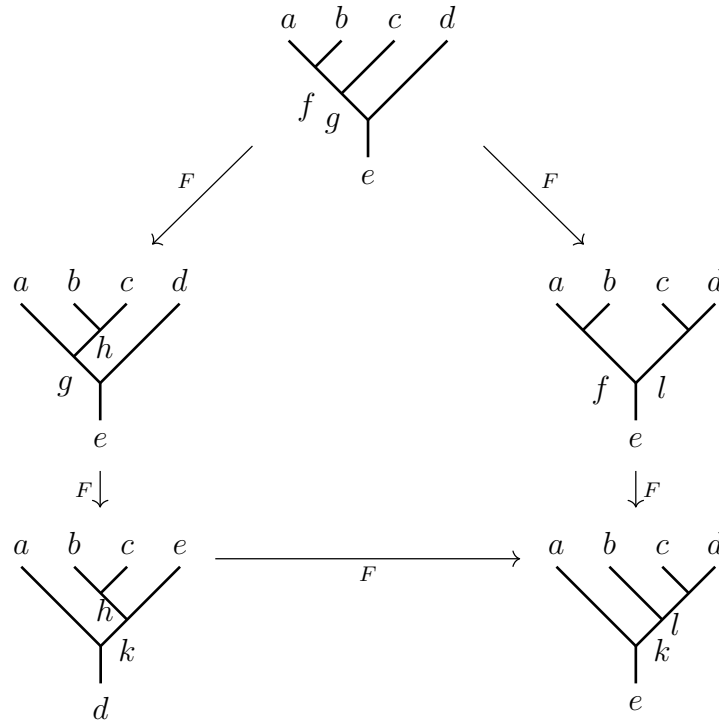
$$l_b \cdot [F^{a1b}]_c = r_a \cdot I_n \tag{1.18}$$

where $n = N_c^{ab}$.

One can verify that these equations are satisfied for all admissible $a, b, c \in \mathcal{L}$ by taking $l_b = 1, r_a = 1$ we pick bases for the fusion spaces and use gauge freedom to set $[F_d^{abc}] = I$ whenever at least one of a, b, c is the vacuum charge 1.

For this reason in the graphical calculus when drawing vacuum lines i.e. edges labeled by $1 \in \mathcal{L}$ we either draw it with dashed lines or omit it completely.

The pentagon axiom is encoded diagrammatically by the equivalence of sequences of F -moves.



This yields the pentagon equations

$$\begin{aligned} & \sum_{\delta} [F_e^{fcd}]_{(g,\beta,\gamma)(l,\delta,\nu)} [F_e^{abl}]_{(f,\alpha,\delta)(k,\delta,\mu)} \\ &= \sum_{h,\sigma,\psi,\rho} [F_g^{abc}]_{(f,\alpha,\beta)(h,\sigma,\psi)} [F_e^{ahd}]_{(g,\sigma,\gamma)(k,\lambda,\rho)} [F_k^{bcd}]_{(h,\psi,\rho)(l,\mu,\nu)} \end{aligned} \quad (1.19)$$

where $a, b, c, d, e, f, g, h, k, l \in \mathcal{L}$ and the greek subscripts index the multiplicity of the trivalent vertices.

By MacLane's coherence theorem, any re-association of an n -fold tensor product can be realized as a sequence of reparenthesizations of triples $(a \otimes b) \otimes c \rightarrow a \otimes (b \otimes c)$, and any two fusion trees with the same external edge labels can be related by a sequence of F -moves.

1.2.4 Rigidity and quasiparticle generation/annihilation

With the monoidal structure in place there is the notion of left and right dual objects in $(\mathcal{C}, \otimes, 1, \alpha)$, which for simple objects in the presence of unitarity gives the notion of anti-quasiparticles for anyons.

Definition 1.15. *An object X^* in \mathcal{C} is a left dual of X if there exist morphisms $\text{ev}_X : X^* \otimes X \rightarrow 1$ and $\text{coev}_X : 1 \rightarrow X \otimes X^*$ such that*

$$(\text{id}_X \otimes \text{ev}_X) \circ \alpha_{X, X^*, X} \circ (\text{coev}_X \otimes \text{id}_X) = \text{id}_X \quad (1.20)$$

$$(\text{ev}_X \otimes \text{id}_{X^*}) \circ \alpha^{-1}(X^*, X, X^*) \circ (\text{id}_{X^*} \otimes \text{coev}_X) = \text{id}_{X^*}. \quad (1.21)$$

*Similarly, an object *X is said to be a right dual of X if there exists morphisms*

$ev'_X : X \otimes^* X \rightarrow 1$ and $coev' : 1 \rightarrow^* X \otimes X$ such that

$$(ev'_X \otimes id_X) \circ \alpha_{X, X, X}^{-1} \circ (id_X \otimes coev'_X \otimes) = id_X \quad (1.22)$$

$$(id_{*X} \otimes ev'_X) \circ \alpha_{*X, X, *X} \circ (coev'_X \otimes id_{*X}) = id_{*X} \quad (1.23)$$

and similarly for $coev'$ and ev' .

The morphisms ev_X, ev'_X and $coev_X, coev'$ are called evaluation and coevaluation morphisms respectively.

Definition 1.16. *A monoidal category is rigid if every object has left and right duals.*

For $f \in \text{Hom}(X, Y)$, left and right dual morphisms f^* and $*f$ are defined by the compositions

$$f^* = ev_Y \otimes id_{X^*} \circ ((id_{Y^*} \otimes f) \otimes id_{X^*}) \circ \alpha_{Y^*, X, X^*}^{-1} \circ id_{Y^*} \otimes coev_X \quad (1.24)$$

$$*f = id_{*X} \otimes ev'_Y \circ id_{*X} \otimes (f \otimes id_{*Y}) \circ \alpha_{*X, X, *Y} \circ coev'_X \otimes id_{*Y} \quad (1.25)$$

$$f^* = \text{[Diagram]}$$

Remark 1.1.

When \mathcal{C} is also unitary as a fusion category, the notion of left and right duals coincide and definitions involving dual objects and morphisms are greatly simplified. Since our interest here is the unitary case, from now on we will assume $*X \cong X^*$ for all $X \in \text{Obj}(\mathcal{C})$, and when we wish to denote the dual of an object X we write X^* .⁵

⁵In particular we will state the definition of the pivotal structure and braiding for unitary fusion categories and avoid a bit of bookkeeping.

As with the unitors, they are taken to be trivial in the sense they carry 1 to the copy of 1 in $X \otimes X^*$ by the identity morphism. Then in terms of string diagrams, coevaluation and evaluation morphisms are drawn as cups and caps, respectively.

Below we record some properties of duality that we will use implicitly throughout the remaining chapters.

Proposition 1.1. 1. $1^* \cong 1$

2. *Dual objects are unique (up to isomorphism).*

3. *For all objects X and Y and morphisms $f, g \in \text{Hom}(X, Y)$*

$$(X \otimes Y)^* \cong Y^* \otimes X^* \quad (1.26)$$

$$(f \circ g)^* = g^* \circ f^*. \quad (1.27)$$

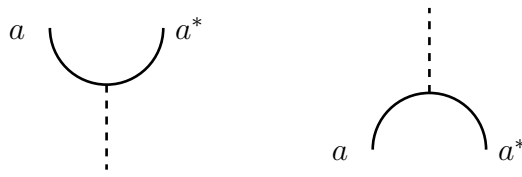
We are finally ready to state the definition of a fusion category.

Definition 1.17. *A tensor category is a locally finite, \mathbb{C} -linear, rigid monoidal category with simple tensor unit.*

Definition 1.18. *A fusion category is a finite semisimple \mathbb{C} -linear tensor category.*

1.2.5 Rigidity in a skeletal UMTC

The diagrams for these coevaluation and evaluation morphisms on simple objects are the worldlines of quasiparticle generation and annihilation.



$$(1.28)$$

which can then be identified with the trivalent vertices $|a, a^*; 1\rangle$ and $\langle a, a^*; 1|$.

$$(1.29)$$

The rigidity axiom concerns trivalent vertices of the form $|a, a^*; 1\rangle$ and $\langle a, a^*; 1|$.

For any $a \in \mathcal{L}$, the F -symbols must satisfy

$$([F_{a^*}^{a^*aa^*}]^{-1})_{11} = [F_a^{aa^*a}]_{11} \quad (1.30)$$

Rigidity axiom (Take $f = \text{id}$)

$$(1.31)$$

where we have suppressed the a and a^* labels. In words, rigidity says that cups and caps in a charge line can be straightened. Thus rigidity is encoded in diagrams through a kind of isotopy invariance.

1.2.6 Unitarity

Definition 1.19. *A fusion category is unitary if there exists a conjugation on Hom spaces: for every $f \in \text{Hom}(X, Y)$, there exists $\bar{f} \in \text{Hom}(Y, X)$ which is conjugate linear with*

$$\overline{\bar{f}} = f \tag{1.32}$$

$$\overline{f \otimes g} = \bar{f} \otimes \bar{g} \tag{1.33}$$

$$\overline{f \circ g} = \bar{g} \circ \bar{f} \tag{1.34}$$

satisfying

$$\overline{\text{coev}_X} = \text{ev}'_X \quad \overline{\text{ev}_X} = \text{coev}'_X \tag{1.35}$$

Up until now all of our string diagrams have been oriented from the bottom up. The string diagram of a conjugate morphism \bar{f} is the reflection of the string diagram for f across a horizontal axis.

$$\boxed{\bar{f}} = \boxed{f}$$

Skeletal unitarity

The compatibility condition satisfied by unitary and the coevaluation/evaluation morphisms ensures that the notions of time reversal symmetry and anti-quasiparticle coincide. Now wordlines carrying topological charge a can be expressed in terms of orientation-reversed wordlines carrying topological charge a^* .

The F -symbols then satisfy

$$[(F_d^{abc})^{-1}]_{fe} = [(F_d^{abc})^\dagger] \quad (1.36)$$

1.2.7 Pivotal fusion categories

The fusion structure of an MTC is sufficient to describe the state spaces of collections of anyons as vector spaces, but in order to get a Hilbert space of states we need an inner product $\langle \cdot, \cdot \rangle$ for which the Hom spaces are complete with respect to the associated norm $|\langle \cdot, \cdot \rangle|$. To this end, we need the notion of a *quantum trace* of morphisms. In the presence of a *pivotal structure*, the quantum traces will lead to a pairing between states that satisfies the definition of an inner product.

The pivotal structure ensures further compatibility between time reversal and duality: it says that the dual of the dual of an anyon type a (or process f) is just a (f), a straightforward categorification of something that is clear from physical considerations at the level of the fusion ring.

Pivotality

In what follows we will assume that \mathcal{C} is a fusion category, although more generally one considers pivotal structures on more general rigid monoidal categories, see Section 4.7 of [38]. Our definition of pivotality is adapted from that in [81], which is slightly different.

Definition. A *pivotal structure* on \mathcal{C} is a collection of natural isomorphisms $\phi_X : X \rightarrow X^{**}$ satisfying $\phi_{X \otimes Y} = \phi_X \otimes \phi_Y$ for all $X, Y \in \text{Obj}(\mathcal{C})$.

Skeletally, a pivotal structure amounts to a choice of *pivotal coefficient* for each simple object, $\{t_a\}_{a \in \mathcal{L}}$. The $\{t_a\}$ are required to be roots of unity and must satisfy the pivotal

1.2.8 Braided fusion categories

In order to describe the Hilbert state spaces of anyons it was enough to understand MTCs at the level of pivotal fusion categories. But in order to understand the evolution of anyonic systems we need the third and final fundamental structure possessed by an MTC, its *braiding*.

Definition 1.21. A braiding on a monoidal category $(\mathcal{C}, \otimes, 1, \alpha)$ is a family of natural isomorphisms $c_{X,Y} : X \otimes Y \rightarrow Y \otimes X$ so that the following commute:

(i) the hexagon diagram

$$\begin{array}{ccccc}
 & & (X \otimes Y) \otimes Z & & \\
 & \swarrow^{c_{X,Y} \otimes \text{id}_Z} & & \searrow^{\alpha_{X,Y,Z}} & \\
 (Y \otimes X) \otimes Z & & & & X \otimes (Y \otimes Z) \\
 \downarrow \alpha_{Y,X,Z} & & & & \downarrow c_{X,Y \otimes Z} \\
 Y \otimes (X \otimes Z) & & & & (Y \otimes Z) \otimes X \\
 & \searrow^{\text{id}_Y \otimes c_{X,Z}} & & \swarrow_{\alpha_{Y,Z,X}} & \\
 & & Y \otimes (Z \otimes X) & &
 \end{array}$$

and

(ii) the hexagon diagram

$$\begin{array}{ccccc}
 & & (X \otimes Y) \otimes Z & & \\
 & \swarrow^{\alpha_{X,Y,Z}} & & \searrow^{c_{X \otimes Y,Z}} & \\
 X \otimes (Y \otimes Z) & & & & Z \otimes (X \otimes Y) \\
 \downarrow \text{id}_X \otimes c_{Y,Z} & & & & \downarrow \alpha_{Z,X,Y}^{-1} \\
 X \otimes (Z \otimes Y) & & & & (Z \otimes X) \otimes Y \\
 & \searrow^{\alpha_{X,Z,Y}^{-1}} & & \swarrow_{c_{X,Z} \otimes \text{id}_Y} & \\
 & & (X \otimes Z) \otimes Y & &
 \end{array}$$

for all $X, Y, Z \in \text{Obj}(\mathcal{C})$.

A category with a braiding is called a braided category.

Definition 1.22. *A ribbon fusion category is a spherical braided fusion category.*

As with MacLane’s coherence theorem for monoidal categories, there is a braided coherence theorem due to Joyal and Street [57].

Theorem 1.2 (Braided coherence). *Whenever two morphisms between the same objects in a braided category are given by a sequence of associators and braidings and their inverses, they are equal.*

Represented using string diagrams, the braiding isomorphisms are depicted by

$$\begin{array}{ccc}
 \begin{array}{c} Y \quad X \\ | \quad | \\ \boxed{c_{X,Y}} \\ | \quad | \\ X \quad Y \end{array} & =: & \begin{array}{c} Y \quad X \\ | \quad | \\ \text{crossing} \\ | \quad | \\ X \quad Y \end{array}
 \end{array} \tag{1.43}$$

and similarly for $c_{X,Y}^{-1}$ but with the opposite crossing. Then the braided coherence theorem interpreted topologically is a statement about two braids being related by Reidemeister II and III moves.

Skeletal BFCs

Passing to a skeletonization, the matrix entries of the braiding isomorphisms are called the R -symbols, and they dictate how exchange transforms a basis of states. Throughout the chapters we try to be consistent about following the standard but sometimes counterintuitive conventions for skeletalizing the braiding from [3, 81].

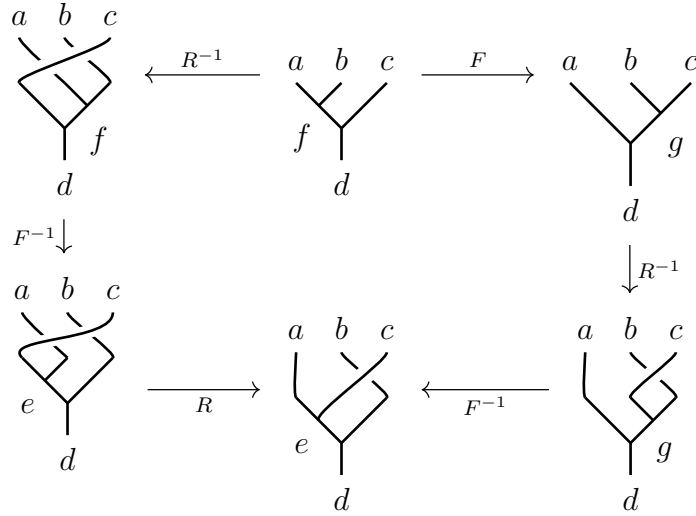
$$\begin{array}{ccc}
 \begin{array}{c} a \quad b \\ \diagdown \quad / \\ \diagup \quad \diagdown \\ b \quad a \end{array} & = \sum_c \sqrt{\frac{d_c}{d_a d_b}} R_c^{ab} & \begin{array}{c} a \quad b \\ \diagdown \quad / \\ | \\ \diagup \quad \diagdown \\ b \quad a \end{array}
 \end{array} \tag{1.44}$$

So in the graphical calculus, crossings can be resolved in terms of R -symbols and quantum dimensions. Another useful form of this local relation which can be derived from the one above is

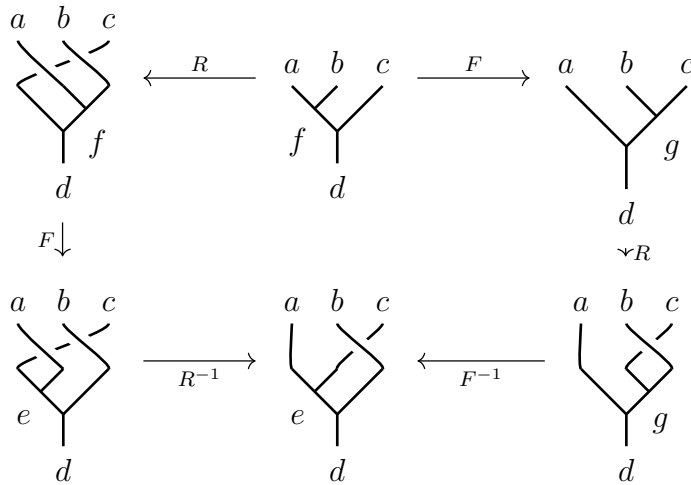
$$\begin{array}{ccc}
 \begin{array}{c} a \quad b \\ \diagdown \quad / \\ \diagup \quad \diagdown \\ \mu \\ c \end{array} & = [R_c^{ab}]_{\mu\mu} & \begin{array}{c} a \quad b \\ \diagdown \quad / \\ | \\ c \end{array}
 \end{array} \tag{1.45}$$

Exchanging the crossing gives the analogous equation involving R^{-1} .

The hexagons that need to commute are encoded by equivalent sequences of local moves involving F -moves and R -moves. Suppressing vertex labels, these take the form



and



As matrix equations the hexagon axioms become

$$\begin{aligned}
 & \sum_{\lambda, \gamma} [R_e^{ac}]_{\alpha, \lambda} [F_d^{acb}]_{(e, \lambda, \beta); (g, \gamma, \nu)} [R_g^{bc}]_{\gamma, \mu} \\
 &= \sum_{f, \sigma, \delta, \psi} [F_d^{cab}]_{(e, \alpha, \beta); (f, \delta, \sigma)} [R_d^{fc}]_{\sigma \psi} [F_d^{abc}]_{(f, \delta, \psi); (g, \mu, \nu)}
 \end{aligned} \tag{1.46}$$

and

$$\begin{aligned} & \sum \lambda, \gamma [(R_e^{ca})^{-1}]_{\alpha, \lambda} [F_d^{acb}]_{(e, \lambda, \beta); (g, \gamma, \nu)} [(R_n^{cb})^{-1}]_{\gamma, \mu} \\ &= \sum_{f, \sigma, \delta, \psi} [F_d^{cab}]_{(e, \alpha, \beta); (f, \delta, \sigma)} [(R_d^{cl})^{-1}]_{\sigma, \psi} [F_d^{abc}]_{(f, \delta, \psi); (g, \mu, \nu)}. \end{aligned} \quad (1.47)$$

Nondegenerate braided fusion categories

Let \mathcal{C} be a spherical braided fusion category. The matrix

$$S_{ab} = \frac{1}{\mathcal{D}} \text{Tr}(c_{b, a^*} \circ c_{a^*, b}) = \frac{1}{\mathcal{D}} a \begin{array}{c} \circlearrowleft \\ \circlearrowright \end{array} b$$

given by the quantum trace of the double braiding is called the S -matrix.

Definition 1.23. A braided monoidal category \mathcal{C} called *symmetric* if

$$c_{Y, X} \circ c_{X, Y} = \text{id}_{X \otimes Y}$$

for all $X, Y \in \text{Obj}(\mathcal{C})$.

For example, the fusion category $\text{Rep}(G)$ is symmetric. On the other hand, abraiding is nondegenerate if the only objects X such that $c_{Y, X} \circ c_{X, Y} = \text{id}_{X \otimes Y}$ for all $Y \in \text{Obj}(\mathcal{C})$ are direct sums of 1.

This is equivalent to the following definition.

Definition 1.24. A ribbon fusion category (RFC) is nondegenerate if $\det(S) \neq 0$.

Unitary modular tensor categories

Definition 1.25. An RFC is unitary if it is unitary as a fusion category and $\overline{c_{X, Y}} = c_{X, Y}$, $\overline{\theta_X} = \theta_X^*$. (See the next section 1.3 for the definition of θ .)

We have arrived at the definition of a modular tensor category.

Definition 1.26. *A modular tensor category \mathcal{C} is a nondegenerate ribbon fusion category. A unitary modular tensor category is a unitary nondegenerate RFC.*

In fact unitarity implies nondegeneracy, and every braiding on a unitary fusion category is automatically unitary [45].

Definition 1.27. *A skeletal MTC is a collection of complex numbers*

$$\{N_c^{ab}, [R_c^{ab}]_{\mu,\nu}, [F_d^{abc}]_{(n,\alpha,\beta);(m,\mu,\nu)}\}$$

satisfying the pentagon and hexagon equations.

Skeletal unitary MTCs have unitary R - and F -matrices.

1.3 Invariants and classification of MTCs

Next we introduce several important invariants of a UMTC \mathcal{C} which are preserved by braided-tensor autoequivalence functors of \mathcal{C} , which give the right notion of equivalence of topological orders. See Definition 3.1 in Chapter 3.

In particular, given a skeletal UMTC, invariant quantities will be independent of the specific set of solutions $\{N_c^{ab}, R_c^{ab}, [F_d^{abc}]_{nm}\}$ to the consistency equations.

We denote the rank of the UMTC by $rank(\mathcal{C}) = |\mathcal{L}| = n$. Orientations on diagrams are mostly suppressed.

1.3.1 Quantum dimensions, twists, and Frobenius-Schur indicators

The traces of the identity morphisms on simple objects id_a give invariants called *quantum dimensions* d_a .

$$\text{Tr}(\text{id}_a) = \bigcirc \! \! \! \rightarrow a = d_a.$$

The quantum dimensions satisfy $d_1 = 1$ and $d_a = d_{a^*}$ for all $a \in \mathcal{L}$.

A related invariant of UMTCs is the *global quantum dimension* \mathcal{D} , which is the positive square root

$$\mathcal{D} = \sqrt{\sum_a d_a^2}.$$

Twists

The trace of the braiding isomorphism of a simple object with itself is an invariant.

$$\text{Tr}(c_{aa}) = \! \! \! \left. \begin{array}{c} a \\ \circlearrowleft \\ a \end{array} \right\} = \sum_c R_c^{aa} \! \! \! \left. \begin{array}{c} a \quad a \\ \circlearrowleft \\ c \\ \circlearrowright \\ a \quad a \end{array} \right\} = \sum_c \sqrt{\frac{d_c}{d_a^2}} R_c^{aa} \sqrt{d_a d_a d_c} = \sum_c d_c R_c^{aa}$$

Dividing by the quantum dimension of the anyon a gives the invariant θ_a , called the *topological twist* of a .

$$\theta_a = \frac{1}{d_a} \! \! \! \left. \begin{array}{c} a \\ \circlearrowleft \\ a \end{array} \right\} = \sum_c \frac{d_c}{d_a} R_c^{aa}$$

The twists can be organized into the diagonal T -matrix $T_{ab} = \theta_a \delta_{ab}$. It is known that each θ_i is a root of unity, a result referred to as Vafa's theorem [81]. Put $\theta_i = e^{2\pi i/r_i}$. Then it follows that $|T| = \text{lcm}(r_1, r_2, \dots, r_n)$.

anyon type a	quantum dimension d_a	twist θ_a
abelian	1	
boson	1	1
fermion	1	-1
semion	1	i or -i
nonabelian	> 1	
integral	$\in \mathbb{Z}$	
weakly integral	$d_a^2 \in \mathbb{Z}$	

Table 1.3: Names for common anyon types based on their invariants. A blank entry mean that the designation does not constrain the quantity of interest, although we note that all twists are required to be roots of unity $e^{i\theta}$, $\theta = 2\pi i/n$ for some $n \in \mathbb{Z}_{\geq 0}$. The bosons here are emergent quasiparticles, as opposed to the constituent bosons in the corresponding (2+1)D TPM.

The ribbon property

The R -symbols and twists satisfy the equation

$$\sum_c R_c^{ab} R_c^{ba} = \frac{\theta_c}{\theta_a \theta_b}$$

The quantum dimension and twist of an anyon determine some of its important physical properties, and in both math and physics there are special names for anyons with specific values of these invariants.

The central charge

Define

$$\Theta = \frac{1}{\mathcal{D}} \sum_{a \in \mathcal{L}} \theta_a d_a^2 \quad , \quad \Theta^* = \frac{1}{\mathcal{D}} \sum_{a \in \mathcal{L}} \theta_a^{-1} d_a^2 \quad (1.48)$$

When \mathcal{C} is an MTC,

$$\Theta = e^{2\pi ic/8}$$

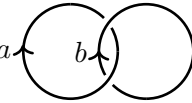
for some $c \in \mathbb{Q}$, known as the *central charge* of \mathcal{C} . The *topological central charge* c_{top} of \mathcal{C} is

$$c_{top} = c \pmod{8}.$$

1.3.2 The modular data and modular representation

S-matrix

Another important invariant is given by the trace of the double braiding:

$$S_{ab} = \frac{1}{\mathcal{D}} \text{Tr}(c_{b,a^*} \circ c_{a^*,b}) = \frac{1}{\mathcal{D}} \text{tr} \left(\begin{array}{c} \text{a} \leftarrow \text{b} \end{array} \right)$$


Resolving the diagram in the graphical calculus and using the ribbon property one can show that the *S*-matrix satisfies

$$S_{ab} = \frac{1}{\mathcal{D}} \sum_c N_c^{a^*b} \frac{\theta_c}{\theta_a \theta_b} d_c. \quad (1.49)$$

Taken together, the set of matrices $\{S, T\}$ is called the modular data of a modular tensor category.

The origin of the word “modular” in modular tensor category is the projective representation of the modular group $SL(2, \mathbb{Z})$ that is provided by the category.

The modular representation

Let C be the *charge conjugation* matrix $C_{ab} = \begin{cases} 1 & b = a^* \\ 0 & b \neq a^* \end{cases}$. Observe that $C^2 = I$, since the dual of an anyon a^* is a .

Theorem 1.3. [81] *The matrices S and T satisfy the equations*

$$(ST)^3 = \Theta C, \quad S^2 = C, \quad C^2 = I_n \quad (1.50)$$

where

$$\Theta = \frac{1}{\mathcal{D}} \sum_{a \in \mathcal{C}} d_a^2 \theta_a = e^{2\pi i c/8}.$$

Recall c is the central charge of \mathcal{C} .

It follows that the map $\rho : PSL(2, \mathbb{Z}) \rightarrow U(n)$ that sends

$$\begin{pmatrix} 0 & -1 \\ 1 & 0 \end{pmatrix} \mapsto S \quad \begin{pmatrix} 1 & 1 \\ 1 & 0 \end{pmatrix} \mapsto T$$

is a linear representation of $PSL(2, \mathbb{Z})$, and hence a projective representation of $SL(2, \mathbb{Z})$. Thus every UMTC gives a projective representation of the mapping class group of the torus $SL(2, \mathbb{Z})$. More generally, the nondegeneracy of the S -matrix means that we get projective representations of all mapping class groups.

On the one hand, the modular data are a powerful invariant. For example, MTCs which are equivalent to Drinfeld centers of finite groups are determined by their modular data for groups G with $|G| < 32$ [51, 66].

However, they are not a complete invariant of MTCs. The first counterexamples are due to Mignard and Schauenberg, and come in families of MTCs of the form $\mathcal{Z}(\text{Vec}_{\mathbb{Z}_q \times \mathbb{Z}_p}^\omega)$, where p and q are odd primes with $q \mid 2p - 1$ [66]. The smallest of these counterexamples is the family of five rank 49 categories $\mathcal{Z}(\text{Vec}_{\mathbb{Z}_{11} \times \mathbb{Z}_5}^\omega)$, where $[\omega] \in H^3(\mathbb{Z}_{11} \times \mathbb{Z}_5, U(1))$.

1.3.3 Knot and link invariants from MTCs

We have already seen that several link invariants that come from MTCs, the quantum dimensions associated to the unknot, the twists of the twisted unknot, and the S -matrix from the Hopf link. More generally, an MTC gives an invariant of any framed link.

In light of the modular data failing to be complete invariants of MTCs, it is an open question whether there is some minimal data set extending $\{S, T\}$ that is. Alternatively, one can ask whether there are other sets of link invariants that distinguish equivalence classes of MTCs.

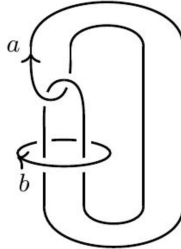
The following result says that such links necessarily must come from closures of words in B_n for $n > 2$ that involve more than one braid group generator.

Theorem 1.4 (Bonderson, D., Galindo, Rowell, Tran, Wang). *Any framed knot or link which can be represented by the closure of a braid word in \mathcal{B}_2 is determined by the modular data $\{S, T\}$.*

Beyond modular data

Along these lines in [14] and [34] we investigate small knot and link invariants as invariants of MTCs, and in particular those coming from the 5 Mignard-Schauenberg categories of rank 49.

We pay particular attention the invariants of the Whitehead link, and define the W -matrix

$$W_{ab} = \frac{\theta_a}{\theta_b} \widetilde{W}_{ab} = \frac{\theta_a}{\theta_b} \cdot$$


Proposition 1.2 (Bonderson, D., Galindo, Rowell, Tran, Wang). *The W -matrix is*

determined by the punctured S -matrices

$$S_{(a\mu)(b\nu)}^{(x)} = \frac{1}{D\sqrt{d_x}} \text{ (diagram) }$$

according to

$$W_{ab} = \frac{\theta_a D^2}{\theta_b d_a} \sum_{x,\mu} S_{bx}^* S_{(a\mu)(a\mu)}^{(x)}$$

We find that the W -matrices taken with the twists are enough to distinguish the rank 49 Mignard-Schauenburg that failed to be distinguished by the S - and T -matrices as sets.

Theorem 1.5 (Bonderson, D. , Galindo, Rowell, Tran, Wang). *The data $\{T, W\}$ gives a complete invariant of the categories $D^\omega(G)$ for $G = \mathbb{Z}_{11} \rtimes \mathbb{Z}_5$.*

In [34] we tabulate the invariants for knots and links up to 9 crossings which come from braid closures in \mathcal{B}_3 . It is not uncommon for such knots and links to distinguish the rank 49 Mignard-Schauenburg categories when taken with the T -matrix, and sometimes even give a complete invariant. For example,

Theorem 1.6 (D., Tran (2018)). *The 5_2 knot is a complete invariant of the $D^\omega(G)$ for $G = \mathbb{Z}_{11} \rtimes \mathbb{Z}_5$.*

The T -matrix together with the figure eight knot or the Borromean rings distinguish the categories.

1.3.4 Classification and structure theory of MTCs

A classification of MTCs charts a “periodic table” of topological phases of matter. We seek an understanding of what the “atoms” of MTCs are - analogous to finite simple

groups - from which all MTCs can be generated. Examples of ways to generate or combine MTCs include Galois conjugation, Deligne products (see Chapter 5) and G -gauging/condensation (Chapter 4)

A classification of UMTCs begins with considerations about its objects - rank, quantum dimension, and fusion rules.

TABLE 1. Unitary MTCs of rank ≤ 4

	A	2							
	1								
	A	4		N	4				
	\mathbb{Z}_2			$(A_1, 3)_{\frac{1}{2}}$	U				
	A	4	N	16	N	4			
	\mathbb{Z}_3		$(A_1, 2)$		$(A_1, 5)_{\frac{1}{2}}$	U			
A	10	A	8	N	8	N	4	N	6
$\mathbb{Z}_2 \times \mathbb{Z}_2$		\mathbb{Z}_4		$(A_1, 3)$	U	$(A_1, 7)_{\frac{1}{2}}$	U	$Fib \times Fib$	U

Figure 1.6: Low rank classification of UMTCs, from [75].

An MTC whose objects all have quantum dimension 1 (every simple object is invertible) is said to be pointed. Topological phases whose topological order is pointed are known as *abelian* topological phases. This is because the quantum dimensions being one is equivalent to the anyons having statistics which generate an abelian (and hence projectively trivial) subgroup of the unitary group $U(1)$ [77], see the next chapter for the details.

1.4 Examples

We will work with many examples in the later chapters, and it will be helpful to record their algebraic data, common invariants, and other properties.

Any admissible UMTC data not explicitly listed is understood to be trivial. We give the fusion rules either as a list of the nontrivial fusion products or in the form of a fusion table depending on which is more suitable.

1.4.1 Semion UMTC

Low rank examples exhibit many of the features that characterize different UMTCs.

Example 1.3 (Semion topological order). [75]

Anyons	$\mathcal{L} = \{1, s\}$
Fusion	$s \otimes s = 1$
R -symbols	$R_1^{ss} = i$
F -symbols	$F_s^{sss} = -1$
<hr/>	
Quantum dimensions	$d_s = 1$
	$\mathcal{D} = \sqrt{2}$
Twists	$\theta_s = i$
S -matrix	$S = \frac{1}{\sqrt{2}} \begin{pmatrix} 1 & 1 \\ 1 & -1 \end{pmatrix}$
Frobenius-Schur indicators	$v_s = -1$
Anomaly and central charge	$\Theta = \frac{1}{\sqrt{2}}(1 + i), c = 1$

The semion MTC is the smallest MTC with nontrivial F -symbols.

1.4.2 Fibonacci UMTC

Example 1.4 (Fibonacci topological order). [81]

Anyons	$\mathcal{L} = \{1, \tau\}$
Fusion	$\tau \otimes \tau = 1 \oplus \tau$
R -symbols	$R_1^{\tau\tau} = e^{-4\pi i/5}$ $R_\tau^{\tau\tau} = e^{3\pi i/5}$
F -symbols	$F_\tau^{\tau\tau\tau} = \begin{pmatrix} \phi^{-1} & \phi^{-1/2} \\ \phi^{-1/2} & -\phi^{-1} \end{pmatrix}$
Quantum dimensions	$d_\tau = \phi$ $\mathcal{D} = \sqrt{2 + \phi}$
Twists	$\theta_\tau = e^{4\pi i/5}$
S -matrix	$S = \frac{1}{\sqrt{2+\phi}} \begin{pmatrix} 1 & \phi \\ \phi & -1 \end{pmatrix}$
Frobenius-Schur indicator	$v_\tau = 1$

1.4.3 Ising UMTCs

There are eight inequivalent MTCs of rank 3 with the same fusion rules which all go by the name of Ising, distinguished by writing $\text{Ising}^{(\nu)}$ where ν parametrizes the quantum twist of the anyon σ [53]. Throughout these chapters by Ising we mean $\text{Ising}^{(1)}$, the category with modular data given in [81].

Example 1.5 (Ising topological order). [81]

Anyons	$\mathcal{L} = \{1, \sigma, \psi\}$
Fusion	$\sigma \otimes \sigma = 1 \oplus \psi$ $\psi \otimes \psi = 1$ $\psi \otimes \sigma = \sigma$
R -symbols	$R_1^{\sigma\sigma} = e^{-\pi i/8}, R_1^{\psi\psi} = -1$ $R_\sigma^{\psi\sigma} = R_\sigma^{\sigma\psi} = -i, R_\psi^{\sigma\sigma} = e^{3\pi i/8}$
F -symbols	$F_\sigma^{\sigma\sigma\sigma} = \frac{1}{\sqrt{2}} \begin{pmatrix} 1 & 1 \\ 1 & -1 \end{pmatrix}$ $F_\sigma^{\psi\sigma\psi} = F_\psi^{\sigma\psi\sigma} = -1$
Quantum dimensions	$d_\sigma = \sqrt{2}, d_\psi = 1$ $\mathcal{D} = 2$
Twists	$\theta_\sigma = 1, \theta_\psi = e^{2\pi i/16}, \theta_\psi = -1$
S -matrix	$S = \frac{1}{2} \begin{pmatrix} 1 & \sqrt{2} & 1 \\ \sqrt{2} & 0 & -\sqrt{2} \\ 1 & -\sqrt{2} & 1 \end{pmatrix}$
Frobenius-Schur indicators	$\nu_\psi = 1, \nu_\sigma = 1$
Anomaly and central charge	$\Theta = \frac{1+i}{\sqrt{2}}, c = 1$

1.4.4 Quantum doubles of finite groups and Dijkgraaf-Witten

TQFT

Example 1.6 ($D(\mathbb{Z}_2)$ topological order). [3]

Anyons	$\mathcal{L} = \{1, e, m, f\}$
Fusion	$\langle e, m \rangle \cong \mathbb{Z}_2 \times \mathbb{Z}_2$
R -symbols	$R_c^{ab} = e^{\pi i a_2 b_1}$ where $a = (e^{a_1}, m^{a_2}), a = (e^{b_1}, m^{b_2})$
F -symbols	$F_d^{abc} = 1$ for all $a, b, c, d \in \mathcal{L}$
Quantum dimensions	$d_e = d_m = d_f = 1$ $\mathcal{D} = 2$

For the next example we will only need the fusion table.

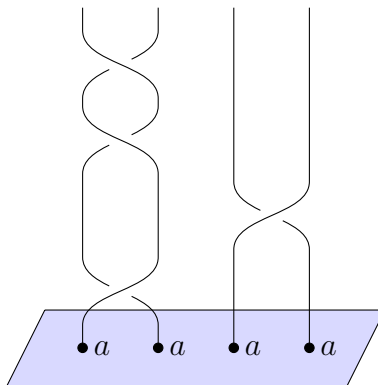
Example 1.7 ($D(S_3)$ topological order). [21]

Anyons $\mathcal{L} = \{A, B, C, D, E, F, G, H\}$
 Fusion table

\otimes	A	B	C	D	E	F	G	H
A	A	B	C	D	E	F	G	H
B	B	A	C	E	D	F	G	H
C	C	C	$A \oplus B \oplus C$	$D \oplus E$	$D \oplus E$	$G \oplus H$	$F \oplus H$	$F \oplus G$
D	D	E	$D \oplus E$	$A \oplus C \oplus F \oplus G \oplus H$	$B \oplus C \oplus F \oplus G \oplus H$	$D \oplus E$	$D \oplus E$	$D \oplus E$
E	E	D	$D \oplus E$	$B \oplus C \oplus F \oplus G \oplus H$	$A \oplus C \oplus F \oplus G \oplus H$	$D \oplus E$	$D \oplus E$	$D \oplus E$
F	F	F	$G \oplus H$	$D \oplus E$	$D \oplus E$	$A \oplus B \oplus F$	$H \oplus C$	$G \oplus C$
G	G	G	$F \oplus H$	$D \oplus E$	$D \oplus E$	$H \oplus C$	$A \oplus B \oplus G$	$F \oplus C$
H	H	H	$F \oplus G$	$D \oplus E$	$D \oplus E$	$G \oplus C$	$F \oplus C$	$A \oplus B \oplus H$

Chapter 2

Quantum representations from MTCs and topological quantum computing



In this chapter we review the mathematical foundations of quantum computation and the algebraic theory of topological quantum computing (TQC). We discuss TQC with anyons as well as the more general mathematical framework of TQC with excitations, boundaries, and defects in topological phases of matter to be applied in Parts II & III.

The reader comfortable with quantum computation may wish to skip ahead to [Section](#)

2.2, and if already familiar with the physics of TQC, Section 2.3. As with the material in Chapter 1, we note that there are already many excellent references covering this material, and recall it here only for the sake of self-containment. On the whole Section 2.1 follows Nielsen and Chuang [68].

2.1 Quantum computation

One of the beautiful things about the quantum world is that quantum mechanics and quantum information are the same theory - the idea of a quantum computer is simply to engineer a quantum system whose evolution can be precisely controlled. Like in Chapter 1 where we examined MTC theory from physical principles, here too we will use the postulates of quantum mechanics as our guide.

There are three main pieces of any computation: input, process, and output. For a *quantum computation* each of these stages is quantum mechanical: the input is a quantum state, the process a unitary evolution, and the output a measurement. Thus the stages of a quantum computation follow the postulates of quantum mechanics.

2.1.1 Encoding quantum information

The input to a quantum computation is a quantum state, which per the laws of quantum mechanics, we know to be given by a unit vector in some Hilbert space.

Postulate 1. *A quantum state $|\psi\rangle$ of an isolated quantum system is a unit vector in a complex Hilbert space \mathcal{H} .*

The smallest nontrivial Hilbert space over \mathbb{C} comes at dimension 2, $\mathcal{H} \cong \mathbb{C}^2$. A phys-

ical system whose space of quantum states is 2-dimensional is called a 2-level quantum system.

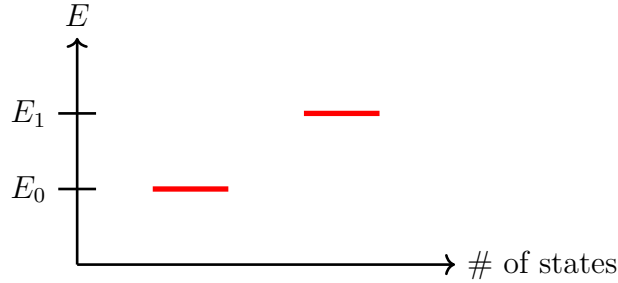


Figure 2.1: Depiction of basis states of a 2-level quantum system. In general $E_0 \neq E_1$, and there is a ground state with energy E_0 and an excited state with energy E_1 . When $E_0 = E_1$ there are two ground states both with energy E_0 , an example of a phenomenon called *ground state degeneracy*, see [Figure 2.3](#).

Thus the smallest unit of quantum information, called a *qubit* for quantum bit, is just a unit vector in a two-dimensional Hilbert space.

And thus whereas the classical bit is discrete, with bit states taking on a value of either 0 or 1, a qubit has a continuum of states. When a qubit is identified with \mathbb{C}^2 , the standard basis $\{e_1 = (1, 0)^T, e_2 = (0, 1)^T\}$ of \mathbb{C}^2 is referred to as the computational basis and written using Dirac notation, $\{|0\rangle, |1\rangle\}$.

Qubits

Then in analogy with a classical bit, one says that a qubit state is a *quantum superposition* of the states 0 and 1, meaning a normalized complex linear combination of basis states

$$|\psi\rangle = \alpha|0\rangle + \beta|1\rangle \quad (2.1)$$

where $|\alpha|^2 + |\beta|^2 = 1$.

Examples of two-level systems include the polarization of a photon, the spin of an electron, and any collection of anyons with a two-fold degeneracy. For instance, Fibonacci anyons τ have the property that when they fuse with another τ , the result is a quantum superposition of 1 and τ . This multiplicity in the fusion product, or *multi-fusion channel*, is essentially a two-level system.¹

Qubit states admit a powerful visualization as points on a two-dimensional sphere called the Bloch sphere representation. Rewriting the qubit state $|\psi\rangle = \alpha|0\rangle + \beta|1\rangle$ using the normalization condition, the qubit state can be rewritten in terms of 3 real degrees of freedom, θ , ϕ , and γ [68].

$$|\psi\rangle = e^{i\gamma} \left(\cos \frac{\theta}{2} |0\rangle + e^{i\phi} \sin \frac{\theta}{2} |1\rangle \right).$$

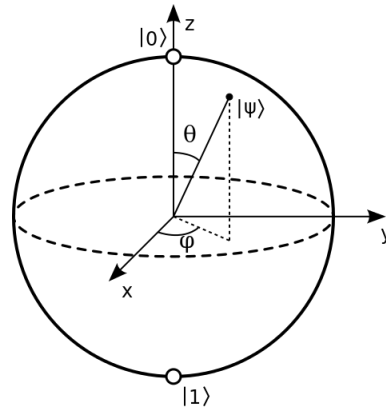


Figure 2.2: Parametrization of pure qubit states and visualization in terms of the Bloch sphere.

Since states are really only defined up to an overall phase, the factor of $e^{i\gamma}$ out in front can be ignored. Thus we are left with two real degrees of freedom, θ and ϕ , which parametrize the polar and azimuthal angles of a point on a 2-sphere, respectively.

Interpreted with these conventions the sphere is called the Bloch sphere. The state $|0\rangle$ corresponds to $\theta = 0, \phi = 0$, or the north pole, and $|1\rangle$ to $\theta = \pi, \phi = 0$.

¹We will see in the next section that in order to encode a logical qubit one actually needs four Fibonacci anyons, but this oversimplification is fine for now.

Qudits

More generally, a quantum system with d energy levels, *d-level quantum system* is modeled by a d -dimensional Hilbert space with orthonormal basis, which we will denote by \mathcal{H}^d . While the Bloch sphere provides a nice way to visualize qubit states, pure qudit states for $d > 2$ lie on a convex polytope in higher dimensions, and not so easy to visualize [65].

Encoding quantum information

We have discussed two different notions of a qubit, the mathematical definition and the physical realization, namely a two-level system. *Encoding* a qubit is to identify these two notions.

More precisely, a qubit encoding in a two-level system is an isomorphism of the vector spaces

$$\mathcal{H}_{logical}^2 \cong \mathcal{H}_{physical}^2.$$

In general a qubit can be encoded in a d -level system where $d > 2$,

$$\mathcal{H}_{logical}^2 \rightarrow \mathcal{H}_{physical}^d.$$

A *qudit*, or d -dimensional Hilbert space can be encoded in a d -level system

$$\mathcal{H}_{logical}^d \rightarrow \mathcal{H}_{physical}^d$$

or of course in full generality in any n -level system for $n > d$. Some get special names: three-dimensional qudits are called *qutrits*, and p -dimensional qudits for p prime are called *qupits*.

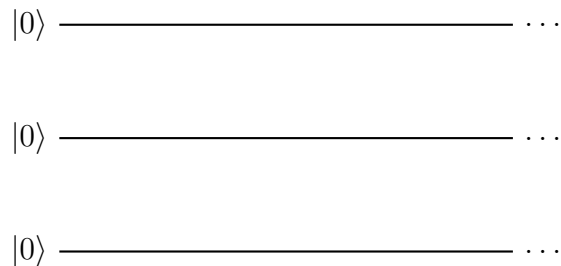
When smaller Hilbert spaces are encoded into larger Hilbert space, there is the pos-

sibility of *leakage*.

Taking the tensor product of Hilbert spaces, one combines qubits and qudits so that they can be coupled together to perform specific operations.

Postulate 2. *The Hilbert space of states of a composite quantum system is given by the tensor product of the Hilbert spaces of its components.*

Quantum algorithms are often illustrated using *quantum circuits*. Each strand corresponds to a qudit, whose initial state is labeled on one end, often some ground state written $|\psi\rangle = |0\rangle$.



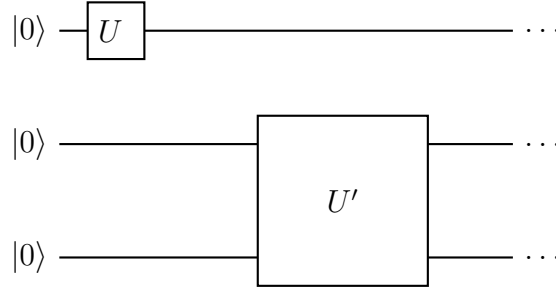
2.1.2 Processing quantum information

Given a 2-level physical system identified as a qubit, the input to a qubit computation is initialized by preparing the system in a certain state. By the second postulate of quantum mechanics, a quantum computation will transform such an input state unitarily.

Postulate 3. *The evolution of a closed quantum system is given by a unitary transformation on Hilbert space $U \in \mathcal{B}(\mathcal{H})$.*

With respect to the computational qubit states, a quantum logical operation on a qubit, or *qubit gate* is simply a 2×2 unitary matrix, depicted in quantum circuits as a

rectangle on a strand.



These look a lot like our string diagrams from fusion categories in Chapter 1. Indeed quantum circuits are just string diagrams in the category of finite dimensional vector spaces with some extra decorations.

In terms of the Bloch sphere, where points in $\mathbb{C}P^1$ are identified with points on the Riemann sphere, unitary evolution corresponds to rotation of the sphere through some angle.

Below we provide a list of the most common single qubit gates, which will come in handy when analyzing gate sets arising from anyons later in the chapter, and gate sets from defects in Parts II and III.

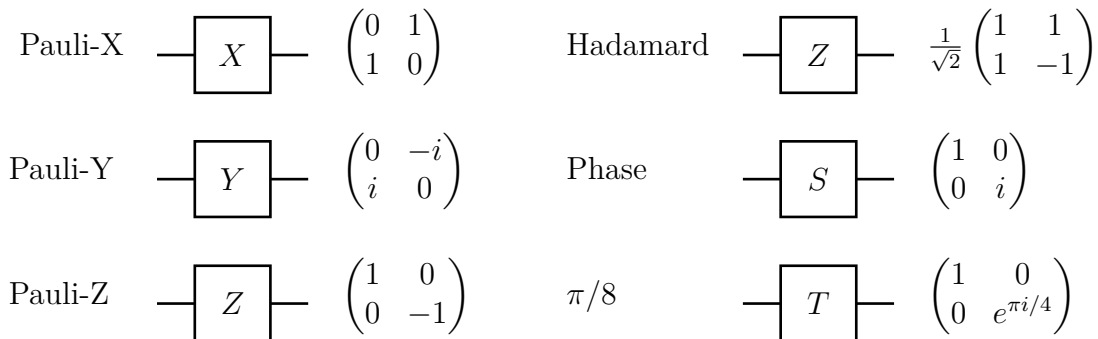


Figure 2.3: Common single qubit gates and their quantum circuit notation. We remark that the 2×2 matrices here for the S -gate and T -gate have no relation to the S - and T -matrices of Chapter 1.

More generally, there are $d \times d$ single-qudit gates, depicted in quantum circuits as a rectangle on a strand. Multi-qubit and multi-qudit gates are unitary matrices on tensor product Hilbert spaces, and depicted as rectangles with the appropriate number of input and output strands.

Given an array of n qudits $\otimes_i \mathcal{H}_i$ and a small set of qudit gates \mathcal{S} , ideally one wants to be able to effectively perform any unitary operation U in an efficient way. Efficient meaning that U should be a composition of gates in \mathcal{S} , of polynomial length in n .

Typically one studies elements of a small *gate set*, say, $\mathcal{S} = \{g_1, \dots, g_m\}$, where each g_i is a 2×2 or 4×4 unitary matrix, i.e. each acts on a one qubit (\mathbb{C}^2) or two-qubit ($\mathbb{C}^2 \otimes \mathbb{C}^2$) subspace of $(\mathbb{C}^2)^{\otimes n}$. These gate sets, while acting on a few qubits at a time, are extended trivially on the remaining qubits by tensoring with the identity.

Definition 2.1 (Universal gate set [68]). *A gate set is universal for quantum computation if any unitary operation may be approximated to arbitrary accuracy by a quantum circuit involving only those gates.*

More precisely, if we consider the set of all quantum circuits on $(\mathbb{C}^2)^{\otimes n}$ that can be built from our gate set, then it is universal if it is dense in $PU(2^n)$. (Recall that we are interested in things up to a phase.)

For the most part considerations about single qubits will suffice for our purposes in the later chapters. The following theorem provides some justification.

Theorem 2.1. *A universal gate set for $SU(2)$ together with an entangling gate generates universal quantum computation.*

Theorem 2.2. *The gate set $\{H, T, CNOT\}$ is universal for quantum computation.*

2.1.3 Measurement and readout

The final stage of a quantum computation is to measure the state of the system.

Postulate 4. *Measurement of a quantum system is described by the action of a set of projection operators $\{P_\lambda\}$ on \mathcal{H} whose projections form a basis of \mathcal{H} .*

Given a computational basis for an array of qudits, measurement proceeds by measuring the overlap of the state of the system with a computational basis state. The result is a complex probability amplitude that relays some information about how the initial state was transformed by the computation. In general such measurements must be repeated to produce a probabilistic understanding of the final state.

2.1.4 Towards quantum computers

We have seen that the recipe for a qubit is a 2-level quantum system whose evolution can be precisely controlled and shielded from decoherence. Several decades out from Feynman's articulation of the idea of a quantum computer [41] with noisy intermediate-scale quantum devices on the horizon [71] there is a proliferation of approaches to quantum computing architecture. They exhibit a wide variety of materials and control schemes, but generally speaking each involves some tradeoff between feasibility, power, efficiency, noisiness, and scalability.

2.2 Topological quantum computing with anyons

The *topological* approach to quantum computing is based on using materials in topological phases of matter as the hardware for a computer: a robust gap between degenerate ground states and excited states is a good home for a qubit.

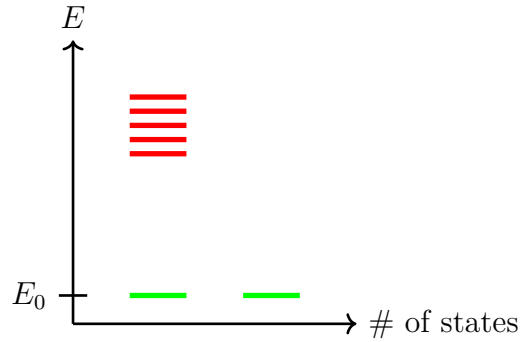


Figure 2.4: Illustration of a gapped quantum system with ground state degeneracy.

Generically the lowest two energies will have two different energy levels E_0 and E_1 , with $E_0 < E_1$. A qubit can be encoded in the superposition of states with those energies. But if the energy levels E_0 for $n > 1$ are close by, it will be hard to keep the system from evolving, or leaking, into an excited state.

There is an energy gap Δ that separates the E_0 states from the excited states $E_n > E_0$. The larger this gap, the safer the encoding. Topological phases of matter have the property that the gap is exponentially small in the length scale of the system. Quantum information encoded in the ground states of a gapped system is said to be *topologically protected*.

While the technology to engineer materials in topological phases of matter is at its early stages, topological error protection makes them a very appealing candidate for large-scale quantum computers [61].

Even in the absence of applications to quantum devices, the theory of TQC is a powerful tool for gaining physical insight. As we saw in the previous section, quantum physics and information are really one and the same. This is the perspective we take in the rest of the chapters, and the scope of our treatment of topological quantum computing is mostly formal with the exception of a few comments about applications to devices and

experiment when interesting.

2.2.1 Topological qubits

There are two ways that a bulk topological phase can give rise to topologically protected quantum information, either through the topology of its underlying space manifold or through the multi-fusion channel of a collection of anyons.

Encoding quantum information in surface states

The unitary representations of mapping class groups of punctured surfaces afforded by a TQFT are in general projective, so that they only satisfy the equation $\rho(gh) = \rho(g)\rho(h)$ up to a scalar. In other words one has a group homomorphism with target the group of *projective unitaries*

$$\rho : MCG(\Sigma_g) \longrightarrow U(d)/U(1). \quad (2.2)$$

Now the $\rho(g)$ are only defined up to a $U(1)$ phase and $\rho(gh)$ and $\rho(g)\rho(h)$ are *projectively equal*, so that for a fixed choice of $\rho(g)$ for all $g \in G$, there exists some phase $\omega(g, h)$ such that $\rho(gh) = \omega(g, h)\rho(g)\rho(h)$. In other words, the failure of ρ to be a linear representation is measured by the phases $\omega(g, h)$. It can be shown that such $\omega(g, h)$ satisfy the definition of a 2-cocycle, hence the notation from cohomology.

2.2.2 Fault-tolerant gates from anyon exchange

In TQC, the gates that are topologically-protected are those arising from anyon exchange. These are precisely elements of the image of a braid group representation.

2.3 Braid group representations from MTCs

The algebraic structure organizing the topology of the spacetime trajectories of point-like particles is the fundamental group of their configuration space $\pi_1(\text{Conf}_n(\Sigma_g^b))$. For n anyons of type a on a closed disk $\Sigma_0^1 = D^2$, this is isomorphic to the n -strand braid group \mathcal{B}_n .

Anyon exchange-generated gates are elements in the image of a unitary representation of the braid group. In this section we cover how to compute matrix representations from the data of an skeletal MTC $\{N_c^{ab}, R_c^{ab}, [F_d^{abc}]_{nm}\}$, beginning with some braid group basics.

2.3.1 The n -strand braid group

The n -strand braid group \mathcal{B}_n has presentation

$$\mathcal{B}_n = \left\langle \sigma_1, \sigma_2, \dots, \sigma_{n-1} \mid \begin{array}{l} \sigma_i \sigma_j = \sigma_j \sigma_i \text{ for } |i - j| \geq 2 \\ \sigma_i \sigma_{i+1} \sigma_i = \sigma_{i+1} \sigma_i \sigma_{i+1} \text{ for } i = 1, 2, \dots, n-1 \end{array} \right\rangle.$$

It is easy to see that \mathcal{B}_1 is the trivial group and $\mathcal{B}_2 \cong \mathbb{Z}$. More generally, the \mathcal{B}_n are infinite groups with center $Z(\mathcal{B}_n) \cong \mathbb{Z}$. Taking the quotient of \mathcal{B}_n by the normal subgroup generated by the σ_i^2 results in a group isomorphic to S_n . Thus there is a surjection of the braid group onto the symmetric group, and we have an exact sequence

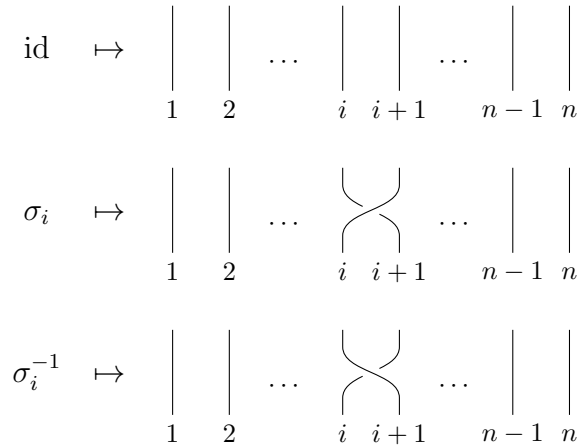
$$1 \longrightarrow P\mathcal{B}_n \longrightarrow \mathcal{B}_n \longrightarrow S_n \longrightarrow 1.$$

This implicitly defines $P\mathcal{B}_n$, the *pure braid group* on n -strands. In particular, we can get a representation of the braid group by postcomposing with a representation of the symmetric group. However, such a representation will not encode all of the informa-

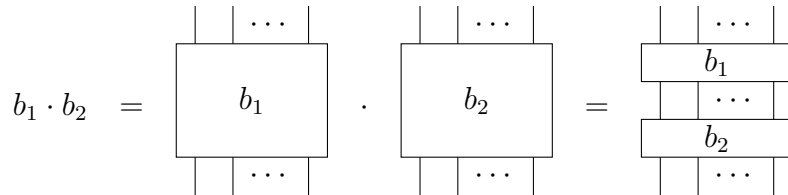
tion about the braid group that is needed for computation. Instead one must look for representations which do not factor through S_n .

Diagrammatic presentation

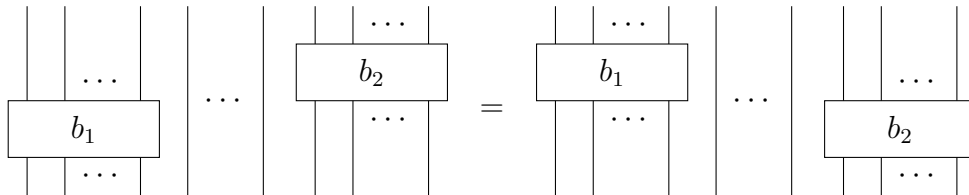
The n braid group can be understood diagrammatically by identifying its elements as elementary braid diagrams on n -strands. We use the following conventions.



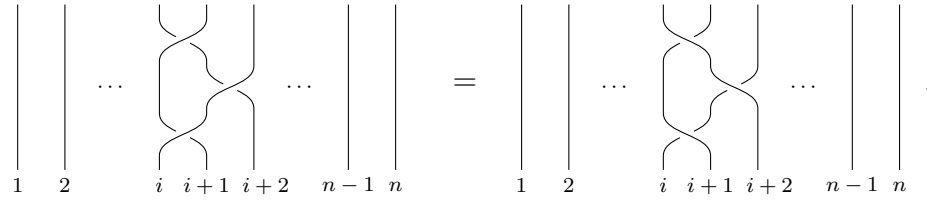
Multiplication is given by stacking of diagrams, and we take the convention that $b_1 \cdot b_2$ is b_1 stacked on top of b_2 .



The far commutativity and braid relations then correspond to the freedom to braid-isotope

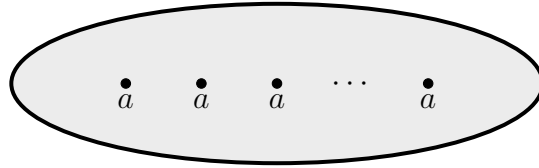


and the Reidemeister III move



2.3.2 Action of \mathcal{B}_n on $\text{Hom}(i, a^{\otimes n})$

Consider the Hilbert space of states $\text{Hom}(i, a \otimes a \otimes \cdots \otimes a)$ associated to a collection of n anyons of type a with total charge i .



The n -strand braid group acts on $\text{Hom}(i, a \otimes a \otimes \cdots \otimes a)$ as follows. Given a braid generator $\sigma_k \in \mathcal{B}_n$ and a morphism $f : i \rightarrow a^{\otimes n}$, the generator acts by postcomposition with the braiding isomorphism on the k^{th} and $k + 1^{\text{st}}$ factors of $a^{\otimes n}$, with suitable associators interspersed. Suppressing the associators,

$$b \cdot f = (\text{id}^{\otimes k-1} \otimes_{C_{a,a}} \otimes \text{id}^{\otimes n-k-1}) \circ f \tag{2.3}$$

This gives a unitary representation

$$\rho_{n,a,i} : \mathcal{B}_n \longrightarrow U(d) \tag{2.4}$$

where $d = \dim(\text{Hom}(i, a \otimes a \otimes \cdots \otimes a))$.

Explicit matrix representations with respect to a fixed fusion tree basis can be calcu-

lated with the data of a skeletal UMTC according to the following procedure. Let $V_i^{a^{\otimes n}}$ to indicate the vector space $\text{Hom}(i, a^{\otimes n})$ with basis.

1. Fixing a fusion tree with external edge labels a and total charge i , enumerate the admissibly labeled trees v_j of $V_i^{a^{\otimes n}}$.
2. For each generator of the n -strand braid group σ_k and each basis vector $v \in \{v_j\}$, stack the diagram for σ_k on the diagram for v_j and resolve in the $\{v_j\}$ basis via the graphical calculus using a sequence of R - and F -moves. These give the columns of the matrices representing the generators.
3. To calculate the matrix representation of any braid b , write it as a word in braid generators and multiply the generator images.

$$\rho(b) = \rho(\sigma_{i_m}^{p_m} \cdots \sigma_{i_1}^{p_1}) = \rho(\sigma_{i_m})^{p_m} \cdots \rho(\sigma_{i_1})^{p_1}.$$

While computing elements in the image of a representation from the data of UMTC is straightforward, in general analysis of the image is less so. For small n and low dimensions there are some techniques for characterizing the images, but a general method for determining density is lacking. That being said, there are many results about the representations for specific UMTCs whose algebraic data is well understood, see the examples in Section 2.4.

2.3.3 The action of \mathcal{B}_3 on state spaces of three anyons

When a pair of anyons a and a^* is generated from the vacuum, their total charge is fixed to the vacuum charge 1 and does not support a logical qubit, even if a is a nonabelian anyon. Thus one needs a minimum of two pairs to be generated in order to

support a logical qubit. In light of these physical considerations, for our purposes the most elementary anyonic quantum systems are those where $a = a^*$ of the form $\text{Hom}(1, a^{\otimes 4})$.

In this case, the four anyons of type a support a qudit of dimension d where $d = \sum_{c \in \mathcal{L}} (N_c^{aa})^2$, and their exchange generates a unitary representation of the four-strand braid group into $d \times d$ unitary matrices: $\rho : \mathcal{B}_4 \longrightarrow U(d)$.

However, by duality we have the isomorphism

$$\text{Hom}(1, a \otimes a \otimes a \otimes a) \cong \text{Hom}(a, a \otimes a \otimes a)$$

where we have used that $a = a^*$.

Thus with some loss of generality we can study the representation of \mathcal{B}_3 associated to three anyons of type a with total charge a . The \mathcal{B}_3 representations are simpler to analyze, having only two generators and satisfying only one relation (the braid relation). The examples we present here are all self-dual and so the representations are actually equal.

Next we describe how to calculate explicit matrix representations of \mathcal{B}_3 given a topological order \mathcal{C} .

In the later chapters we will primarily be interested in representations of the 3-strand braid group $\mathcal{B}_3 = \langle \sigma_1, \sigma_2 \mid \sigma_1 \sigma_2 \sigma_1 = \sigma_2 \sigma_1 \sigma_2 \rangle$. Observe that the far commutativity relation does not apply because none of the strands are ever more than one strand apart.

$$\text{Hom}(i, a \otimes a \otimes a) \cong \mathbb{C} \left[\left[\begin{array}{c} a \quad a \quad a \\ \mu \quad \quad \nu \\ c \\ i \end{array} \right] \right]$$

where $N_c^{aa} \cdot N_i^{ca} \neq 0, 1 \leq \mu \leq N_c^{aa}, 1 \leq \nu \leq N_i^{ca}$.

For multiplicity-free theories, this simplifies to

$$\text{Hom}(i, a \otimes a \otimes a) \cong \mathbb{C} \left[\left\{ \begin{array}{c} a \quad a \quad a \\ \diagdown \quad \diagup \\ c \\ | \\ i \end{array} \right\} \mid N_c^{aa} \cdot N_i^{ca} \neq 0 \right]$$

Below we use the notation $|a, a, a; i; c\rangle$ to indicate the fusion tree basis vector of $V_i^{a^{\otimes 3}}$ with internal edge labeled by $c \in \mathcal{L}$.

To understand the group action of \mathcal{B}_3 on $V_i^{a^{\otimes 3}}$, it suffices to understand how the generators σ_1 and σ_2 act.

Image of σ_1

With the left-associated basis, the braid that results from stacking σ_1 can be resolved with a single R -move.

$$\sigma_1 \cdot |a, a, a; i; c\rangle = \begin{array}{c} \text{Braid diagram} \\ \diagdown \quad \diagup \\ c \\ | \\ i \end{array} = R_c^{aa} \begin{array}{c} \text{Fusion tree} \\ \diagdown \quad \diagup \\ c \\ | \\ i \end{array} = R_c^{ab} |a, a, a; i; c\rangle$$

It follows that the matrix representation of σ_1 is diagonal in the left associated basis:

$$\rho(\sigma_1) = \text{diag}(R_{c_1}^{aa}, R_{c_2}^{aa}, \dots, R_{c_d}^{aa})$$

Image of σ_2

As for the second generator, we have

$$\begin{aligned}
 \sigma_2 \cdot |a, a, a; i; c\rangle &= \text{Diagram 1} \\
 &= \sum_d [F_i^{aaa}]_{d,c} \text{Diagram 2} \\
 &= \sum_d [F_i^{aaa}]_{d,c} R_d^{aa} \text{Diagram 3} \\
 &= \sum_{d,e} [F_i^{aaa}]_{d,c} R_d^{aa} [F_i^{aaa}]_{e,d}^{-1} \text{Diagram 4} \\
 &= \sum_{d,e} [F_i^{aaa}]_{d,c} R_d^{aa} [F_i^{aaa}]_{e,d}^{-1} |a, a, a; i; e\rangle
 \end{aligned}$$

Equivalently one can show that

$$\rho(\sigma_2) = [F_i^{aaa}]^{-1} \rho(\sigma_1) [F_i^{aaa}].$$

The image of the 3-strand braid group associated to n anyons of type a with total charge i in a UMTC $\mathcal{C} = \{N_c^{ab}, R_c^{ab}, [F_d^{abc}]_{ef}\}$ is generated by the two matrices $\rho(\sigma_1)$ and $\rho(\sigma_2)$.

Whether the subgroup of $d \times d$ unitary matrices realized by braiding anyons is finite,

infinite, or dense depends on the UMTC at hand.

2.3.4 Measurement

While measurement is necessary for readout of a quantum computation, it is also a viable tool for performing computation itself.

Generically most examples of topological order are not universal by braiding alone, see Section 2.4. The smallest known topological order featuring universal braiding is the Fibonacci UMTC [43]. Fibonacci topological order has several expected realizations: for example in fractional quantum Hall (fqH) liquids with filling fraction $\nu = 12/5$, superconductor networks, and interacting Majorana fermions [28].

One alternative approach to realizing nonabelian anyons for topological quantum computing involves engineering non-abelian objects like symmetry defects and more generally domain walls, including gapped boundaries [21, 22, 23, 82]. The general mathematical framework for topological quantum computing with domain walls is briefly described at the end of this chapter, and the particular case of symmetry defects is covered in detail in Part II.

But even when suitable objects be they anyons or something else can be realized in a topological phase, adiabatically moving them in a way that maintains the system in its ground state is also an experimental challenge.

And thus another approach, which can be combined with the previous one, is to perform braiding operations effectively instead of physically. In a scheme known as *measurement-only topological quantum computation*, the exchange-generated quantum gates can be realized instead through a series of topological charge projections [15].

Incorporating such *projective measurement* into protocols for realizing quantum gates can be rigorously translated into the mathematical framework of topological quantum

computing. As projection operators on a Hilbert space, measurement operators are not unitary, and hence not directly related to the associators or braiding of a UMTC.

Projective measurement

Given a skeletal UMTC interpreted as an anyon model, up to a normalization projective measurement of a (multiplicity-free) fusion channel is given by the diagram

$$P_c^{ab} = \begin{array}{c} a \quad b \\ \diagdown \quad / \\ \quad c \\ / \quad \diagdown \\ a \quad b \end{array} \quad (2.5)$$

Applying the measurement to an anyon process involving the fusion of a and b corresponds to stacking the diagram P_c^{ab} , possibly extended by the identity, for example:

$$\begin{array}{c} a \quad b \\ \diagdown \quad / \\ \quad c \\ / \quad \diagdown \\ a \quad b \\ | \\ d \end{array} = \sqrt{\frac{d_a d_b}{d_c}} \delta_{cd} \begin{array}{c} a \quad b \\ \diagdown \quad / \\ \quad c \end{array} \quad (2.6)$$

Resolving using the graphical calculus shows that this has the effect of forcing the fusion channel of a and b to produce c .

In executing a protocol with a projective measurement, projecting onto a specific anyon in a fusion channel means measuring the channel until it gives the desired result: the channel is measured and if the answer is not correct, the computation is scrapped and the protocol is run from the beginning. In practice when incorporating measurement one must make considerations about the overhead that this introduces, as the probability

of producing a desired fusion outcome depends on the particulars of a topological order.

It is reasonable to ask why one should bother studying exchange-only gates if the measurement-only approach seems destined to reign supreme. In fact, our main result in Chapter 6 suggests that projective measurement is *required* for universal quantum computation when the underlying phase is not universal by braiding itself.

However, knowing how to employ projective measurement to produce a desired operation still requires a detailed understanding of the braiding operations native to a given topological order.

2.4 Examples

Next we present some known results about TQC with anyons and examples of single-qubit logical gates that can be realized by anyon exchange. Later we will be interested in comparing the gate sets from topological orders related by a kind of topological phase transition called *gauging*, and it will be helpful to have such examples on hand.

2.4.1 TQC with metaplectic anyons

An N -metaplectic category is any UMTC with the same fusion rules as $SO(N)_2$. The specifics of the fusion rules depend on the residue of N modulo 4: they fall into one of three types: the odd N -metaplectic, $N \equiv 0 \pmod{4}$, and $N \equiv 2 \pmod{4}$. When N is odd it is known that the braid group representations have finite image [53]. In other words, the N odd metaplectic anyons have Property F - hence any universal quantum computing scheme based on these anyons require projective measurement. See for example [29] for a universal gate set based on metaplectic anyons and measurement.

The Ising ν categories are the smallest examples of metaplectic categories.

Example 2.1 (Ising anyon qubit).

A qubit can be encoded in the state space of four Ising anyons σ with trivial total charge. The single qubit operations realizable from exchanging Ising anyons is then given by a representation of the 4-strand braid group \mathcal{B}_4 . This representation was discovered in the context of type II_1 factors prior to the advent of TQC, and its projective image classified [56].

There is a qubit supported on $\text{Hom}(\sigma, \sigma^{\otimes 3})$. With respect to the basis

$$\left\{ \begin{array}{c} \sigma \quad \sigma \quad \sigma \\ \diagdown \quad \diagup \quad \diagdown \\ \quad \quad \quad \diagup \\ \quad \quad \quad \sigma \\ 1 \end{array}, \begin{array}{c} \sigma \quad \sigma \quad \sigma \\ \diagdown \quad \diagup \quad \diagdown \\ \quad \quad \quad \diagup \\ \quad \quad \quad \sigma \\ \psi \end{array} \right\}.$$

one has

$$\rho(\sigma_1) = e^{-\pi i/8} \begin{pmatrix} 1 & 0 \\ 0 & i \end{pmatrix} \quad \text{and} \quad \rho(\sigma_2) = e^{-\pi i/8} \begin{pmatrix} 1+i & 1-i \\ 1-i & 1+i \end{pmatrix}. \quad (2.7)$$

Theorem 2.3 (Jones [56]). *The projective image of \mathcal{B}_3 on $\text{Hom}(\sigma, \sigma^{\otimes 3})$ is finite and isomorphic to $Z_2^2 \rtimes S_3$.*

Consequently Ising anyons cannot generate universal single qubit quantum computation. In particular, the image does not contain a T -gate. Chapter 4 contains an example of a protocol to generate a T -gate that uses projective measurement and braiding with symmetry defects.

2.4.2 TQC with Fibonacci anyons

Example 2.2 (Fibonacci anyon qubit).

The fusion rule $\tau \otimes \tau = 1 \oplus \tau$ allows for two possibilities for the total charge of three Fibonacci anyons, either 1 or τ . One can check that the vector space $\text{Hom}(1, \tau \otimes \tau \otimes \tau)$ is 1-dimensional, and $\text{Hom}(\tau, \tau \otimes \tau \otimes \tau)$ is 2-dimensional.

A left-associated fusion basis is given by

$$\left\{ \begin{array}{c} \tau \quad \tau \quad \tau \\ \diagdown \quad \diagup \\ \tau \\ | \\ 1 \\ | \\ \tau \end{array} , \begin{array}{c} \tau \quad \tau \quad \tau \\ \diagdown \quad \diagup \\ \tau \\ | \\ \tau \end{array} \right\}.$$

With respect to this basis the matrix representation of \mathcal{B}_3 is determined by

$$\rho(\sigma_1) = \begin{pmatrix} e^{-4\pi i/5} & 0 \\ 0 & e^{3\pi i/5} \end{pmatrix} \quad \text{and} \quad \rho(\sigma_2) = \begin{pmatrix} \phi^{-1} e^{4\pi i/5} & \phi^{-1/2} e^{-3\pi i/5} \\ \phi^{-1/2} e^{-3\pi i/5} & -\phi^{-1} \end{pmatrix}. \quad (2.8)$$

Theorem 2.4 (Freedman, Larsen, Wang). *The Fibonacci representation on $V_\tau^{\tau^{\otimes 3}}$ is dense in $U(2)$:*

$$\overline{\rho(\mathcal{B}_3)} \supset U(2).$$

2.4.3 TQC with twisted doubles of finite groups

As with the metaplectic anyons, it is known that the images of the braid group representations arising from $D^\omega(G)$ are finite [40]. Moreover, the mapping class group representations for any oriented, compact surface with boundary are also finite [52].

However, a universal gate set based on the D anyons in $D(S_3)$ that uses projective measurement and ancillary states was found in [26]. It has also been suggested to use gapped boundaries (see the next section 2.5) to enlarge the $D(S_3)$ gate set [23]. Their gate set also relies on measurement.

2.5 Topological quantum computing beyond anyons

The original concept of topological quantum computing by Kitaev [64] and later Preskill as well as Freedman, Larsen, and Wang [43] involved anyons in (2+1)D topological phases. However, the requirements for a topological quantum computer, namely a quantum system with degenerate ground states protecting from excited states by a topological gap, can in principle be met in other ways. The idea of TQC has grown to encompass the idea of using excitations in higher-dimensional topological phases, i.e. materials whose physics governed by higher-dimensional TQFTs, as well as with other phenomena like domain walls or defects.

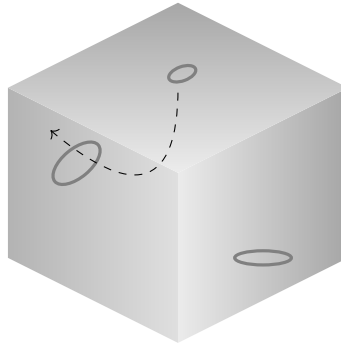
The algebraic setting for studying higher dimensional TPMs is higher category theory, whereby the statistics of excitations would be given by unitary representations of *motion groups* [49, 50], which generalize the idea of braid and mapping class groups to higher dimensions [82]. Roughly speaking domain walls (codimension one defects) between phases and defects of all codimension can be understood through higher bimodule categories, functors between them, and their equivalences, and so on [3, 6, 7].

TQC with excitations in (3+1)D

The generalization of anyon exchange-based quantum computing is to consider the fusions and motions of excitations in higher-dimensional TPM.

For example, in (3+1)D topological phases excitations are no longer restricted to

being point-like, and they can be loop-like and knotted.



However, the right generalizations of MTCs for (3+1)D TQFTs, are not quite yet well established. While there is a body of work investigating the low-dimensional representation theory of simple motion groups of knots and links in three-manifolds, like the loop braid group or necklace braid group [18, 19, 60], there is not yet a framework in place for a systematic understanding of excitation statistics in higher dimensions. Nevertheless, physicists have other methods to investigate topological order and related phenomena in (3+1)D. One topic of great interest is the possibility of (3+1)D topological phases to host a stable quantum memory using *fractons* [54].

2.5.1 TQC with domain walls and defects in (2+1)D

Domain walls between topological phases and their interaction with excitations gives rise to interesting physics that can potentially be utilized for quantum information processing.

In (2+1)D, where MTC theory for topological order is well established, domain walls within or between topological order are described by *module categories* over MTCs.

Since every finite module category over a braided tensor category \mathcal{C} is equivalent to a category of modules over an algebra object (see Definition 3.4) A internal to \mathcal{C} [38], the

notion of a domain walls can be equivalently formulated using algebra objects, see for example [62].

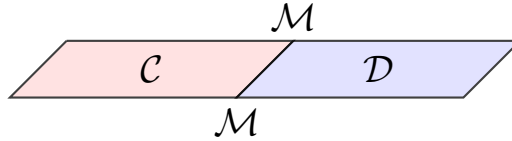


Figure 2.5: Schematic illustration of a domain wall between two different topological orders \mathcal{C} and \mathcal{D} , modeled by a $(\mathcal{C}, \mathcal{D})$ -bimodule category.

Domain walls are a sense in which topological orders can be fused together, and domain walls too can be fused.

Special types of domain walls have algebraic theories with lots of structure.

Gapped boundaries/holes

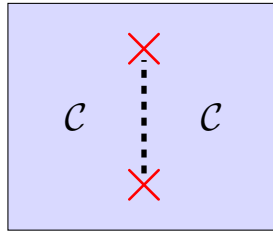
One example that has received a lot of attention by condensed matter physicists as well as a mathematical treatment is that of *gapped boundaries* or *gapped holes*, which are domain walls between doubled topological orders $\mathcal{C} \boxtimes \bar{\mathcal{C}}$ and the vacuum Vec . They are classified by Lagrangian algebras in $\mathcal{C} \boxtimes \bar{\mathcal{C}}$ [62], and viewed as nonabelian objects in their own right have been used in schemes to generate universal quantum computation when projective measurement is available.

Another type of nonabelian object that arises from domain walls are point-like *symmetry defects*, also called *twist defects* in the early physics literature on the subject. Here we give a brief overview of symmetry defects, which are the subject of the remaining chapters and are discussed in detail in [Chapter 4](#) and [Chapter 5](#).

Symmetry defects

A trivial example of a domain wall is a line-like boundary between a topological phase and itself which is “transparent” in the sense that it is invisible to anyons.

Mathematically, a UMTC \mathcal{C} is an invertible $(\mathcal{C}, \mathcal{C})$ -bimodule over itself, see [Chapter 4](#). When a topological order has a symmetry, meaning that \mathcal{C} has a categorical action by a group G , it can host transparent domain walls which terminate in point-like objects that are said to carry g and g^{-1} flux.



While anyons can pass through these defect lines, they no longer do so in a trivial way - the exchange of an anyon with a symmetry defect can permute its topological charge type by the action of G on \mathcal{C} .

In the presence of quantum (categorical group) symmetry, these domain walls form a family of invertible $(\mathcal{C}, \mathcal{C})$ -bimodule categories \mathcal{C}_g extending \mathcal{C} , which then characterizes its symmetry-enriched topological (SET) order. For so-called anomaly-free symmetries, these invertible bimodule categories form a fusion category, in which case the algebraic theory of symmetry defects is given by a G -crossed braided fusion category extending \mathcal{C} . This extension theory of MTCs was developed by mathematicians [\[39\]](#) and later used to characterize SET order in [\[3\]](#).

The anomaly vanishing means that these SET orders are purely (2+1)D - when the anomaly does not vanish the \mathcal{C}_g do not form a fusion category and instead they characterize SET order which can only occur at the boundary of a (3+1)D TPM.

In [Part II](#) we formulate the mathematical theory of quantum computing with symmetry defects in terms of unitary representations coming from G -crossed braided fusion categories, giving examples and applications. We will see that symmetry defects and their algebraic theory are at the heart of a connection between symmetry, topological order, and quantum information.

Part II

G-crossed braided fusion categories, SET phases, and TQC

Chapter 3

Symmetry, gauging, and condensation in topological order

3.1 Symmetries of MTCs

There are many different notions of symmetry for MTCs, each of which plays an important role in the theory of *symmetry gauging*, a procedure that takes an MTC \mathcal{C} and a categorical group G symmetry and produces a new MTC \mathcal{C}^G .

Understanding how these notions of symmetries are related and the role they play in modeling symmetry defects and certain topological phase transitions in (2+1)D TPM requires a solid understanding of autoequivalences of braided tensor categories, which is our starting point.

Symmetry in (2+1)D TPM	Symmetry in MTC theory
Topological symmetry	Braided tensor autoequivalence $T \in \underline{\text{Aut}}_{\otimes}^{\text{br}}(\mathcal{C})$
Gauge symmetry	Braided tensor autoequivalence which is trivial on $\mathcal{L} = \text{Irr}(\mathcal{C})$
Global G symmetry	Monoidal functor $\rho : \underline{G} \rightarrow \underline{\text{Aut}}_{\otimes}^{\text{br}}(\mathcal{C})$
Local G symmetry	$\text{Rep}(G) \subset \mathcal{C}$ as symmetric fusion subcategory
Generalized symmetry	Hypergroup symmetry [9] Hopf monad symmetry [27] (?)

Table 3.1: Notions of symmetry in topological phases and their categorical meaning. Here we assume G is a finite group. There are several notions of generalized symmetries of topological order beyond groups but not yet a complete theory.

3.1.1 Braided tensor autoequivalences and topological symmetry

A braided tensor autoequivalence gives the right notion of a structure preserving map of an MTC: it is an equivalence of categories that respects the braiding and tensor structure. When we discussed invariants of MTCs in Section 1.3 like the modular data, we were studying quantities that are invariant under the action of braided tensor autoequivalences.

Definition 3.1 (Braided tensor autoequivalence). *Let \mathcal{C} be a braided tensor category. A functor $F : \mathcal{C} \rightarrow \mathcal{C}$ is a braided tensor autoequivalence if*

- F is a monoidal functor
i.e. there exists a family of natural isomorphisms

$$U_{X,Y} : F(X \otimes Y) \rightarrow F(X) \otimes F(Y)$$

such that $F(1) \cong 1$ and the following diagram commutes for all $X, Y, Z \in \text{Obj}(CC)$.

$$\begin{array}{ccc}
F((X \otimes Y) \otimes Z) & \xrightarrow{F(\alpha_{X,Y,Z})} & F(X \otimes (Y \otimes Z)) \\
U_{X \otimes Y, Z} \downarrow & & \downarrow U_{X, Y \otimes Z} \\
F(X \otimes Y) \otimes F(Z) & & F(X) \otimes F(Y \otimes Z) \\
U_{X, Y \otimes \text{id}_{F(Z)}} \downarrow & & \downarrow \text{id}_{F(X)} \otimes U_{Y, Z} \\
(F(X) \otimes F(Y)) \otimes F(Z) & \xrightarrow{\alpha_{F(X), F(Y), F(Z)}} & F(Z) \otimes (F(Y) \otimes F(Z))
\end{array}$$

- F is braided

i.e.

$$\begin{array}{ccc}
F(X \otimes Y) & \xrightarrow{F(c_{X,Y})} & F(Y \otimes X) \\
U_{X,Y} \downarrow & & \downarrow U_{Y,X} \\
F(X) \otimes F(Y) & \xrightarrow{c_{F(X), F(Y)}} & F(Y) \otimes F(X)
\end{array}$$

for all $X, Y \in \text{Obj}(\mathcal{C})$.

- F is an equivalence of categories i.e. there exists a functor $G : \mathcal{C} \rightarrow \mathcal{C}$ such that $G \circ F$ and $F \circ G$ are naturally isomorphic to the identity functor $\text{id}_{\mathcal{C}}$ by a natural transformation η where η_1 is an isomorphism and

$$\begin{array}{ccc}
(G \circ F)(X) \otimes (G \circ F)(Y) & \xrightarrow{U_{X,Y}^{G \circ F}} & (G \circ F)(X \otimes Y) \\
\eta_X \otimes \eta_Y \downarrow & & \downarrow \eta_{X \otimes Y} \\
\text{id}(X \otimes Y) & \xrightarrow{U_{X,Y}^{\text{id}}} & \text{id}(X) \otimes \text{id}(Y)
\end{array}$$

and similarly for $F \circ G$.

The isomorphism classes of braided tensor autoequivalences form a group under composition, denoted by $\text{Aut}_{\otimes}^{br}(\mathcal{C})$. The braided tensor autoequivalences themselves can

also be organized into a category $\underline{\text{Aut}}_{\otimes}^{br}(\mathcal{C})$, with objects now honest braided tensor autoequivalences and morphisms natural isomorphisms between tensor autoequivalences. Composition of autoequivalences gives $\underline{\text{Aut}}_{\otimes}^{br}(\mathcal{C})$ the structure of a monoidal category, which is sometimes called the category of topological symmetries of \mathcal{C} .

For our purposes it will be helpful to think about braided tensor autoequivalences in terms of how they transform the algebraic data of an MTC interpreted as an anyon model.

Remark 3.1. *Let F be a braided tensor autoequivalence of \mathcal{C} .*

- The vacuum is preserved: $F(1) \cong 1$.
- Quantum dimensions of anyons are preserved: $d_{F(a)} = d_a$.
- F restricts to a permutation on the set of anyon types $\text{Irr}(\mathcal{C})$.
- F induces conjugates the modular data by a permutation matrix.
- R - and F -symbols are not necessarily preserved i.e. $R_c^{ab} \neq R_{F(c)}^{F(a)F(b)}$ in general.

For a full understanding of symmetry in topological order, braided tensor autoequivalence may be too strict a notion, and one wants to relax the requirement that a symmetry be a monoidal functor [27]. We comment briefly about more general symmetries towards the end of the chapter.

3.1.2 Skeletal autoequivalences and gauge symmetry

Skeletalizing the definition of a braided tensor autoequivalence of an UMTC results in U -symbols and η -symbols, which are the matrix entries of the tensorators and compositors of F . Essentially they are a collection of unitary matrices that keep track of how objects

and morphisms are transformed by the action of F . We will encounter U -symbols and η -symbols in the next chapter when we discuss the algebraic theory of SET order.

Gauge versus topological symmetry of anyon models

For those autoequivalences that act trivially on isomorphism classes of objects, their skeletonization is given by a collection of unitary matrices that keep track of how the trivalent fusion spaces $\text{Hom}(c, a \otimes b)$ transform. This kind of symmetry is called *gauge symmetry* in the physics literature to distinguish from the weaker *topological symmetry*, which also allows for label permutations. Two different anyon models are said to be *gauge equivalent* if they can be related by a gauge symmetry, and any quantity which is left invariant by gauge transformations is called *gauge invariant*.

Trivalent morphisms transform as

$$|\widetilde{a, b; c, \mu}\rangle = \sum_{\mu'} [\Gamma_c^{ab}]_{\mu\mu'} |a, b; c, \mu'\rangle \quad (3.1)$$

How trivalent vertices transform under gauge symmetry determines how any ribbon fusion graph transforms.

In particular, the F - and R -symbols are transformed by

$$[\tilde{F}_d^{abc}]_{(e,\alpha,\beta);(f,\mu,\nu)} = \sum_{\alpha',\beta',\mu',\nu'} [\Gamma_e^{ab}]_{\alpha\alpha'} [\Gamma_d^{ec}]_{\beta,\beta'} [F_d^{abc}]_{(e',\alpha',\beta');(f',\mu',\nu')} [(\Gamma_f^{bc})^{-1}]_{\mu'\mu} [(\Gamma_d^{af})^{-1}]_{\nu'\nu} \quad (3.2)$$

$$[\tilde{R}_c^{ab}]_{\mu\nu} = \sum_{\mu',\nu'} [\Gamma_c^{ba}]_{\mu\mu'} [R_c^{ab}]_{\mu'\nu'} [(\Gamma_c^{ab})^{-1}]_{\nu'\nu} \quad (3.3)$$

In other words, with respect to a fixed basis of anyons, two sets of algebraic data

$\{N_c^{ab}, [R_c^{ab}], [F_d^{abc}]\}$ $\{N_c^{ab}, [\tilde{R}_c^{ab}], [\tilde{F}_d^{abc}]\}$ describe the same anyon model if they are related by a gauge equivalence.

This ambiguity in the algebraic data for a UMTC, or *gauge freedom* is one reason why finding concrete solutions to the pentagons and hexagons is computationally challenging. In practice the notion of a gauge transformation allows one to determine when two different numerical descriptions of UMTCs (and also more general fusion categories like UGxBFCs) are the same, but applying it successfully can take some work, see our discussion about skeletonizations of bilayer Fibonacci UMTC and its unitary S_2 -extension in Example 5.3 and Chapter 6.

Skeletonizations are an invaluable tool for working with topological order, and finding solutions to the consistency equations that define UMTCs and UGxBFCs by computer contribute much to our understanding.

However, solutions produced in this way will lack structure in the sense that they do not readily provide a way to reconstruct the families of natural isomorphisms that they encode. And while solutions do allow for concrete physical predictions and applications, the full algebraic theory of the topological order/symmetry-enriched topological order provides a deeper understanding of the physical theory. For this reason we take an abstract but constructive approach to symmetry-enriched topological order, which we discuss in Chapter 6.

3.1.3 Categorical group symmetry and global symmetry in TPM

Now let G be a finite group, and notice that a group homomorphism

$$\rho : G \longrightarrow \text{Aut}_{\otimes}^{br}(\mathcal{C})$$

is not enough to provide an action of G on \mathcal{C} by braided tensor autoequivalences, since the elements of $\text{Aut}_{\otimes}^{br}(\mathcal{C})$ are isomorphism classes of such autoequivalences.

In order to have a meaningful notion of group symmetry, we need to access the additional category level available with $\underline{\text{Aut}}_{\otimes}^{br}(\mathcal{C})$ and “categorify” the group homomorphism to produce an action of G by braided tensor autoequivalences.

To do this, one has to promote G to a *categorical group* \underline{G} in the trivial way, namely objects of \underline{G} are identified with elements of G , and morphisms are given by $\text{Hom}(g, g) = \text{id}_G$ and $\text{Hom}(g, h) = \emptyset$ if $g \neq h$. The group multiplication gives the category \underline{G} a monoidal structure.

With a categorical group in hand one looks to promote the homomorphism ρ to a monoidal functor

$$\underline{\rho} : \underline{G} \rightarrow \underline{\text{Aut}}_{\otimes}^{br}(\mathcal{C}).$$

Given G and \mathcal{C} the obstruction to lifting ρ to a monoidal functor $\underline{\rho}$ is given by a cohomology class in $H_{\rho}^3(G, \mathcal{A})$. Provided this obstruction vanishes, the monoidal functor $\underline{\rho}$ is called a *categorical group symmetry*. The data of a monoidal functor $\underline{\rho}$ is equivalent to a G -action on \mathcal{C} , see [38]. We say G acts on \mathcal{C} by categorical symmetries and think of $\underline{\rho}$ as a representation of the group G on the category \mathcal{C} .

3.2 From global symmetries to defects

How does symmetry-enriched topological order emerge from symmetry? How do defects manifest?

Mathematicians and physicists alike will be familiar with the fact that representations of groups on a vector space V and G -modules are equivalent notions: unpacking the

definition of a homomorphism $G \rightarrow GL(V)$ defines an action $G \times V \rightarrow V$, and vice versa.

Defectification [3] is simply a categorification of this equivalence.¹

Promoting the group G to the categorical group \underline{G} , and the vector space V to a UMTC \mathcal{C} , on the one hand we have that the group representation categorifies to a categorical group representation. On the other hand, the notion of a G -module categorifies to a group of *module categories* over \mathcal{C} .

Mathematically, the categorification of the correspondence yields a monoidal functor from \underline{G} to $\underline{\text{Pic}(\mathcal{C})}$ that factors through the equivalence of the categories $\underline{\text{Aut}}_{\otimes}^{br}(\mathcal{C})$ and $\underline{\text{Pic}(\mathcal{C})}$ [39]: the category of braided tensor autoequivalences of an MTC \mathcal{C} is equivalent to another category associated to \mathcal{C} , called the Picard 1-category.

$$\underline{\text{Aut}}_{\otimes}^{br}(\mathcal{C}) \cong \underline{\text{Pic}(\mathcal{C})}.$$

The category $\underline{\text{Pic}(\mathcal{C})}$ has objects given by invertible $(\mathcal{C}, \mathcal{C})$ -bimodule categories and morphisms are isomorphism classes of $(\mathcal{C}, \mathcal{C})$ -bimodule category equivalences, with tensor product given by the relative tensor product of bimodule categories.

Definition 3.2 ($(\mathcal{C}, \mathcal{D})$ -bimodule category). *Let \mathcal{C} and \mathcal{D} be monoidal categories. A category \mathcal{M} is a $(\mathcal{C}, \mathcal{D})$ bimodule category if there are families of natural isomorphisms*

$$l_{X,Y,M} : (X \otimes Y) \triangleright M \rightarrow X \triangleright (Y \triangleright M)$$

$$r_{M,W,Z} : (M \triangleleft W) \triangleleft Z \rightarrow M \triangleleft (W \otimes Z)$$

$$m_{X,M,Z} : (X \triangleright M) \triangleleft Z \rightarrow X \triangleright (M \triangleleft Z)$$

¹In fact we have already seen a form of categorification of this correspondence in the analogy between UMTCs and “quantum” finite groups. In analogy with $\text{Rep}(G)$, the simple objects (c.f. irreducible representations of G) of a UMTC are *quasiparticles*.

such that the following diagrams commute for all $X, Y \in \text{Obj}(\mathcal{C})$, $W, Z \in \text{Obj}(\mathcal{D})$, and $M \in \text{Obj}(\mathcal{M})$.

(i) *Left module pentagon*

$$\begin{array}{ccc}
 & ((X \otimes Y) \otimes Z) \triangleright M & \\
 \alpha_{X,Y,Z \triangleright \text{id}_M}^{\mathcal{C}} \swarrow & & \searrow l_{X \otimes Y, Z, M} \\
 (X \otimes (Y \otimes Z)) \triangleright M & & (X \otimes Y) \triangleright (Z \triangleright M) \\
 l_{X, Y \otimes Z, M} \downarrow & & \downarrow l_{X, Y, Z \triangleright M} \\
 X \triangleright ((Y \otimes Z) \triangleright M) & \xrightarrow{\text{id}_X \otimes l_{Y, Z, M}} & X \triangleright (Y \triangleright (Z \triangleright M))
 \end{array}$$

(ii) *Right module pentagon*

$$\begin{array}{ccc}
 & ((M \triangleleft X) \triangleleft Y) \triangleleft Z & \\
 r_{M, X, Y \otimes \text{id}_Z} \swarrow & & \searrow r_{M \otimes X, Y, Z} \\
 (M \triangleleft (X \otimes Y)) \triangleleft Z & & (M \triangleleft X) \triangleleft (Y \otimes Z) \\
 r_{M, X \otimes Y, Z} \downarrow & & \downarrow r_{M, X, Y \otimes Z} \\
 M \triangleleft ((X \otimes Y) \otimes Z) & \xrightarrow{\text{id}_M \triangleleft \alpha_{X, Y, Z}^{\mathcal{D}}} & M \triangleleft (X \otimes (Y \otimes Z))
 \end{array}$$

(iii) *Middle module pentagons*

$$\begin{array}{ccc}
 & ((X \triangleright M) \triangleleft Y) \triangleleft Z & \\
 m_{X, M, Y \triangleleft \text{id}_Z} \swarrow & & \searrow r_{X \triangleright M, Y, Z} \\
 (X \triangleright (M \triangleleft Y)) \triangleleft Z & & (X \triangleright M) \triangleleft (Y \otimes Z) \\
 m_{X, M \triangleleft Y, Z} \downarrow & & \downarrow r_{X \triangleright M, Y, Z} \\
 X \triangleright ((M \triangleleft Y) \triangleleft Z) & \xrightarrow{\text{id}_X \triangleright r_{M, Y, Z}} & X \triangleright (M \triangleleft (Y \otimes Z))
 \end{array}$$

and

$$\begin{array}{ccc}
 & ((X \otimes Y) \triangleright M) \triangleleft Z & \\
 l_{X,Y,M} \triangleright \text{id}_Z \swarrow & & \searrow m_{X \otimes Y, M, Z} \\
 (X \triangleright (Y \triangleright M)) \triangleleft Z & & (X \otimes Y) \triangleright (M \triangleleft Z) \\
 m_{X,Y} \triangleright M, Z \downarrow & & \downarrow l_{X,Y,M} \triangleleft Z \\
 X \triangleright ((Y \triangleright M) \triangleleft Z) & \xrightarrow{\text{id}_X \triangleright m_{Y,M,Z}} & X \triangleright (Y \triangleright (M \triangleleft Z))
 \end{array}$$

In the remaining chapters we will only be interested in $(\mathcal{C}, \mathcal{C})$ -bimodule categories, and hereafter abbreviate notation and refer them as \mathcal{C} -bimodule categories unless indicated otherwise.

Let \mathcal{C} be a braided fusion category. Given two \mathcal{C} -module categories \mathcal{M} and \mathcal{N} there is the notion of the relative tensor product category $\mathcal{M} \boxtimes_{\mathcal{C}} \mathcal{N}$, which is again a \mathcal{C} -bimodule category. A precise definition is given in terms of a universal property, for which we refer the reader to [30].

When the $H^4(G, U(1))$ obstruction vanishes, fusion between the g -sectors can be consistently defined and the bimodule categories \mathcal{C}_g together with the original MTC form a new fusion category, called a G -crossed braided extension of \mathcal{C} [39].

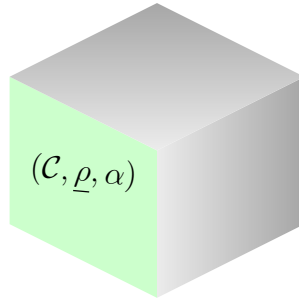
Definition 3.3 (Gaugable categorical symmetry). *A categorical action by a group G is called anomaly-free, or gaugable, if it has vanishing $H^4(G; U(1))$ obstruction.*

These extensions characterize so called anomaly-free symmetry-enriched topological (SET) phases, anomaly-free meaning they can be realized in a purely (2+1)D system [24]. In the special case that the underlying topological order that one starts out with is trivial, i.e. $\mathcal{C} = \text{Vec}$, extensions characterize symmetry-protected topological (SPT)

phases. In reality, not every gaugable group symmetry of a topological order will be physically realizable, but it is still interesting to study from the mathematical point of view.

Gauging anomaly and (2+1)D SET phases at the boundary of higher phases

When G acts on \mathcal{C} categorically but the $H^4(G, U(1))$ obstruction does not vanish, there is a physical bulk-boundary correspondence between (3+1)D SPT phases and (2+1)D SET phases, which suggests that the “weak” fusion categories formed by the invertible \mathcal{C} -bimodule categories with nonvanishing H^4 obstruction α characterizes (2+1)D SET order which can be realized at the boundary of certain (3+1)D SPT phases [24].



This correspondence poses many interesting mathematical questions, but our focus here is on non-anomalous (2+1)D SET phases.

3.2.1 Examples of categorical symmetries

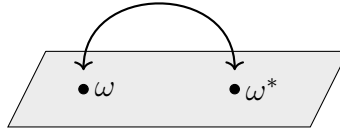
We restrict our attention so *on-site* symmetries, see [3], which in terms of Hamiltonian models roughly means that locality of operators is preserved by the symmetry transformation. Off-site symmetries like translational symmetries of topological phases with lattice models [24] are also studied in physics.

Next we introduce some examples of gaugable symmetries of fusion rings whose

symmetry-enriched topological order and applications to TQC are described later in [Chapter 4](#).

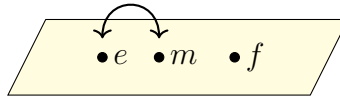
Charge-conjugation duality in $D(\mathbb{Z}_3)$

The UMTC $D(\mathbb{Z}_3)$ has three anyon types, labeled by $1, \omega$, and ω^* , with fusion rules given by the group multiplication in \mathbb{Z}_3 . The category has a categorical \mathbb{Z}_2 symmetry given by interchanging ω and ω^* , with vanishing H^4 obstruction [3].



Charge conjugation is not always a gaugable symmetry, however.

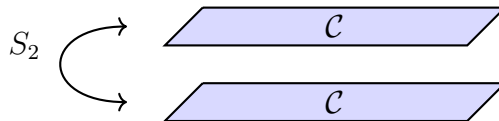
Electromagnetic duality in $D(\mathbb{Z}_2)$



There is a categorical \mathbb{Z}_2 -symmetry exchanging e and m with vanishing H^4 obstruction [3].

Layer exchange symmetry in $\mathcal{C}^{\boxtimes n}$

A simple type of SET order that does not involve symmetries specific to an MTC is the action of the symmetric group S_n on the factors in the Deligne product of UMTCs $\mathcal{C}^{\boxtimes n}$, see [Chapter 5](#). When $n = 2$, this models the layer-exchange symmetry given by two decoupled layers of topological order.



More generally, this permutation symmetry is a unitary, on-site symmetry modeling layer-exchange symmetry of multi-layered topological order. This family of examples and the $n = 2$ case is the subject of [Part III](#).

3.3 Gauging topological order: local symmetry from global symmetry

For each topological order \mathcal{C} with an anomaly-free categorical group symmetry G , there is a corresponding topological order \mathcal{D} which contains $\text{Rep}(G)$ as a symmetric fusion subcategory. The topological order \mathcal{D} is referred to as the gauging or the gauged theory. The two-step procedure to produce the gauged category \mathcal{D} from the category \mathcal{C} models a sort of topological phase transition whereby a global symmetry $\underline{\rho} : \underline{G} \rightarrow \underline{\text{Aut}}_{\otimes}^{br}(\mathcal{C})$ gets turned into a local symmetry $\text{Rep}(G)$.

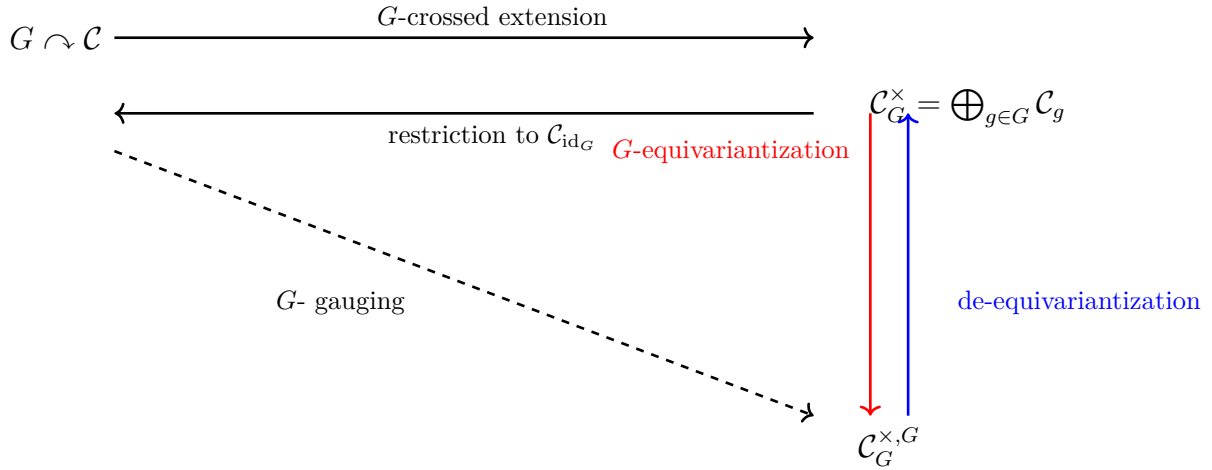


Figure 3.1: Two-step gauging of UMTCs corresponds to G -gauging of a global symmetry a topological phase of matter. First the UMTC is extended by a family of invertible bimodule categories \mathcal{C}_g , which has the structure of a unitary G -crossed braided fusion category (UxGBFC) \mathcal{C}_G^\times , see [Chapter 4](#) for a definition. In particular, there is a G -action on \mathcal{C}_G^\times that can be equivariantized, resulting in the gauged UMTC $\mathcal{C}_G^{\times, G}$.

The inverse procedure, or de-gauging, proceeds by G de-equivariantization followed by restriction to the trivially graded component.

Theorem. *[38, 63, 79] G equivariantization and G de-equivariantization are inverse processes that establish a bijection between equivalence classes of G -crossed braided fusion categories and equivalence classes of braided fusion categories containing $\text{Rep}(G)$ as a symmetric fusion subcategory.*

3.4 Anyon condensation and generalized symmetry breaking

In the last section we saw that gauging and de-gauging of MTCs provides two different ways of producing a GxBFC. Interpreted physically, SET order can be thought of as either coming from gauge coupling a global symmetry of a topological order or as coming from a broken local symmetry of a topological order.

Part III concerns the first case, namely using extension theory of UMTCs to construct the algebraic theory of SET order, which we define shortly in Section 4.1.

To conclude our discussion of symmetry in this chapter, we consider the second case, where the SET order can be realized without the definition of a UGxBFC as a category of modules over certain algebra objects internal to a UMTC.

Definition 3.4 (Algebra objects). *An algebra object A in a tensor category \mathcal{C} consists of the data (A, m, u) , where $A \in \text{Obj}(\mathcal{C})$, $m : A \otimes A \rightarrow A$ and $u : 1 \rightarrow A$ are morphisms in \mathcal{C} satisfying the following commutative diagrams.*

$$\begin{array}{ccc}
 (A \otimes A) \otimes A & \xrightarrow{\alpha_{A,A,A}} & A \otimes (A \otimes A) \\
 \downarrow m \otimes \text{id}_A & & \downarrow \text{id}_A \otimes m \\
 A \otimes A & & A \otimes A \\
 \searrow m & & \swarrow m \\
 & A &
 \end{array}$$

$$\begin{array}{ccc}
 1 \otimes A & \xrightarrow{l_A} & A \\
 u \otimes \text{id}_A \downarrow & & \downarrow \text{id}_A \\
 A \otimes A & \xrightarrow{m} & A
 \end{array}$$

$$\begin{array}{ccc}
A \otimes 1 & \xrightarrow{r_A} & A \\
\text{id}_A \otimes u \downarrow & & \downarrow \text{id}_A \\
A \otimes A & \xrightarrow{m} & A
\end{array}$$

Definition 3.5 (Modules over algebra objects). A left module over an algebra object (A, m, u) in a tensor category \mathcal{C} is a pair (M, λ) consisting of an object $M \in \text{Obj}(\mathcal{C})$ and a morphism $\lambda : A \otimes M \rightarrow M$ such that the diagrams

$$\begin{array}{ccc}
(A \otimes A) \otimes M & \xrightarrow{\alpha_{A,A,M}} & A \otimes (A \otimes M) \\
m \otimes \text{id}_M \downarrow & & \downarrow \lambda \\
A \otimes M & & A \otimes M \\
& \searrow \lambda & \swarrow \lambda \\
& M &
\end{array}$$

and

$$\begin{array}{ccc}
1 \otimes M & \xrightarrow{l_M} & M \\
u \otimes \text{id}_M \downarrow & & \downarrow \text{id}_M \cdot \\
A \otimes M & \xrightarrow{\lambda} & M
\end{array}$$

A right module over an algebra object and bimodules are defined in the obvious way.

The algebras most interesting from the gauging perspective have some additional properties.

Definition 3.6. An algebra object A in a (\mathbb{C} -linear) tensor category \mathcal{C} is connected if $\text{Hom}(1, A) \cong \mathbb{C}$ and separable if the multiplication morphism $m : A \otimes A \rightarrow A$ splits as a A -bimodule morphism.

When \mathcal{C} is braided there is a notion of commutativity of algebra objects.

Definition 3.7. An algebra object (A, m, u) in a braided tensor category \mathcal{C} is commutative if the diagram

$$\begin{array}{ccc}
 A \otimes A & \xrightarrow{c_{A,A}} & A \otimes A \\
 & \searrow m & \swarrow m \\
 & A &
 \end{array}$$

commutes.

Left (or right) modules over an algebra object A form a category $\text{Mod}_{\mathcal{C}}(A)$ with objects given by modules and morphisms by A -module homomorphisms between their underlying objects. The category of modules over A is then a right (respectively left) module category over \mathcal{C} . The following theorem says that this correspondence also goes in the other direction.

Theorem 3.1 ([38]). *Every finite module category over a finite tensor category \mathcal{C} is of the form $\text{Mod}_{\mathcal{C}}(A)$ for some algebra object A .*

Motivated by the fact that $\text{Mod}_{\mathcal{C}}(A)$ is indecomposable when A is connected, inherits the structure of a \mathcal{C} -bimodule category when A is commutative, and is semisimple whenever A is separable, whereupon $\text{Mod}_{\mathcal{C}}(A)$ has the proper structure to characterize domain walls between \mathcal{C} and itself, we have the following definition [27].

Definition 3.8. *An algebra object in a braided tensor category \mathcal{C} is called *condensible* if it is connected as well as commutative and separable (aka *étale*).*

Definition 3.9. *The condensation of a UMTC with respect to a condensible algebra object A is the category of modules over A , $\text{Mod}_{\mathcal{C}}(A)$.*

Then Theorem 3.1 interpreted physically says that every domain wall can be understood as coming from some broken generalized symmetry.

Some use the phrase condensation to refer to the category of *local* modules over \mathcal{A} , i.e. to describe the UMTC that results after the second deconfinement step of de-gauging.

However, the meaning of condensation used here is that we do not throw out our confined objects.

The G -symmetry breaking by de-equivariantization of $\text{Rep}(G)$ is a special case.

3.4.1 $D(S_3)$ defect fusion rules from boson condensation

Example 3.1 ($D(S_3)$ with $C \leftrightarrow F$ symmetry).

$$\begin{array}{ccc} \underbrace{D(S_3)}_{\{A,B,C,D,E,F,G,H\}} & \longrightarrow & D(S_3)_{\mathbb{Z}_2}^X = D(S_3) \oplus \{X_1, X_2, X_3, X_4, X_5, X_6\} \\ & & \uparrow \\ & & \text{Rep}(\mathbb{Z}_2) \subset TL_4 \boxtimes \overline{TL_4} \end{array}$$

- “condense” the boson $(0 \boxtimes \bar{0}) \oplus (4 \boxtimes \bar{4}) \in TL_4 \boxtimes \overline{TL_4}$.

$D(S_3)_{\mathbb{Z}_2}^X$ fusion rules from de-equivariantization

Proposition 3.1. *The fusion rules for the symmetry defects in $D(S_3)$ with $C - F$ exchange symmetry are given by*

\otimes	X_1	X_2	X_3	X_4	X_5	X_6
X_1	$A \oplus G$	$B \oplus G$	D	$D \oplus E$	E	$C \oplus F \oplus H$
X_2		$A \oplus G$	E	$D \oplus E$	D	$C \oplus F \oplus H$
X_3			$A \oplus H$	$C \oplus F \oplus G$	$B \oplus H$	$D \oplus E$
X_4				$A \oplus B \oplus C$ $\oplus F \oplus G \oplus 2H$	$C \oplus F \oplus G$	$2D \oplus 2E$
X_5					$A \oplus H$	$D \oplus E$
X_6						$A \oplus B \oplus C$ $\oplus F \oplus 2G \oplus H$

3.4.2 Example: non-boson condensation in $D(S_3)$

The object $A \oplus C$ in the UMTC $D(S_3)$, see Example 4 in Chapter 1, admits the structure of a condensible algebra object but does not correspond to a local symmetry $\text{Rep}(\mathbb{Z}_2) \subset D(S_3)$, in contrast with the algebra object $A \oplus B$.

Nevertheless one can pass to the category of modules over the algebra object $A \oplus C$, which realize a non-group extension of the UMTC $D(\mathbb{Z}_2)$.

The following result was first known to N. Seiberg, and likely others, who could deduce it in a rigorous way using DW theory [78]. We simply translated the problem into the language of UMTCs and module categories and confirmed his calculation by a computer-assisted calculation, see [27].

Proposition 3.2. *The fusion rules in $\text{Mod}_{\mathcal{C}}(A)$ are given by the following table.*

\otimes	1	e	m	f	X	Y
1	1	e	m	f	X	Y
e	e	1	f	m	Y	X
m	m	f	1	e	Y	X
f	f	m	e	1	X	Y
X	X	Y	Y	X	$1 \oplus f \oplus X$	$e \oplus m \oplus Y$
Y	Y	X	X	Y	$e \oplus m \oplus Y$	$1 \oplus f \oplus X$

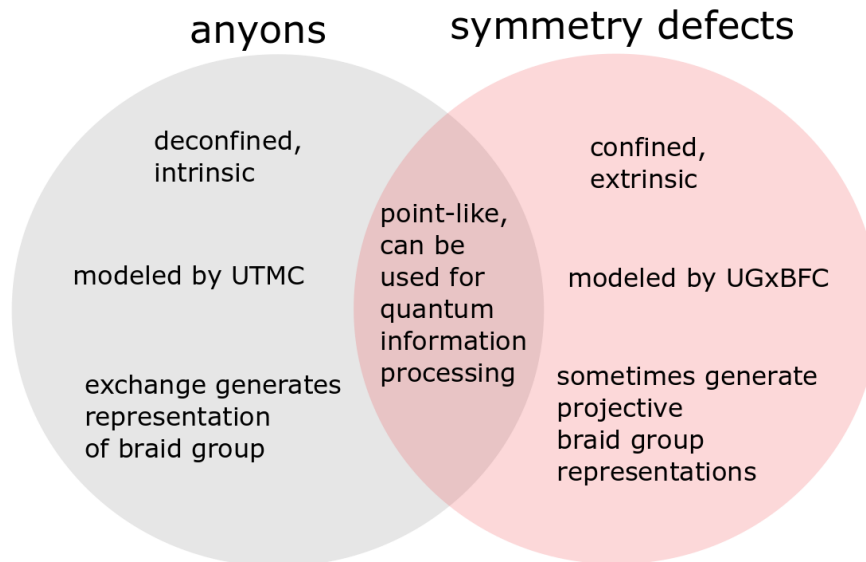
where we have identified the objects which are $A \oplus C$ modules in $D(S_3)$ with simple objects in $D(\mathbb{Z}_2)$ by

$A \oplus C$	1
E	e
D	m
$B \oplus C$	f
$F \oplus G \oplus H$	X
$D \oplus E$	Y

In particular the quantum dimensions are given by $d_1 = d_e = d_m = d_f = 1$, $d_X = d_Y = 2$. It is perhaps worth noting that should this example fit into a coherent theory of generalized symmetry extension and gauging, it says that a DW TQFT with abelian gauge group is related by generalized gauging to one with a non-abelian gauge group.

Chapter 4

(2+1)D Symmetry-enriched topological order and TQC



In [Chapter 3](#) we saw that G -crossed braided fusion categories arise from categorical group actions on MTCs as well as from de-equivariantizations of MTCs with $\text{Rep}(G)$ as a symmetric fusion subcategory. Interpreted physically for UMTCs, this reflects that

SET order can emerge from topological order either in the presence of global symmetry or by anyon condensation.

In the former case where a global symmetry is modeled by a monoidal functor $\rho : G \rightarrow \underline{\text{Aut}}_{\otimes}^{br}(\mathcal{C})$, there is an associated family \mathcal{C}_g of invertible \mathcal{C} -bimodules extending $\mathcal{C}_{\text{id}} = \mathcal{C}$ whose simple objects are interpreted as symmetry defects. For anomaly-free symmetries with a vanishing $H^4(G; U(1))$ obstruction, these bimodule categories admit the structure of a fusion category, specifically a G -crossed braided fusion category (GxBFC), see [Chapter 3](#).

Section [4.1](#) covers the basics of GxBFCs, their skeletonizations, and associated graphical calculus and their interpretation as the algebraic theory of symmetry defects. We use elementary facts about GxBFCs to prove some statements about SET order, for example that enriching abelian topological order by a symmetry which permutes anyons nontrivially necessarily produces nonabelian defects. We introduce the terminology of g -confinement and g -deconfinement of anyons and g -defects, respectively, which we apply in [Part III](#) to construct concrete models for permutation SET order.

In Section [4.1.1](#) we discuss braid group quantum representations that are sometimes afforded by GxBFCs and their application to symmetry-enriched topological quantum computing along with examples of UGxBFCs and their single qubit gates, with several examples to illustrate in Section [4.2](#). As further motivation for the final chapters in Section [4.3](#) we give a categorical argument that supports the claim bilayer symmetry defects and projective measurement give a universal gate set based on Ising anyons [[4](#), [35](#)].

4.1 Algebraic theory of symmetry defects

The following definition is taken directly from [[38](#)], adapted to our notation and terminology.

Definition 4.1 (GxBFC). A G -crossed braided fusion category \mathcal{C}_G^\times is a fusion category equipped with

(i) a grading $\mathcal{C}_G^\times = \bigoplus_{g \in G} \mathcal{C}_g$

(ii) an action $g \mapsto T_g$ of G on \mathcal{C}_G^\times with $T_g(\mathcal{C}_h) \subset \mathcal{C}_{ghg^{-1}}$

(iii) a natural collection of isomorphisms

$$c_{X,Y} : X \otimes Y \longrightarrow T_g(Y) \otimes X \quad (4.1)$$

for all $X \in \text{Obj}(\mathcal{C}_g)$, $g \in G$, and $Y \in \text{Obj}(\mathcal{C}_G^\times)$.

satisfying the following coherences.

(a)

$$\begin{array}{ccc}
 T_g(X \otimes Y) & \xrightarrow{(U_g)_{X,Y}} & T_g(X) \otimes T_g(Y) \\
 \downarrow T_g(c_{X,Y}) & & \downarrow c_{T_g(X), T_g(Y)} \\
 T_g(T_h(Y) \otimes X) & & T_{ghg^{-1}}(T_g(Y)) \otimes T_g(X) \\
 \downarrow (U_g)_{T_h(Y), X} & & \downarrow (\gamma_{ghg^{-1}, g})_Y \otimes \text{id}_{T_g(X)} \\
 T_g(T_h(Y)) \otimes T_g(X) & \xrightarrow{(\gamma_{g,h})_Y \otimes \text{id}_{T_g(X)}} & T_{gh}(Y) \otimes T_g(X)
 \end{array}$$

and compatibility between the G -crossed braiding and the fusion:

(b) G-crossed “hexagon” #1:

$$\begin{array}{ccc}
& (X \otimes Y) \otimes Z & \\
\alpha_{X,Y,Z} \swarrow & & \searrow c_{X,Y} \otimes \text{id}_Z \\
X \otimes (Y \otimes Z) & & (T_g(Y) \otimes X) \otimes Z \\
c_{X,Y} \otimes \text{id}_Z \downarrow & & \downarrow \alpha_{T_g(Y),X,Z} \\
T_g(Y \otimes Z) \otimes X & & T_g(Y) \otimes (X \otimes Z) \\
(U_g)_{Y,Z} \otimes \text{id}_X \downarrow & & \downarrow \text{id}_{T_g(Y)} \otimes c_{X,Z} \\
(T_g(Y) \otimes T_g(Z)) \otimes X & \xrightarrow{\alpha_{T_g(Y),T_g(Z),X}} & T_g(Y) \otimes (T_g(Z) \otimes X)
\end{array}$$

(c) G-crossed “hexagon” #2:

$$\begin{array}{ccc}
& X \otimes (Y \otimes Z) & \\
\alpha_{X,Y,Z} \swarrow & & \searrow \text{id}_X \otimes c_{Y,Z} \\
(X \otimes Y) \otimes Z & & X \otimes (T_h(Z) \otimes Y) \\
c_{X \otimes Y,Z}^{-1} \uparrow & & \downarrow \alpha_{X,T_h(Z),Y}^{-1} \\
T_{gh}(Z) \otimes (X \otimes Y) & & (X \otimes T_h(Z)) \otimes Y \\
(\gamma_{g,h})_Z \otimes \text{id}_{X \otimes Y} \uparrow & & \downarrow c_{X,T_h(Z)} \otimes \text{id}_Y \\
T_g T_h(Z) \otimes (X \otimes Y) & \xrightarrow{\alpha_{T_g T_h(Z),X,Y}^{-1}} & (T_g T_h(Z) \otimes X) \otimes Y
\end{array}$$

The definition of a GxBFC does not require the G -grading to be faithful, so that some sectors \mathcal{C}_g may be empty. As mentioned in [3], we remark that non-faithful G -graded fusion categories are faithfully graded by some normal subgroup $H \triangleleft G$. In particular, the restriction of a non-faithful GxBFC to such a subgroup H , i.e. ignoring all structure and coherences coming from $g \notin H$, will simply be a faithful H xBFC. However, the action by elements $g \notin H$ introduces additional bimodule functors between the h -sectors.

On the other hand, given a faithful H xBFC with a G -action, there may be an $H^4(G; U(1))$ obstruction that precludes the existence of a faithful GxBFC, in which

case the additional bimodule equivalences afforded by the G -action are not simply those for some larger G xBFC.

However to this point both the math and physics literature have focused on faithful extension theory, and in this work too we are interested only in the faithful case. Hereafter we will assume that all G xBFCs are faithful. Briefly, a unitary G xBFC is unitary as a fusion category, with inverses of G -crossed braiding isomorphisms given by conjugation (of morphisms, skeletally matrix components of isomorphisms will be unitary matrices).

4.1.1 Symmetry defects in SET phases and TQC

The algebraic theory of symmetry defects and characterization of SET order in terms of unitary G xBFCs was given in [3]. The mathematical definition of a symmetry defect in a (anomaly-free) (2+1)D SET phase is the following.

Definition 4.2. *A symmetry defect with flux g is a simple object in the g -graded component of a unitary G -crossed braided extension of a UMTC.*

Proposals for physical realizations of specific symmetry defects include lattice dislocations and coupling fqH edge states [3].

Projective representations from G xBFCs and TQC

While symmetry defects are not intrinsic quasiparticle excitations of a topological phase, they can nevertheless be used for quantum information processing. However, their exchange does not in general give braid group representations due to the fact that the G -crossed braiding permutes the defect charge labels, sending simple objects in \mathcal{C}_h to simple objects in the conjugate sector $\mathcal{C}_{ghg^{-1}}$.

If the G -action extends to the \mathcal{C}_g in a way that is trivial on the level of isomorphism classes, i.e. so that braiding defects within a sector \mathcal{C}_g does not change their charge

labels, then the g -defects give rise to braid group representations in the same manner as anyons.

When the isomorphism class of a simple object $X \in \mathcal{C}_g$ is fixed by the autoequivalence T_g , the G -crossed braiding gives an isomorphism $c_{X,X} : X \otimes X \rightarrow X \otimes X$.

$$\begin{array}{ccc}
 X & & X \\
 & \swarrow & \searrow \\
 & & \\
 & \nwarrow & \nearrow \\
 X & & T_{g^{-1}}(X) \cong X
 \end{array}$$

In this case there is a well-defined action of the braid group \mathcal{B}_n on $\text{Hom}(X^{\otimes n}, X^{\otimes n})$, but it is only projective in general due to the fact that the G -action can still be nontrivial on the level of morphisms. For g -defects fixed by the action of g we can consider the projective braid group representations afforded by the associators and braidings in a GxBFC as “ g -defect statistics”. Projective unitary representations can still be interpreted as quantum gates applications to quantum computing since states and operators are really projectively unitary in quantum mechanics.

In analogy with MTCs and due to the shared formalism one can interpret the quantum representation theory of GxBFCs as *symmetry-enriched topological quantum computation*. With a fixed skeletal UGxBFC in hand, see Section 4.1.2, calculating the projective braid group representations is done in the same way as with UMTCs, which we demonstrate in Section 4.3.

Properties of GxBFCs and SET order

When a G -extension of \mathcal{C} exists, its rank can be quickly deduced from the data of the group action on \mathcal{C} .

Lemma 4.1 (Rank of g -sectors [10]). *The rank of the g -graded component of a $GxBFC$ is the number of isomorphism classes of simple objects fixed by the action of g ,*

$$\text{Rank}(\mathcal{C}_g) = |\{a \in \text{Irr}(\mathcal{C}) \mid T_g(a) \cong a\}| \quad (4.2)$$

Lemma 4.2 (Rank of G -extensions). *The rank of a G -extension satisfies the formula*

$$\text{Rank}(\mathcal{C}_G^\times) = |G| |\text{Irr}(\mathcal{C})/G|.$$

where $|\text{Irr}(\mathcal{C})/G|$ is the number of orbits of the anyon types under the action of G .

This is an immediate consequence of Lemma 4.1 Burnside's Lemma applied to $\text{Irr}(\mathcal{C})$ under the action of G .

Lemma 4.3 (Dimension of g -sectors [3]). *Let \mathcal{C} be a UMTC and $\mathcal{C}_G^\times = \bigoplus_{g \in G} \mathcal{C}_g$ a unitary faithful G -crossed braided extension of \mathcal{C} . Then*

$$\mathcal{D}_g^2 = \mathcal{D}_{\text{id}}^2 \quad (4.3)$$

i.e. the global quantum dimension of a g -sector \mathcal{C}_g is equal to that of the trivial sector.

The examples in Section 4.2 and the remaining chapters will exhibit several features of SET order which can be established algebraically.

1. Abelian phases have non-abelian symmetry defects whenever a symmetry permutes topological charge labels.
2. Quantum systems of defects evolving under exchange have the potential to realize the same quantum operations as a quantum systems of anyons under exchange.

3. Symmetry defects can simulate topological order on high-genus surfaces.

Statement 1 for example is elementary from the GxBFC theory.

Proposition 4.1 (Criterion for nonabelian SET order from abelian order). *Let \mathcal{C} be a pointed UMTC with a categorical global symmetry $\underline{\rho} : \underline{G} \rightarrow \underline{\text{Aut}}_{\otimes}^{\text{br}}(\mathcal{C})$ and vanishing $H^4(G, U(1))$ obstruction.*

If the action of G is nontrivial on isomorphisms classes of objects, then there exists a simple object X with $d_X > 1$ in any G -crossed braided extension of \mathcal{C} .

Proof. Since the obstruction vanishes there exists a UGxBFC $\mathcal{C}_G^\times = \bigoplus_{g \in G} \mathcal{C}_g$, with $\mathcal{C}_{\text{id}} = \mathcal{C}$ [3, 39]. Since the action of G is nontrivial on $\text{Irr}(\mathcal{C})$, there exists some $g \in G$ and a simple object $a \in \text{Obj}(\mathcal{C})$ with $T_g(a) \not\cong a$.

By Lemma 4.1 this implies $\text{Rank}(\mathcal{C}_g) < \text{Rank}(\mathcal{C})$, but by Lemma 4.3 we also have $\mathcal{D}_{\mathcal{C}_g}^2 = \mathcal{D}_{\mathcal{C}}^2$. Put $m = \text{Rank}(\mathcal{C}_g)$ and $n = \text{Rank}(\mathcal{C})$. Then

$$\sum_{1 \leq i \leq m} d_{X_i}^2 = \sum_{a \in \text{Irr}(\mathcal{C})} d_a^2 = \sum_{1 \leq i \leq n} 1^2 \quad (4.4)$$

where the last step used that \mathcal{C} is pointed. Since $m < n$ and $d_{X_i} \geq 1$ for all $X_i \in \mathcal{C}_g$ by unitarity, there must exist at least one i with $d_{X_i} > 1$. □

While defects can generate nonabelian topological order from abelian topological order, and the example in the Section 4.3 demonstrates that defects and measurement can be used to generate universal gate sets from non-universal topological order, we caution against thinking of them as inherently providing more computational power.

However, the availability of defects may permit more efficient protocols for realizing certain gates than braiding or measurement alone, and they can simulate other topological orders (see Section 4.2.1) potentially on space manifolds with nontrivial topology (see the introduction to Part 3).

We conjecture that accessing topology or symmetry defects without measurement or ancillae will not be universal if braiding fails to be.

Conjecture 1. *If the simple objects of an MTC \mathcal{C} have finite braid group representations then*

- *the representations of the mapping class groups afforded by \mathcal{C} are also finite image, and*
- *when they exist, the projective braid and mapping class group representations associated to simple objects of any G -crossed braided extension \mathcal{C}_G^\times are finite image.*

Nevertheless they are very interesting to us and as with modular tensor categories, we will want to be able to freely pass between the categorical definition of a G -crossed braided fusion category, the algebraic data defining a skeletonization, and a graphical calculus.

4.1.2 Skeletal G -crossed braided extensions of MTCs

Recall that the skeletonization of an MTC \mathcal{C} is given by N -matrices, R -matrices, and F -matrices with respect to an ordered basis of anyon types \mathcal{L} .

$$\{N_c^{ab}, [R_c^{ab}]_{\mu\nu}, [F_d^{abc}]_{(n,\alpha,\beta);(m,\mu,\nu)}\}$$

satisfying certain equations.

A skeletal G -crossed braided extension \mathcal{C}_G^\times of \mathcal{C} can be represented by a set of complex numbers

$$\{N_Z^{X,Y}, [R_Z^{XY}]_{\mu\nu}, [F_W^{XYZ}]_{(I,\alpha,\beta);(J,\mu,\nu)}, [U_g(X,Y;Z)], [\eta_X(g,h)]\}$$

satisfying the pentagon equations and the matrix equations that express the axioms of a G -crossed braided fusion category.

Here we use capital Roman letters to emphasize that the simple objects now include defects $X, Y, Z, W \in \text{Irr}(\mathcal{C}) \cup_g \text{Irr}(\mathcal{C}_g)$, and continue to use Greek letters for indexing fusion multiplicity, with the exception of η . The R -symbols are now matrix entries of G -crossed braiding isomorphisms, which recall are not actual braiding isomorphisms even though we use the same notation. The new U - and η -symbols are the matrix entries of the tensorators and compositors of the action respectively, and give a skeletalization of the G -action on \mathcal{C}_G^\times .

In our examples we fix a skeletonization $\{N, R, F\}$ of \mathcal{C} and work with skeletal extensions $\{N, R, F, U, \eta\}$ of \mathcal{C}_G^\times whose restriction to the trivial sector $\mathcal{C}_{\text{id}} = \mathcal{C}$ recovers is equal to $\{N, R, F\}$, in which case it is safe to think of $\{N, R, F, U, \eta\}$ as an enlargement of the skeletal UMTC data. Of course in general given a skeletonization of \mathcal{C} and a skeletonization of \mathcal{C}_G^\times - as can happen in practice when obtaining G -crossed data from de-equivariantization and trying to identify the underlying anyon model - the restriction of the G -crossed skeletal data to $X, Y, Z, W \in \text{Irr}(\mathcal{C})$ gives a skeletonization of \mathcal{C} that is equivalent by a gauge transformation but not necessarily equal to the original data for \mathcal{C} .

Notation for symmetry defects

We will use the notation $X^g \in \text{Irr}(\mathcal{C}_g)$ for symmetry defect types, which regrettably departs from the notation $x_g \in \text{Irr}(\mathcal{C}_g)$ established in [3], and write $h \cdot X^g$ instead of ${}^h x_g$

to indicate the action on defects.

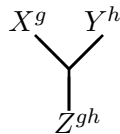
4.1.3 The graphical calculus for G -crossed braided fusion categories

Before we can apply UGxBFCs for TQC in Sections 4.2 and 4.3 we need to introduce the graphical calculus associated to their skeletonizations. The graphical calculus extends that of MTCs to include defect labels, with important differences at trivalent vertices and crossings.

As with anyons, the consistency equations that ensure the various categorical structures are compatible with one another are encoded in the topological properties of the diagrams. Here we point out only the parts of the G -crossed graphical calculus that differ from the usual one for MTCs.

Diagrams are still read from bottom to top and when unitary can be interpreted as quantum mechanical processes between anyons and symmetry defects. For simplicity, in what follows we use multiplicity-free notation and suppress the vertex labels.

Trivalent vertices encode admissible splitting/fusion processes between anyons and defects, implicitly encoding the N -matrix entries $N_{Z^{gh}}^{X^g Y^h}$.



The F -symbols have the same diagrammatic definition as for anyons, except now the topological charges carry group element labels.

$$\begin{array}{c} X^g \quad Y^h \quad Z^k \\ \diagdown \quad \diagup \\ J^{gh} \\ | \\ W^{ghk} \end{array} = \sum_{I^{hk}} \left[F_{W^{ghk}}^{X^g Y^h Z^k} \right]_{I^{hk}, J^{gh}} \begin{array}{c} X^g \quad Y^h \quad Z^k \\ \diagdown \quad \diagup \\ I^{hk} \\ | \\ W^{ghk} \end{array}$$

As we saw above, the algebraic data of a G xBFC differs in three main ways: the R -symbols are extended to become the matrix entries of a G -braiding, and new symbols U and η arise.

The G -crossed R -symbols are written in the same way as in a UMTC, although they are no longer the matrix entries of a braiding isomorphism $c_{X,Y} : X \otimes Y \rightarrow Y \otimes X$ but a G -crossed braiding, $c_{X,Y} : X \otimes Y \rightarrow g \cdot Y \otimes X$. As in Chapter 1 we follow the standard conventions for skeletalizing the braiding.

$$\begin{array}{c} X^g \quad Y^h \\ \diagdown \quad \diagup \\ Y^h \quad h^{-1} \cdot X^g \end{array} = \sum_{Z^{gh}} \sqrt{\frac{dz}{d_X d_Y}} R_{Z^{gh}}^{X^g Y^h} \begin{array}{c} X^g \quad Y^h \\ \diagdown \quad \diagup \\ Z^{gh} \\ | \\ Y^h \quad X^g \end{array} \quad (4.5)$$

Crossings of defect lines are resolved in the same manner as for anyons, except now the R -symbols are G -crossed.

$$\begin{array}{c} X^g \quad Y^h \\ \diagdown \quad \diagup \\ Z^{gh} \end{array} = R_{Z^{gh}}^{X^g Y^h} \begin{array}{c} X^g \quad Y^h \\ \diagdown \quad \diagup \\ Z^{gh} \end{array}$$

The picture is similar for a left-handed crossing, but with a factor of R^{-1} . The G -crossed R -symbols satisfy G -crossed hexagon equations, see [3].

While in the graphical calculus for anyons strands can be freely moved over and under vertices, U - and η - symbols are picked up when a strand labeled by a symmetry defect

passes over or under a trivalent vertex, respectively. Sliding a defect over a splitting vertex results in a U -symbol as follows.

The picture is similar for fusion vertices, see [3]. Defect lines can be slid under splitting vertices at the cost of an η -symbol as follows.

As with the U -symbols there is a similar picture for sliding defect lines under fusion vertices. Notice that the orientation of the g -defect with respect to the the trivalent vertex results in different arguments to the U - and η -symbols.

The G -crossed consistency equations enforcing compatibility of all of these structures are quite complicated, and the full set of such equations is listed in [3], although there is some redundancy. In particular, many of the diagrams involving compatibility of the U - and η - symbols can be derived from the G -crossed pentagons and hexagons, and hence the consistency equations do not encode additional information [13].

Abstract and skeletal $UGxBFC$ theory gives an algebraic framework for studying certain defects in a materials in topological phases and their interactions with anyonic excitations. Next we investigate some examples of symmetry defects and their applications to TQC using $GxBFC$ theory.

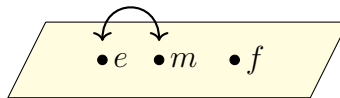
4.2 Examples of defects in SET order and applications to TQC

4.2.1 Non-abelian defects from abelian topological order

By Proposition 4.1, whenever anyon types are nontrivially permuted by a G -action there are non-abelian defects.

$D(\mathbb{Z}_2)$ toric code defect qubit

Recall the algebraic data for $D(\mathbb{Z}_2)$ from Example 1.6 and the anomaly-free \mathbb{Z}_2 -action exchanging e and m from 3.2.1.



gates. The Ising qubit is a Jones representation of \mathcal{B}_4 , whose projective image is finite and given by $\mathbb{Z}_2^2 \rtimes S_3$ [56].

$D(\mathbb{Z}_3)$ charge conjugation defect qubit

The UMTC \mathbb{Z}_3 has three anyon types, labeled by $1, \omega$, and ω^* , with fusion rules given by the group multiplication in \mathbb{Z}_3 . The category has a \mathbb{Z}_2 symmetry given by interchanging ω and ω^* , which lifts to a categorical \mathbb{Z}_2 -action and hence admits a \mathbb{Z}_2 -crossed extension which we write

$$(\mathbb{Z}_3)_{\mathbb{Z}_2}^\times = \{1, \omega, \omega^*\} \oplus \{X_1\}.$$

As a fusion category, $(\mathbb{Z}_3)_{\mathbb{Z}_2}^\times$ is a Tambara-Yamagami (TY) category, whose algebraic data is known and relatively easy to describe [80]. Briefly, given a finite group A a TY category has simple objects $A \sqcup \{m\}$ and fusion rules

$$a \otimes b = ab, \quad a \otimes m = m, \quad \text{and} \quad m \otimes m = \bigoplus_{a \in A} a.$$

A choice of F -symbols for TY categories with this fusion are determined by a choice of nondegenerate symmetric bicharacter $\chi : A \times A \rightarrow \mathbb{C}^\times$ and a choice of square root of $|A|$. One can check that in order to correspond to a unitary \mathbb{Z}_2 -crossed BFC the F -symbols are determined by a choice of a primitive cube root of unity. For calculations in the next section we choose χ to take the value $\xi = e^{2\pi i/3}$ on the non-identity diagonal elements of $\mathbb{Z}_3 \times \mathbb{Z}_3$ and $\bar{\xi}$ on the off-diagonal elements.

and

$$\rho(\sigma_2) \sim \frac{1}{3\sqrt{3}} \begin{pmatrix} 1 & \frac{1}{2}(-1 + i\sqrt{3}) & \frac{1}{2}(-1 + i\sqrt{3}) \\ \frac{1}{2}(-1 + i\sqrt{3}) & 1 & \frac{1}{2}(-1 + i\sqrt{3}) \\ \frac{1}{2}(-1 + i\sqrt{3}) & \frac{1}{2}(-1 + i\sqrt{3}) & 1 \end{pmatrix}.$$

We remark that these matrices form a subset of the matrices generating the Jones representation of \mathcal{B}_4 coming from anyon 1 and total charge 2 in the \mathbb{Z}_2 -gauged theory $\mathbb{Z}_3^{\mathbb{Z}_2} = TL_4$, the Temperley-Lieb-Jones algebra at $A = ie^{-\pi i/12}$. In particular the image of the projective representation is finite [56].

Bilayer defect qudits

The *genons* of [4] in bilayer TPM can be identified with identified as certain defects in S_n -extensions of UMTCs $\mathcal{C}^{\boxtimes n}$ in [3]. The authors of [4] argued that bilayer genons and projective measurement in bilayer Ising theories could be used to generate a universal gate set

$$G_1 = \begin{pmatrix} 1 & 0 \\ 0 & e^{\pi i/4} \end{pmatrix} \quad G_2 = \begin{pmatrix} 1 & 0 & 0 & 0 \\ 0 & 1 & 0 & 0 \\ 0 & 0 & 1 & 0 \\ 0 & 0 & 0 & -1 \end{pmatrix} \quad G_3 = \frac{1}{\sqrt{2}} \begin{pmatrix} 1 & 0 & 0 & -i \\ 0 & 1 & -i & 0 \\ 0 & -i & 1 & 0 \\ -i & 0 & 0 & 1 \end{pmatrix}. \quad (4.6)$$

The gate G_1 is the T -gate, which we recall from Section 2.4 is not in the image of the Ising qubit representation.

Their G_2 is the CNOT gate up to a change of basis, which they give a defect/measurement protocol for but can in fact be realized in the 6 Ising anyon 2-qubit encoding [47], and they claim the G_3 gate can also be realized by monolayer Ising anyons.

Given that G_2 and G_3 can be realized by anyon exchange, the T -gate is really the fundamental contribution of the defects and measurement protocol.

In [35] we formulated their protocol for the T -gate in the language of UxGFCs and quantum representations and were able to confirm their calculation modulo some assumptions about the algebraic data for $(\text{Ising} \boxtimes \text{Ising})_{S_2}^\times$, namely

Conjecture 2 ([35]). *There exists a set of solutions to the \mathbb{Z}_2 -crossed consistency equations associated to $\text{Ising} \boxtimes \text{Ising}$ such that*

$$R_{aa}^{XX} = \theta_a \quad \text{for } a \in \text{Ising}$$

and

$$[F_X^{XXX}] = S_{\text{Ising}} = \frac{1}{2} \begin{pmatrix} 1 & \sqrt{2} & 1 \\ \sqrt{2} & 0 & -\sqrt{2} \\ 1 & -\sqrt{2} & 1 \end{pmatrix}.$$

In Chapter 6 we give an explicit construction of these pieces of data from first principles, and in [33] we prove the conjecture. Results of this nature demonstrate how to leverage category theory for theoretical condensed matter physics and provide further proof-of-concept for quantum experiments involving defects in (2+1)D TPM.

4.3 Example: T -gate from bilayer Ising defects and measurement

The authors of [4] gave a protocol involving genons and projective measurement in bilayer Ising theories to realize a T -gate.

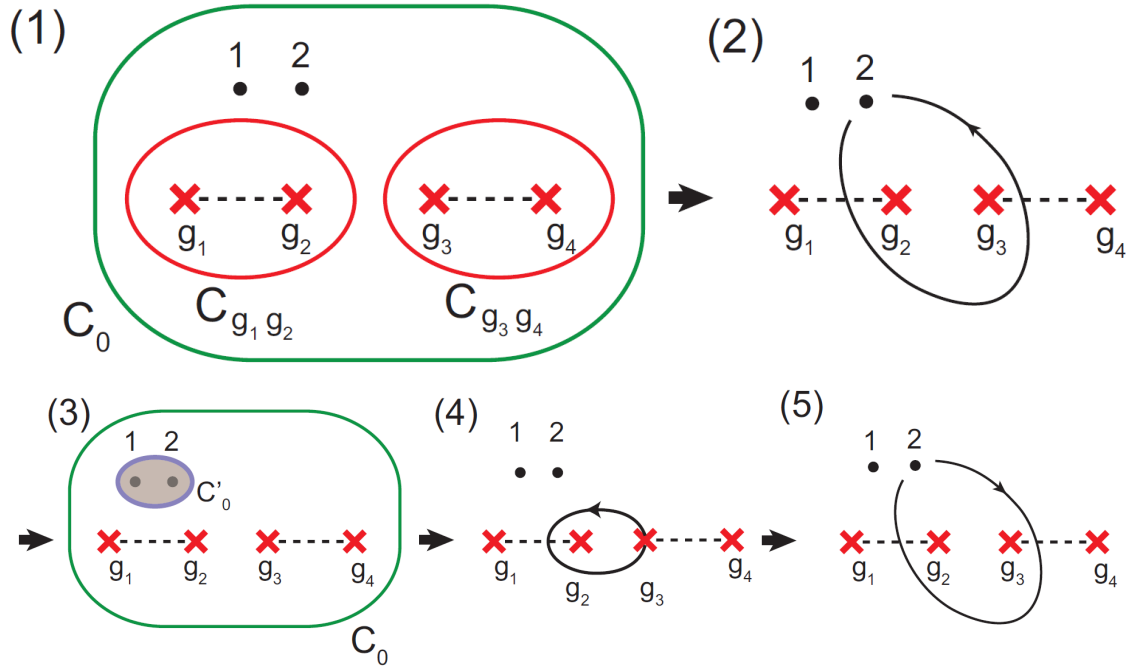


Figure 4.1: Figures from [4] illustrating the braiding and measurement protocol for realization a T -gate using defects in bilayer Ising topological order.

4.3.1 Defect qudit and T -protocol encoding

The protocol to enact the logical T -gate is given by the following sequence of steps.

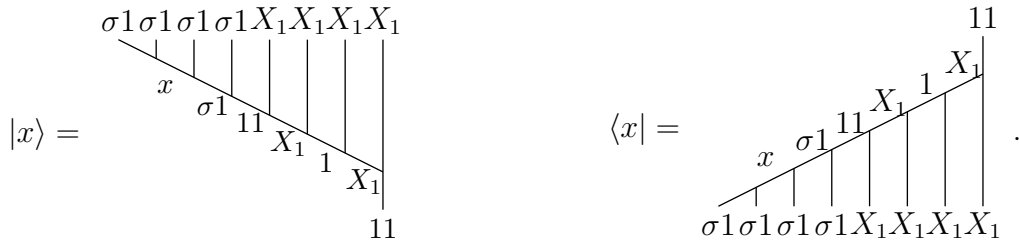
1. Create two pairs of monolayer Ising anyons σ_1 and two pairs of symmetry defects X_1 from the vacuum, using projective measurement if necessary to fix the total charge of each pair of defects to be trivial.
2. Select one of the monolayer Ising anyons from a pair and braid it around the middle two genons in the counterclockwise direction.
3. Fix the pair of Ising anyons from (3) to have trivial total charge with a projective measurement.

4. Perform a full exchange of the middle two defects.
5. Braid the anyon from (3) with the middle two defects in the clockwise direction.

Readout of the computation then proceeds by pair annihilation and projective measurement.

Steps (2-5) determine a morphism in $\text{Hom}(\sigma^{\otimes 4} \otimes X_1^{\otimes 4}, \sigma^{\otimes 4} \otimes X_1^{\otimes 4})$. In the graphical calculus the diagram for this morphism takes the form depicted in Figure 4.3.1.

In terms of the graphical calculus, the qubit is given by the \mathbb{C} -span of the (normalized) fusion tree basis $|x\rangle$, which has the dual basis $\langle x|$.



In terms of diagrams the matrix entries $\langle y|T|x\rangle$ are given by stacking and taking a trace. Below we show the general diagram for the matrix entries alongside the shorthand notation that we use in what follows. In particular, we suppress the index on the symmetry defect, writing $X := X_1$, and since all anyons live in a single layer, we write $a := a1$ for a simple object in **Ising**. Moreover, since the total charge of the fusion trees are trivial, we suppress the labeling of the tracial strand.

As was mentioned in Section 4.3.2, the off diagonal matrix elements vanish by a Schur’s Lemma argument, so it remains to calculate $\langle 1|T|1\rangle$ and $\langle \psi|T|\psi\rangle$.

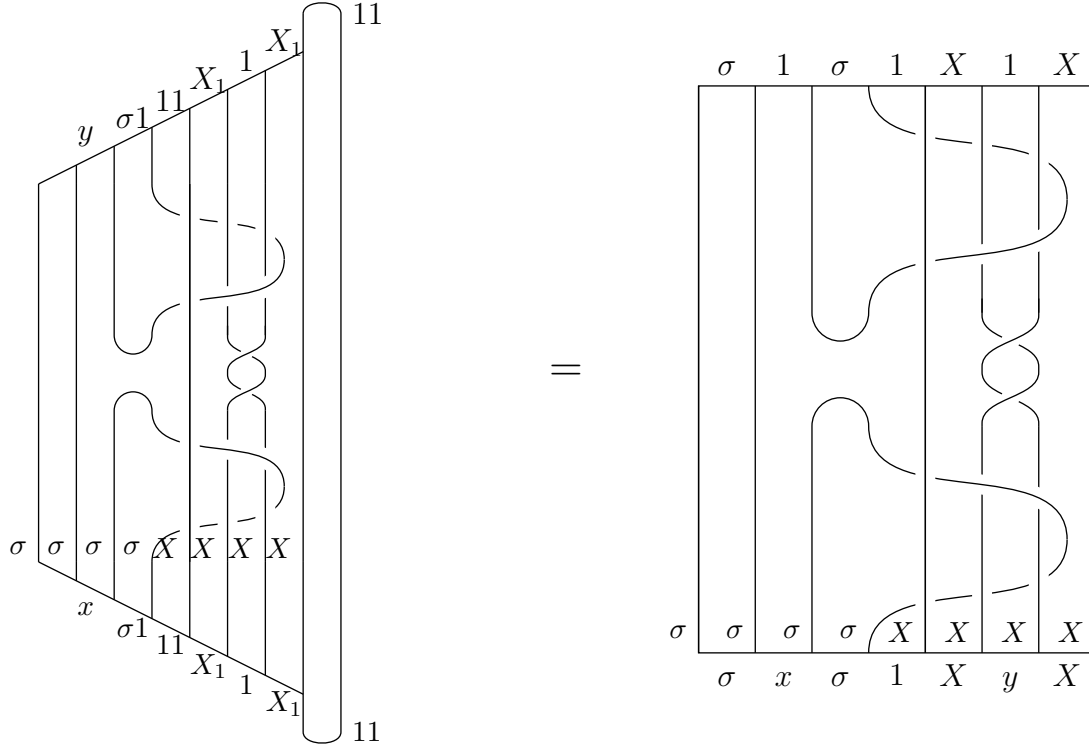


Figure 4.2: On the left is the diagram representing the matrix entries of the protocol. On the right is the shorthand notation we use in the following section.

4.3.2 Calculation of $\langle 1 | T | 1 \rangle$

We break down the calculation of the first matrix entry (up to normalization) into five steps. Below is a formula that shows the contributions from each step, before simplification.

$$\langle 1|T|1\rangle = \underbrace{\frac{1}{d_X} \sum_c \sqrt{d_c} (R_c^{XX})^2}_{\text{Step 1}} \underbrace{\left(\frac{S_{\sigma 1,c}}{S_{11,c}}\right)^2}_{\text{Step 3}} \underbrace{|[F_X^{XXX}]_{c,11}|^2}_{\text{Step 4}} \underbrace{\frac{d_X^2}{d_c} d_{\sigma 1} d_X \sqrt{d_c}}_{\text{Step 5}}$$

The dashed rectangles in each equation indicate the region of the diagram where the graphical calculus is being applied.

Step 1: Unbraid the symmetry defects using equation (1) twice.

$$\begin{array}{c}
 \sigma \ 1 \ \sigma \ 1 \ X \ 1 \ X \\
 \left[\text{Diagram with } \sigma \text{ loop} \right] \\
 \sigma \ \sigma \ \sigma \ \sigma \ \bar{X} \ \bar{X} \ \bar{X} \ \bar{X} \\
 \sigma \ 1 \ \sigma \ 1 \ X \ 1 \ X
 \end{array}
 = \sum_c \sqrt{\frac{d_c}{d_X d_X}} (R_c^{XX})^2
 \begin{array}{c}
 \sigma \ 1 \ \sigma \ 1 \ X \ 1 \ X \\
 \left[\text{Diagram with } c \text{ vertex} \right] \\
 \sigma \ \sigma \ \sigma \ \sigma \ \bar{X} \ \bar{X} \ \bar{X} \ \bar{X} \\
 \sigma \ 1 \ \sigma \ 1 \ X \ 1 \ X
 \end{array}
 \quad (4.7)$$

Note that in this case there is a loop labeled by σ that we can replace with d_σ right away. However, we have left it unsimplified so that the same picture applies for the calculation of $\langle \psi | T | \psi \rangle$.

Step 2: Slide the σ loops under the first defect charge line so that they encircle pairs of defect charge lines using equations (3)-(6). The U - and η -symbols this introduces all cancel, so that the anyons and defects can be moved past each other at no cost.

$$\begin{array}{c}
 \sigma \ 1 \ \sigma \ 1 \ X \ 1 \ X \\
 \left[\text{Diagram with } c \text{ vertex} \right] \\
 \sigma \ \sigma \ \sigma \ \sigma \ \bar{X} \ \bar{X} \ \bar{X} \ \bar{X} \\
 \sigma \ 1 \ \sigma \ 1 \ X \ 1 \ X
 \end{array}
 =
 \begin{array}{c}
 \sigma \ 1 \ X \ 1 \ X \\
 \left[\text{Diagram with } \sigma \text{ loop} \right] \\
 \sigma \ \sigma \ X \ X \ \bar{X} \ \bar{X} \\
 \sigma \ 1 \ X \ 1 \ X
 \end{array}
 \quad (4.8)$$

Step 3: Slide the loops over the trivalent vertices so that they encircle the fusion

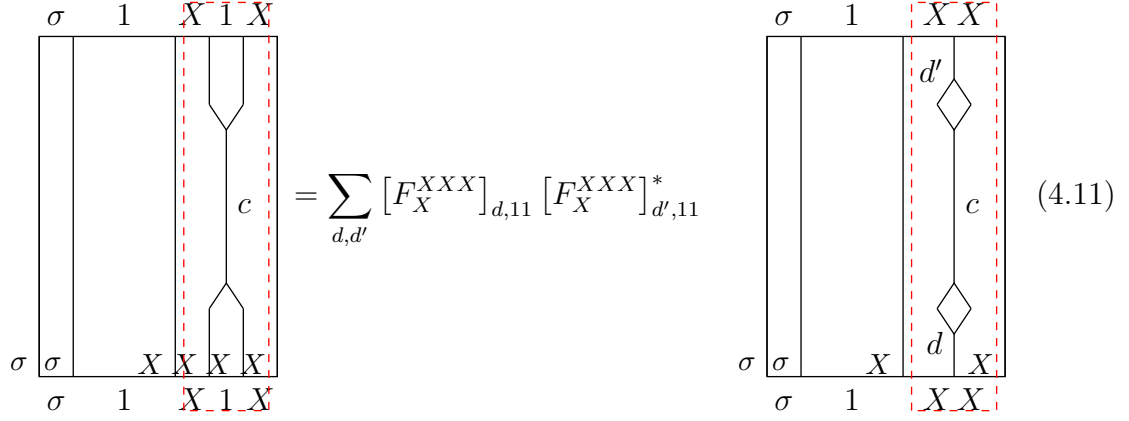
channel labeled by c , flip the tilt of the bottom loop using (6), then use the loop removal relation (7) twice.

In general with loops encircling charge lines in the G -crossed graphical calculus we need to pay careful attention to the relative positions of charge lines, see equations (306) and (307) in [3]. However, in this case the subdiagram involves only anyons, so we can use the graphical calculus of a UMTC and ignore them. Nevertheless, a careful account of the factors using the full G -extended calculus gives the same result: any factors of U - and η - cancel.

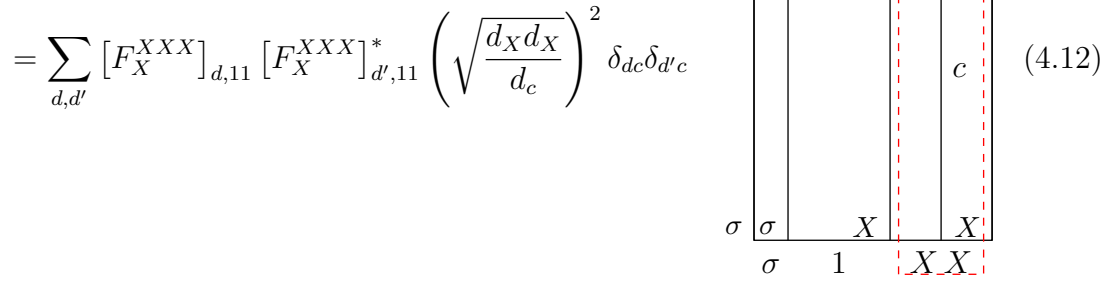
$$(4.9)$$

$$= \left(\frac{S_{\sigma 1, c}}{S_{11, c}} \right)^2 (4.10)$$

Step 4: Perform a sequence of F -moves to change the basis states, then use the bubble-popping relation (9).

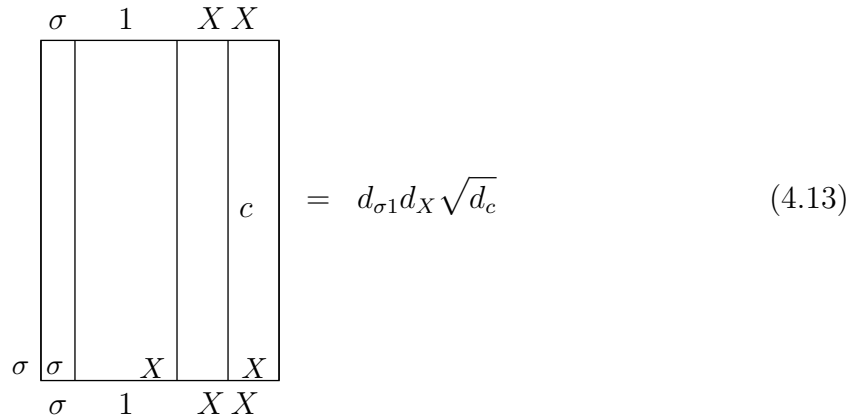


$$\begin{array}{c}
 \sigma \quad 1 \quad X \quad 1 \quad X \\
 \left[\begin{array}{c} \text{Diagram} \end{array} \right] = \sum_{d,d'} [F_X^{XXX}]_{d,11} [F_X^{XXX}]_{d',11}^* \\
 \sigma \quad \sigma \quad X \quad X \quad X \quad X \\
 \sigma \quad 1 \quad X \quad 1 \quad X
 \end{array}
 \quad (4.11)$$



$$\begin{array}{c}
 \sigma \quad 1 \quad X \quad X \\
 \left[\begin{array}{c} \text{Diagram} \end{array} \right] = \sum_{d,d'} [F_X^{XXX}]_{d,11} [F_X^{XXX}]_{d',11}^* \left(\sqrt{\frac{d_X d_X}{d_c}} \right)^2 \delta_{dc} \delta_{d'c} \\
 \sigma \quad \sigma \quad X \quad X \\
 \sigma \quad 1 \quad X \quad X
 \end{array}
 \quad (4.12)$$

Step 5: The diagram that remains contributes a scalar factor that can be calculated using equations (4) and (5) repeatedly until the empty diagram is obtained.



$$\begin{array}{c}
 \sigma \quad 1 \quad X \quad X \\
 \left[\begin{array}{c} \text{Diagram} \end{array} \right] = d_{\sigma 1} d_X \sqrt{d_c} \\
 \sigma \quad \sigma \quad X \quad X \\
 \sigma \quad 1 \quad X \quad X
 \end{array}
 \quad (4.13)$$

Putting these steps together, we arrive at the formula

$$\frac{1}{d_X} \sum_c \sqrt{d_c} (R_c^{XX})^2 \left(\frac{S_{\sigma 1, c}}{S_{11, c}} \right)^2 |[F_X^{XXX}]_{c, 11}|^2 \frac{d_X^2}{d_c} d_{\sigma 1} d_X \sqrt{d_c} \quad (4.14)$$

$$= d_{\sigma 1} d_X^2 \sum_c (R_c^{XX})^2 |[F_X^{XXX}]_{c, 11}|^2 \left(\frac{S_{\sigma 1, c}}{S_{11, c}} \right)^2 \quad (4.15)$$

4.3.3 Calculation of $\langle \psi | T | \psi \rangle$

The first step of resolving the defect braiding is identical to that of the previous subsection for $\langle 1 | T | 1 \rangle$. However, when the fusion channel of the four monolayer Ising anyons $\sigma 1$ is given by $\psi 1$, the loops are not free to slide under the defect line as in Step 2. Instead, we perform an F -move in the middle of the diagram.

$$\begin{array}{c}
 \sigma \quad \psi \quad \sigma \quad 1 \quad X \quad 1 \quad X \\
 \begin{array}{|c|c|c|c|c|c|c|}
 \hline
 \sigma & \sigma & \sigma & \sigma & X & X & X \\
 \hline
 \sigma & \psi & \sigma & 1 & X & 1 & X \\
 \hline
 \end{array}
 \end{array}
 = \sum_d [F_{\sigma 1}^{\sigma 1 \sigma 1}]_{d, 11}
 \begin{array}{c}
 \sigma \quad \psi \quad \sigma \quad 1 \quad X \quad 1 \quad X \\
 \begin{array}{|c|c|c|c|c|c|c|}
 \hline
 \sigma & \sigma & \sigma & \sigma & X & X & X \\
 \hline
 \sigma & \psi & \sigma & 1 & X & 1 & X \\
 \hline
 \end{array}
 \end{array}
 \quad (4.16)$$

When d is the vacuum channel, $d = 11$, we can perform a sequence of sliding moves to resolve all crossings by the same arguments as in the previous subsection.

$$\begin{array}{c}
 \sigma \quad \psi \quad \sigma \quad 1 \quad X \quad 1 \quad X \\
 \left[\text{Diagram 1} \right] = \left[\text{Diagram 2} \right] \\
 \sigma \quad \sigma \quad \sigma \quad \sigma \quad X \quad X \quad X \quad X \\
 \sigma \quad \psi \quad \sigma \quad 1 \quad X \quad 1 \quad X
 \end{array}
 \quad
 \begin{array}{c}
 \sigma \quad \psi \quad X \quad 1 \quad X \\
 \left[\text{Diagram 2} \right] \\
 \sigma \quad \sigma \quad X \quad X \quad X \quad X \\
 \sigma \quad \psi \quad X \quad 1 \quad X
 \end{array}
 \quad (4.17)$$

Now the righthand side can be resolved according as with steps 4 and 5 for $\langle 1|T|1 \rangle$, with the minor difference that the fusion channel of the monolayer Ising anyons is given by $\psi 1$.

However, when $d = \psi 1$ we must use a more involved sequence of moves to resolve the diagram.

(4.18)

(4.19)

(4.20)

Although we have drawn some horizontal lines here, the edges are understood to have the

orientation they inherit from reading the diagram from the bottom up.

What remains can be resolved using a combination of F -moves and bubble-popping relations in a similar manner to the final steps of the calculation for $\langle 1|T|1\rangle$. The contributions from each step in the calculation result in the formula

$$\frac{1}{d_X} \sum_c \sqrt{d_c} (R_c^{XX})^2 \left| [F_X^{XXX}]_{c,11} \right|^2 \left(\sqrt{\frac{d_X d_X}{d_c}} \right)^2 \left([F_{\sigma_1}^{\sigma_1 \sigma_1 \sigma_1}]_{11,11} \left(d_{\sigma_1}^2 \sqrt{d_c} d_X \right) \right) \quad (4.21)$$

$$+ \left(\frac{S_{\psi_1, c}}{S_{11, c}} \right) [F_{\sigma_1}^{\sigma_1 \sigma_1 \sigma_1}]_{\psi_1, 11} [F_{\sigma_1}^{\sigma_1 \sigma_1 \sigma_1}]_{\psi_1, \psi_1} \left(\sqrt{\frac{d_{\sigma_1} d_{\sigma_1}}{d_{\psi_1}}} \right)^2 \left(d_{\sigma_1} \sqrt{d_c} d_X \right) \quad (4.22)$$

$$= d_{\sigma_1} d_{X_1}^2 \sum_c (R_c^{X_1 X_1})^2 \left| [F_{X_1}^{X_1 X_1 X_1}]_{c, 11} \right|^2 \left(1 - \left(\frac{S_{\psi_1, c}}{S_{11, c}} \right) \right) \quad (4.23)$$

These formulas result in the ratio $\frac{\langle \psi|T|\psi\rangle}{\langle 1|T|1\rangle} = e^{\pi i/4}$.

The sequence of moves made here is one of many possible ways to calculate the same quantity, although it has the feature that it does not depend on the U - and η - symbols.

Part III

Permutation extensions of MTCs,
bilayer symmetry defects, and TQC

The remainder of this dissertation is interested in applying modular tensor category theory to understand multi-layer topological order with S_n layer permutation symmetry, in particular the algebraic theory when $n = 2$. This family of SET phases are characterized by S_n -extensions of n -fold Deligne products of MTCs $\mathcal{C}^{\boxtimes n}$.

This fits into a larger program that seeks to understand the interplay between symmetry, topological order, and quantum information. For example, one approach to proving the Property F conjecture (see Chapter 2), which says that braiding anyons with weakly integral quantum dimensions can never give rise to universal quantum computation, involves proving that Property F is preserved by gauging [67]. In other words, there is no such thing as a free lunch: it is expected that if a topological phase doesn't generate universal TQC by braiding, then a topological phase transition (G -gauging) won't change that.

While the extension theory of Etingof, Nikshych, and Ostrik gives a group-cohomological classification of G -crossed braided extensions of MTCs, explicitly constructing the algebraic data of an extension in the form of families of natural isomorphisms satisfying coherences or skeletal solutions to the coherences is still an interesting problem. Furthermore it is necessary to understand the relationship of quantum information with topological phase transitions, by studying how braid and mapping class group representations transform under gauging.

Computing the obstructions to gauging can be a hard problem. For example, a rather simple example of G -extension and G -gauging is the case where S_n acts as a categorical group on the Deligne product of MTCs $\mathcal{C}^{\boxtimes n}$ by permuting indices of objects and morphisms. And while permutation gauging corresponds to the well-established notion of permutation orbifolding of VOAs or conformal nets under the bulk-boundary correspondence between (2+1)D TQFT and (1+1)D CFT, the obstructions to permutation extensions were only recently shown to vanish [46].

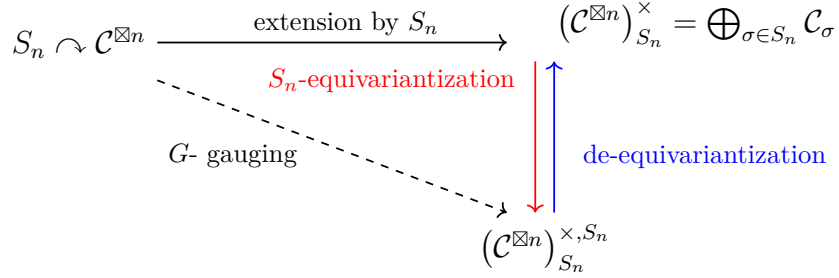


Figure 4.3: Illustration of two-step permutation gauging of modular tensor categories $\mathcal{C}^{\boxtimes n}$.

While simple, the categorical S_n -action and its extension theory exhibits a rich interplay between algebra, topology, and quantum information even in the $n = 2$ case, see Chapter 6. Our goal is to demonstrate how ideas from physics can be helpful for categorification as well as to apply category theory to predict physics in topological phases of matter.

We describe aspects of the algebraic theory of permutation defects and apply it to frame a correspondence between systems of bilayer anyons and defects and monolayer anyons on surfaces with genus first considered in [4].

In Chapter 5 we describe a fusion ring to model defect fusion in permutation enriched topological order which we conjecture generates the $H^2(S_n, \mathcal{A})$ -torsor's worth of possible fusion rings for the S_n -crossed braided extensions of $\mathcal{C}^{\boxtimes n}$. We show that our combinatorial model of permutation defect fusion reproduces known fusion rules in the the $n = 2$ case [3, 4, 37] and use it to derive the fusion rules of the unique rank 24 S_3 -crossed extension of trilayer Fibonacci topological order in Example 5.4.

Borrowing ideas from condensed matter physics, we define g -confinement and g -deconfinement of anyons and g -defects in the language of UMTCs and their G -extensions.

These are the main conceptual and computational tools in [Chapter 6](#) where we discuss how to construct algebraic data for unitary S_2 -crossed braided fusion categories extending bilayer UMTCs $\mathcal{C} \boxtimes \mathcal{C}$ in terms of \mathcal{C} and the S_2 -action. We show that in our algebraic theory of bilayer defects, the quantum gates generated by exchanging certain defects is equivalent to the modular representation coming from its monolayer anyon.

Theorem. *The unitary representation of \mathcal{B}_4 afforded by 4 bare defects $X_1 \in \text{Irr}(\mathcal{C}_{(12)})$ is projectively equivalent to the representation of the mapping class group of the torus $SL(2, \mathbb{Z})$ generated by the S and T matrices of \mathcal{C} . In particular it has finite image.*

The proof follows from the construction of the S_2 -crossed category, the full details of which will appear in [\[33\]](#).

Remark. During the preparation of this manuscript there was a significant amount of work done on the subject of permutation extensions [\[37, 46, 70\]](#) and we learned of the work of [\[5\]](#) that describes algebraic data for S_2 -extensions and discusses S_n -extensions in the language of modular functors and TQFTs. Our account of the overlap of our approach based on [\[3, 4\]](#) with previous work is in progress and we especially welcome help from readers to help attribute previous work.

Chapter 5

Fusion rules for permutation defects

5.1 Introduction

The purpose of this chapter is to describe a model for permutation-enriched topological order from first principles. Per the characterization of SET order by UGxBFCs, the algebraic theory of symmetry defects in multilayer topological order enriched with layer-exchange symmetry - or *permutation defects* - is given by S_n -crossed extensions $(\mathcal{C}^{\boxtimes n})_{S_n}^\times$ of Deligne product UMTCs.

We give a combinatorial description of permutation defects by defining based \mathbb{Z}_+ -rings that form S_n -crossed ring extensions of the fusion ring for $\mathcal{C}^{\boxtimes n}$.

The main idea is the following.

Permutation defect fusion is determined by transposition defect fusion in a way that categorifies how the symmetric group S_n is generated by transpositions.

The details of the categorification of our permutation defect fusion ring to S_n -crossed braided extensions of Deligne product MTCs $\mathcal{C}^{\boxtimes n}$ is discussed in upcoming work [32, 33]. For now it will be enough to work in the de-categorified setting.

5.1.1 Preliminaries

Throughout \mathcal{C} will denote a modular tensor category and $r = \text{rank}(\mathcal{C})$ the number of isomorphism classes of simple objects in \mathcal{C} . We make no further assumptions about \mathcal{C} beyond that it satisfies the axioms of an MTC. Strictly speaking the physical interpretation we give is for unitary MTCs, but the constructions in Part III do not require unitarity and so we state our results for MTCs \mathcal{C} . In this chapter \mathcal{A} denotes the group of abelian anyon types in \mathcal{C} under fusion, see [35], and $\mathcal{A}^{\times n}$ the group of abelian anyon types in $\mathcal{C}^{\boxtimes n}$. As in Chapter 4, underlines of groups or homomorphisms indicate a suitable categorical group or monoidal functor.

We use standard cycle notation for permutation groups, $\sigma \in S_n$. When $n = 2$ we will write $G = S_2$ instead of $G = \mathbb{Z}_2$, so that when we write $(\mathcal{C} \boxtimes \mathcal{C})_{S_2}^{\times}$ the action of \mathbb{Z}_2 by layer-exchange is more clear.

Overview

First we review the categorical S_n -action that permutes the factors in Deligne product MTCs $\mathcal{C}^{\boxtimes n}$ and the multi-layer SET phases that they model, building the dictionary in Table 5.1.1 between the math and physics terminology for reference.

We briefly survey what is known about permutation extensions of MTCs and then apply GxBFC theory to give a model for multi-layer permutation defects.

We define a family of modules \mathcal{C}_g over the fusion ring of a Deligne product MTC \mathcal{C}^{\boxtimes} which form an S_n -graded fusion ring C_G^{\times} and give an algorithm to compute the fusion product of two simple objects $X^\sigma \in \text{Obj}(\mathcal{C}_\sigma)$ and $X^\pi \in \text{Obj}(\mathcal{C}_\pi)$.

(2+1)D TPM	UMTC
multi-layer phase	Deligne product of UMTCs $\mathcal{C}^{\boxtimes n}$
multi-layer SET phase	$(\mathcal{C}^{\boxtimes n})_{S_n}^\times = \bigoplus_{\sigma \in S_n} \mathcal{C}_\sigma$
anyon	$\vec{a} := \boxtimes_i a_i$, where $a_i \in \text{Irr}(\mathcal{C})$
vacuum	tensor unit $1 := 1^{\boxtimes n}$
monolayer anyon	$1 \boxtimes \dots \boxtimes 1 \boxtimes a \boxtimes 1 \boxtimes \dots \boxtimes 1$
g -sector	invertible \mathcal{C} -bimodule category \mathcal{C}_g
transposition defect	simple object $X_{\boxtimes_i f_i}^{(ij)} \in \mathcal{C}_{(ij)}$
m -cycle defect	simple object $X_{\boxtimes_i f_i}^{(i_1 i_2 \dots i_m)} \in \mathcal{C}_{(i_1 i_2 \dots i_m)}$
permutation defect	simple object $X_{\boxtimes_i f_i}^\sigma \in \mathcal{C}_\sigma$
bare defect	$X_{1^{\boxtimes n}}^\sigma$

Table 5.1: Mathematical definitions of the physics terminology we will use when discussing permutation-enriched topological order.

5.1.2 Categorical S_n -symmetry of $\mathcal{C}^{\boxtimes n}$ and multilayer topological order

Let ρ be the monoidal functor that acts strictly on $\mathcal{C}^{\boxtimes n}$ by permutations

$$\begin{aligned}
 \underline{\rho} : \underline{S}_n &\longrightarrow \underline{\text{Aut}}_{\otimes}^{\text{br}}(\mathcal{C}^{\boxtimes n}) \\
 id &\mapsto id : \mathcal{C}^{\boxtimes n} \rightarrow \mathcal{C}^{\boxtimes n} \\
 \sigma &\mapsto \begin{aligned} T_\sigma : \mathcal{C}^{\boxtimes n} &\rightarrow \mathcal{C}^{\boxtimes n} \\ \boxtimes_i X_i &\mapsto \boxtimes_i X_{\sigma(i)} \\ \boxtimes_i f_i &\mapsto \boxtimes_i f_{\sigma(i)} \end{aligned}
 \end{aligned}$$

so that the tensorators $U_\sigma : T_\sigma(X \otimes Y) \rightarrow T_\sigma(X) \otimes T_\sigma(Y)$ and compositors $\eta_X : (T_\rho \circ T_\sigma)(X) \rightarrow T_{\sigma\rho}(X)$ are the identity isomorphisms for all $\sigma, \rho \in S_n$.

Theorem ([46]). *The $H^4(S_n, \mathbb{C}^\times)$ obstruction to S_n -extensions of $\mathcal{C}^{\boxtimes n}$ vanish for the categorical permutation group action $\underline{\rho} : \underline{S}_n \rightarrow \underline{\text{Aut}}_{\otimes}^{\text{br}}(\mathcal{C}^{\boxtimes n})$ and the equivalence classes of*

S_n -extensions form a torsor over $H^3(G, \mathbb{C}^\times)$.

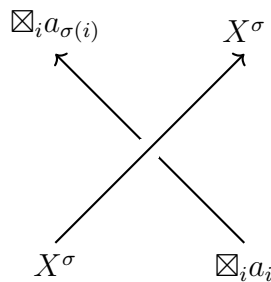
The permutation symmetry then models a global unitary on-site symmetry of *multi-layer topological order* given by n layers of topological order \mathcal{C} [3].

$$S_n \left(\begin{array}{c} \text{---} \text{---} \text{---} \mathcal{C} \\ \text{---} \text{---} \text{---} \mathcal{C} \\ \vdots \\ \text{---} \text{---} \text{---} \mathcal{C} \end{array} \right) \longrightarrow (\mathcal{C}^{\boxtimes n})_{S_n}^\times = \bigoplus_{\sigma \in S_n} \mathcal{C}_\sigma$$

While we been interpreting the factors in the Deligne product as spatially separated layers, the permutation symmetry is technically on-site because $\mathcal{C}^{\boxtimes n}$ can also be interpreted a monolayer topological order. This is what allows us to study the spatial symmetry using the techniques developed for on-site symmetries.

Prior to the development of GxBFCs as the algebraic theory of symmetry defects physicists studied defects in (2+1)D TPM called *genons* because of the way they effectively couple layers of topological phases to create nontrivial topology [4]. Our main result uses GxBFC theory to frame this correspondence algebraically in terms of $(\mathcal{C} \boxtimes \mathcal{C})_{S_2}^\times$ and investigate the relationship between quantum symmetry, topology, and quantum information, see [Chapter 6](#).

The ability of genons to entangle the layers comes from the S_n -crossed braiding, whereby exchange with defects transports (monolayer) anyons between layers.



5.1.3 Bilayer SET order and S_2 -extensions of $\mathcal{C} \boxtimes \mathcal{C}$

The authors of [3] gave fusion rules for bilayer defects and argued that the $H^4(S_2, U(1))$ obstruction vanished and that the symmetry fractionalization $H^2(S_2, \mathcal{A} \times \mathcal{A})$ was trivial.

Formulas for the dimensions of fusion spaces and descriptions of the structure morphisms of S_2 -extensions had already appeared several years prior in [5] using the language of modular functors and TQFT, and the formulas for the fusion coefficients when $\mathcal{A} = 1$ recently appeared in [37] in the language of MTCs. We reproduce their formula below.

Proposition 5.1 ([37]). *Let \mathcal{C} be an MTC with $\mathcal{A} = 1$ and $\mathcal{D} = (\mathcal{C} \boxtimes \mathcal{C})_{\mathbb{Z}_2}^\times = \mathcal{C} \boxtimes \mathcal{C} \oplus \hat{\mathcal{C}}$ a permutation extension. Then*

$$\dim \left(\text{Hom}_{\mathcal{D}}(\hat{X} \otimes \hat{Y}, Z \boxtimes W) \right) = \dim \left(\text{Hom}_{\mathcal{C}}(X \otimes Y, Z \otimes W) \right). \quad (5.1)$$

where $\hat{X}, \hat{Y} \in \text{Obj}(\hat{\mathcal{C}})$, $X, Y, Z, W \in \text{Obj}(\mathcal{C} \boxtimes \mathcal{C})$.

While the algebraic theory for $(\mathcal{C} \boxtimes \mathcal{C})_{S_2}^\times$ has been described in the language of modular functors, our approach gives an explicit construction of the fusion rings (1) in terms of an MTC \mathcal{C} [33] (2) that generalizes to fusion rules for $(\mathcal{C}^{\boxtimes n})_{S_n}^\times$ and (3) suggests the form of their categorification.

We begin with the observation that each transposition sector in the full S_n -extension is related to the transposition sector in an S_2 -extension in a predictable way, so that each bimodule category $\mathcal{C}_{(ij)}$ can be identified as a Deligne product of copies of \mathcal{C} and the bimodule category $\mathcal{C}_{(12)}$.

Observation 5.1. *Let (ij) be a transposition in S_n and let $\mathcal{C}_{(ij)}$ be the corresponding transposition sector in $(\mathcal{C}^{\boxtimes n})_{S_n}^\times \simeq \bigoplus_{\sigma \in S_n} \mathcal{C}_\sigma$. Then*

$$(\mathcal{C}^{\boxtimes n})_{(ij)}^\times \simeq \mathcal{C}^{\boxtimes n-i} \boxtimes (\mathcal{C} \boxtimes \mathcal{C})_{(12)}^\times \boxtimes \mathcal{C}^{\boxtimes n-j+1}.$$

as $\mathcal{C}^{\boxtimes n}$ -bimodule categories.

5.2 Combinatorial model of multilayer anyon and permutation defects

Since the rank of each σ -sector is given by the number of fixed anyons under the action of σ by Lemma 4.1, one can index the simple objects in \mathcal{C}_σ by

$$\text{Irr}(\mathcal{C}_\sigma) = \{X_{\boxtimes_i a_i} \mid \boxtimes_i a_i \in \text{Irr}(\mathcal{C}^{\boxtimes n}) \text{ with } \boxtimes_i a_{\sigma(i)} \cong \boxtimes_i a_i\}. \quad (5.2)$$

We introduce some terminology for symmetry defects for convenience.

Definition 5.1 (Topological charge of defects). *Let X_f^g be a symmetry defect. Then the topological charge of X_f^g is the topological charge (isomorphism class) of f .*

Since the vacuum $\vec{1}$ is always fixed, each sector has a distinguished object $X_{\vec{1}}$ with vacuum charge. Following [3], we make the following definition.

Definition 5.2 (Bare defects). *A simple object in \mathcal{C}_σ isomorphic to $X_{\vec{1}}^\sigma$ is called a **bare** σ -defect.*

Occasionally we use $\vec{a} := \boxtimes_i a_i$ or suppress the Deligne product and write a_i to simplify notation. When we want to indicate which sector a defect belongs to we will use a superscript with the group label, e.g. $X_{\vec{a}}^\sigma \in \text{Irr}(\mathcal{C}_\sigma)$.

On the level of objects we define a direct sum

$$\begin{aligned} \bigoplus : \mathcal{C}_\sigma \times \mathcal{C}_\sigma &\rightarrow \mathcal{C}_\sigma \\ X_{\boxtimes_i a_i} \oplus X_{\boxtimes_i b_i} &\mapsto X_{\boxtimes_i (a_i \oplus b_i)}. \end{aligned} \quad (5.3)$$

As \mathbb{C} -linear abelian categories, our model for permutation sectors is given by $(\mathcal{C}_\sigma, \oplus)$. Decategorifying, this describes $(\mathcal{C}^{\boxtimes n})_{S_n}^\times$ as a free \mathbb{Z} -module on the set $\text{Irr}(\mathcal{C}^{\boxtimes n}) \cup_g \text{Irr}(\mathcal{C}_g)$, which we denote by $C_{S_n}^\times$, using capital instead of calligraphic letters to distinguish the fusion ring from the fusion category. Our goal is to endow $C_{S_n}^\times$ with the structure of a fusion ring, more precisely a unital based \mathbb{Z}_+ ring.¹

Definition 5.3 (Unital based \mathbb{Z}_+ -ring [38]). *Let A be a ring which is free as a \mathbb{Z} -module. A \mathbb{Z}_+ -basis of A is a set of elements $B = \{b_i\}_{i \in I}$ such that $b_i b_j = \sum_{k \in I} c_{ij}^k b_k$, where $c_{ij}^k \in \mathbb{Z}_+$.*

A unital based \mathbb{Z}_+ ring is a ring with a fixed \mathbb{Z}_+ -basis B such that

1. $1 \in B$

2. *there exists an involution $i \mapsto i^*$ of I such that the induced map $a \mapsto a^*$ is an*

$$\text{anti-involution of } A \text{ and whenever } b_i b_j = \sum c_{ij}^k b_k, c_{ij}^1 = \begin{cases} 1 & i = j^* \\ 0 & i \neq j^* \end{cases}.$$

5.2.1 Confinement, deconfinement, and anyon-defect fusion

We define a left and right action of $C^{\boxtimes n}$ on C_g as follows. In [32] we show that these actions categorify to make \mathcal{C}_σ a $C^{\boxtimes n}$ -bimodule category - the idea of the proof is essentially contained in Chapter 6 where we give the proof in the case $n = 2$. But for now we will be content to prove statements at the level of the fusion ring.

Definition 5.4 (σ -confinement). *The (left) confinement map*

$$\triangleright: C^{\boxtimes n} \times C_\sigma \longrightarrow C_\sigma$$

is defined on basis elements by

¹Here \mathbb{Z}_+ denotes $\mathbb{Z}_{\geq 0}$ thought of as a semi-ring.

$$\boxtimes_i a_i \triangleright X_{\boxtimes_i b_i}^\sigma = X_{\boxtimes_i c_i}^\sigma, \text{ where } c_i = \begin{cases} a_i \otimes b_i & \sigma(i) = i \\ (\otimes_{j \neq \sigma(j)} a_j) \otimes b_i & \sigma(i) \neq i \end{cases}. \quad (5.4)$$

and extended linearly to all elements. We define the right confinement map \triangleleft by

$$X_{\boxtimes_i b_i}^\sigma \triangleleft \boxtimes_i a_i = \boxtimes_i a_i \triangleright X_{\boxtimes_i b_i}^\sigma$$

, and call the images of basis elements under these maps σ -**confinements**.

The object $\boxtimes_i c_i$ is fixed by the action of σ , since if $\sigma(i) \neq i$

$$\begin{aligned} \sigma \cdot (\otimes_{j \neq \sigma(j)} a_j \otimes b_i) &= \otimes_{j \neq \sigma(j)} a_{\sigma(j)} \otimes b_{\sigma(i)} \\ &= (\otimes_{j \neq \sigma(j)} a_j) \otimes b_i \end{aligned} \quad (5.5)$$

where we have used that $b_{\sigma(i)} = b_i$ for all i . Thus the confinement map is well-defined. One can also check that the definition of an action is satisfied due to associativity in $C^{\boxtimes n}$.

Confinement map on monolayer anyons and bare defects

The fusion between monolayer anyons $1^{\boxtimes i-1} \boxtimes a \boxtimes 1^{\boxtimes n-i}$ and bare defects $X_{\bar{1}}^\sigma$ is given by

$$1^{\boxtimes i-1} \boxtimes a \boxtimes 1^{\boxtimes n-i} \triangleright X_{\bar{1}}^\sigma = X_{\boxtimes b_j}^\sigma \quad b_j = \begin{cases} 1 & \sigma(j) = j \\ a & \sigma(j) \neq j \end{cases}. \quad (5.6)$$

For example, when $n = 2$,

$$1 \boxtimes a \triangleright X_1 = a \boxtimes 1 \triangleright X_1 = X_a \quad (5.7)$$

for all $a \in \text{Irr}(\mathcal{C})$.

In words, fusing an anyon in the i^{th} layer with the bare defect results in the defect with the topological charge label that has a in every layer which is in the σ -orbit of i . Notice that fusion between anyons and defects is always commutative due to the G -crossed braiding isomorphisms $c_{a, X^g} : a \otimes X^g \rightarrow X^g \otimes a$, but symmetry defect fusion will be noncommutative when G is a nonabelian group.

In this model every σ -defect can be realized by confinement of an anyon with the bare defect:

Lemma 5.1. *Every basis element in C_σ is the image of a pair of basis elements in $C^{\boxtimes n}$ and C_σ under the confinement map.*

Proof. Let $X_{\vec{i}} \in \text{Irr}(C_\sigma)$. Then $\boxtimes b_{\sigma(i)} = \boxtimes b_i$. Define $\vec{a} = \boxtimes a_i$ to be the anyon with $a_i = b_i$ if $\sigma(i) = i$. Then take any k with $\sigma(k) \neq k$ and put $a_k = b_k$, then $a_j = 1$ for all other $j \neq \sigma(j)$ with $j \neq k$. Then one can check that $\boxtimes \vec{a} \triangleright X_{\vec{i}} = \vec{b}$. \square

Thus defects can be realized as confinements in multiple ways, depending on the permutation σ as well as the fusion in \mathcal{C} :

Quantum dimensions and S_n action on permutation defects

Lemma 5.1 immediately determines the quantum dimensions of the defects. We give a formula for the dimensions when $n = 2$ in Chapter 6.

Confinement and deconfinement of anyons and defects

Anyons, being intrinsic quasiparticle excitations corresponding to the ground state of a Hamiltonian which can be moved by local operators without additional energy, are said to be *deconfined*.

On the other hand, point-like symmetry defects are not finite-energy excitations. They are extrinsic in the sense that a Hamiltonian realization of a topological phase enriched with symmetry needs additional terms added in order for it to have excitations which correspond to the symmetry defects [3]. Moreover, the energy needed to spatially separate defects grows differently than it does for anyons [3], and they are said to be *confined* as opposed to deconfined.

We make the following definitions of g -confinement and g -deconfinement, borrowing the ideas from condensed matter theory.²

Definition 5.5 (σ -Deconfinement). *Let $X_{\vec{b}} \in \text{Irr}(\mathcal{C}_\sigma)$, $\vec{a} \in \text{Irr}(\mathcal{C}^{\boxtimes n})$, and suppose they satisfy*

$$\vec{a} \triangleright X_{\vec{1}} = X_{\vec{b}}. \quad (5.8)$$

*Then we say that \vec{a} is a (left) **deconfinement** of $X_{\vec{b}}$, and define right deconfinements in the analogous way using the right action.*

When we want to strip the topological charge from a defect by splitting off an anyon but without making a specific choice of deconfinement, we write

$$X_{\vec{a}} = d(\vec{a}) \triangleright X_{\vec{1}}. \quad (5.9)$$

²Perhaps a better word than borrowed is misappropriated, as our definitions do not align with the usual technical meaning in anyon condensation. We make an effort to consistently use the group element labels to remedy any confusion this causes.

We will see that the notion of deconfinement is central to our construction, as it allows us to intuit the way that the defect theory is built from the anyon theory.

Since all defects are related to a bare defect by fusion with a deconfinement, it suffices to determine the fusion between bare defects, as the following lemma shows.

Lemma 5.2. *The fusion product of two arbitrary defects X_a^σ and X_b^π is determined by the fusion between the bare defects X_1^σ and X_1^π .*

Proof. We have the following equalities between isomorphism classes of objects

$$[X_a^\sigma \otimes X_b^\sigma] = [(d(\vec{a}) \triangleright X_1^\sigma) \otimes (X_1^\pi \triangleleft d(\vec{b}))] \quad (5.10)$$

$$= [(d(\vec{a}) \triangleright (X_1^\sigma \otimes X_1^\pi)) \triangleleft d(\vec{b})] \quad (5.11)$$

where we used that anyon-defect fusion commutes. □

Corollary 1. *The fusion rules are independent of choices of deconfinement.*

Thus we have reduced the problem to determining the fusion between bare defects in non-trivial σ -sectors.

5.2.2 Permutation defect fusion ring

The fusion rules between permutation defects are built from the fusion rules of transposition defects $X \in C_{(ij)}$ in the same way that the symmetric group S_n is generated by its transpositions.

Fusion of transposition defects

Let $(ij) \in S_n$ be a transposition and consider the bare defect $X_1^{(ij)}$. Following Observation 5.1 we make the following definition.

Definition 5.6 (Product of bare transposition defects). *Without loss of generality let (ij) and (kl) be transpositions with $i < j \leq k < l$. Then we define the fusion product of bare defects by*

$$X_{\bar{1}}^{(ij)} \otimes X_{\bar{1}}^{(kl)} = \begin{cases} X_{\bar{1}}^{(ijl)} & k = j \\ X_{\bar{1}}^{(ij)(kl)} & k \neq j \\ \bigoplus_{c \in \text{Irr}(\mathcal{C})} 1^{\boxtimes i-1} \boxtimes c \boxtimes 1^{\boxtimes j-(i+1)} \boxtimes c^* \boxtimes 1^{\boxtimes n-j} & (ij) = (kl) \end{cases} \quad (5.12)$$

That is, when two transpositions multiply to a 3-cycle, the bare transposition defects fuse to the bare 3-cycle defect. When the transpositions are disjoint they fuse to the bare defect in the disjoint-transposition sector.

Now that fusion between any two transposition defects is determined we are ready to describe the fusion product between a transposition defect $X^{(ij)}$ and a general σ -defect X^σ , which will in turn determine more general fusion products. First we define the product of bare defects in disjoint sectors to be the bare defect in the appropriate sector, and thus without loss of generality it suffices to define products between defects $X^{(ij)}$ and X^σ for σ an m -cycle.

Definition 5.7 (Product of disjoint bare defects). *Let $X_{\bar{1}}^\sigma$ and $X_{\bar{1}}^\rho$ be bare defects. Then*

$$X_{\bar{1}}^\sigma \otimes X_{\bar{1}}^\rho = X_{\bar{1}}^{\sigma\rho} = X_{\bar{1}}^{\rho\sigma}. \quad (5.13)$$

Like with fusion of bare transposition defects, there are three cases depending on $\{i, j\} \cap \{k_1, k_2, \dots\}$.

Fusion of transposition defects and cycle defects

Definition 5.8 (Fusion between bare transposition and m -cycle defects). *Let (ij) be a transposition and $(k_1 k_2 \cdots k_m)$ an m -cycle in S_n . Then the fusion product is given by*

$$X_1^{(ij)} \otimes X_1^{(k_1 k_2 \cdots k_m)} = \begin{cases} X_1^{(ij)(k_1 k_2 \cdots k_m)} & |\{i, j\} \cap \{k_1, \dots, k_m\}| \leq 1 \\ (\oplus_a 1^{\boxtimes i-1} \boxtimes a \boxtimes 1^{j-i} \boxtimes a^* \boxtimes 1^{\boxtimes n-j}) \otimes X_1^\sigma & i, j \in \{k_1, \dots, k_m\} \end{cases} \quad (5.14)$$

where σ is a permutation with $X_1^{(k_1 k_2 \cdots k_m)} = X_1^{(ij)} \otimes X_1^\sigma$ and $|\sigma| < m$.

The fusion product with the defect order reversed $X_1^{(k_1 k_2 \cdots k_m)} \otimes X_1^{(ij)}$ is defined analogously. One can check that this is a well-defined associative binary operation.

Proposition 5.2. *The fusion product of bare defects together with the confinement map define a based \mathbb{Z}_+ ring.*

We give a sketch of the proof. Let A be the free \mathbb{Z} -module generated by the set $\{\text{Irr}(\mathcal{C}^{\boxtimes n}) \cup_\sigma \text{Irr}(\mathcal{C}_\sigma)\}$. Combining the multiplication coming from the fusion ring of $\mathcal{C}^{\boxtimes n}$, the confinement map in Definition 5.2, and the definition of bare defect fusion products in Definitions 5.4 and 5.5 defines an associative binary operation $A \times A \rightarrow A$ that gives A the structure of a ring.

As a consequence of our definitions the products are all given by non-negative integer linear combinations of basis elements $\{\text{Irr}(\mathcal{C}^{\boxtimes n}) \cup_\sigma \text{Irr}(\mathcal{C}_\sigma)\}$, and the unit $1 \in \text{Irr}(\mathcal{C}^{\boxtimes n})$ is simple. Therefore we have a unital \mathbb{Z}_+ ring.

Now since $a \cong a^{**}$ for all simple objects in a UMTC by pivotality, and $(g^{-1})^{-1} = g$ for all $g \in G$, the following map defines an involution on basis elements,

$$\vec{a} \mapsto \vec{a}^* \quad \vec{a} \in \text{Irr}(\mathcal{C}^{\boxtimes n}) \quad (5.15)$$

$$X_a^\sigma \mapsto X_{a^*}^{\sigma^{-1}} \quad X_a^\sigma \in \text{Irr}(\mathcal{C}_\sigma) \quad (5.16)$$

which we expand linearly to an involution on all of A . Since that $N_1^{ab} = 1$ if and only if $a \cong b^*$, it remains only to check that this involution corresponds to duality of defects.

Fix $\sigma \in S_n$, $\vec{a} \in \text{Irr}(\mathcal{C}^{\boxtimes n})$ and let $X_{\vec{a}}^\sigma \in \mathcal{C}_\sigma$, $X_{\vec{b}}^\tau \in \mathcal{C}_\tau$. Clearly $N_1^{X_{\vec{a}}^\sigma X_{\vec{b}}^\tau} = 0$ unless $\tau = \sigma^{-1}$.

Given a transposition decomposition of σ , $\sigma = \tau_m \cdots t_1$ with $\tau_j = (j_1 j_2)$, $j_1 < j_2$, we have

$$\begin{aligned} X_{\vec{a}}^\sigma \otimes X_{\vec{b}}^{\sigma^{-1}} &= \left(d(\vec{a}) \otimes d(\vec{b}) \right) \otimes \left(X_{\vec{1}}^\sigma \otimes X_{\vec{1}}^{\sigma^{-1}} \right) \\ &= \left(d(\vec{a}) \otimes d(\vec{b}) \right) \otimes \left(\bigotimes_{1 \leq j \leq m} \left(\bigoplus_{c \in \text{Irr}(\mathcal{C})} 1^{\boxtimes j_1 - 1} \boxtimes c \boxtimes 1^{j_2 - j_1} \boxtimes c^* \boxtimes 1^{n - j_2} \right) \right) \end{aligned} \quad (5.17)$$

In the fusion product over j there is one summand of $\vec{1}$, hence $N_1^{X_{\vec{a}}^\sigma X_{\vec{b}}^{\sigma^{-1}}} = 1$ only if $N_1^{d(\vec{a}), d(\vec{b})} = 1$. So we must have $d(\vec{b}) \cong d(\vec{a})^*$. In other words, the deconfinements must be dual.

Now reconfinement with an arbitrary bare defect gives

$$X_{\vec{1}}^\rho = d(\vec{a}) \otimes d(\vec{b}) \otimes X_{\vec{1}}^\rho = X_{\vec{a} \otimes \vec{b}}^\rho \quad (5.18)$$

and hence $\vec{b} \cong \vec{a}^*$.

5.2.3 Fusion rules for inequivalent permutation extensions

We have given one candidate fusion ring for permutation-extensions of $\mathcal{C}^{\boxtimes n}$, but we know from the general theory that there are in general many such extensions, which form an $H^2(G, \mathcal{A}) \times H^3(G, U(1))$ torsor and should not be expected to have equivalent fusion rules. We claim that these fusion rules can be interpreted as a basepoint

for the $H^2(S_n, \mathcal{A}^{\times n})$ torsor's worth of possible fusion rules corresponding to the trivial cohomology class.

Conjecture 3. *The fusion rules of any S_n -extension of $\mathcal{C}^{\boxtimes n}$ can be obtained from our fusion rules by twisting with a representative ω of a cohomology class $[\omega] \in H^2(S_n, \mathcal{A}^{\times n})$ by*

$$[X_{\vec{a}}^{\sigma, \omega} \otimes X_{\vec{b}}^{\pi, \omega}] = [\omega(\sigma, \pi) \otimes X_{\vec{a}}^{\sigma} \otimes X_{\vec{b}}^{\pi}]$$

where $\sigma, \omega \in S_n$, $\sigma \cdot \vec{a} = \vec{a}$, and $\pi \cdot \vec{b} = \vec{b}$.

Recall that the isomorphism class of the object on the right-hand side of the equation is independent of whether $\omega(\sigma, \pi)$ is fused on the left, right, or between the defect fusion product.

Lemma 5.3. *When $\mathcal{A} = 1$, the permutation defect fusion rules agree with the known $\mathcal{A} = 1$ fusion rules for \mathbb{Z}_2 -extensions of $\mathcal{C} \boxtimes \mathcal{C}$ [37].*

Proof. It suffices to show that their fusion rule $\hat{1} \otimes \hat{1}$ corresponds to our fusion rule of bare transposition defects $X_{\vec{1}}^{(12)} \otimes X_{\vec{1}}^{(12)}$. By their Proposition 4.1 in [37], $N_{a\boxtimes b}^{\hat{1}\hat{1}} = N_1^{ab}$. Since $N_1^{ab} \neq 0$ if and only if $a \cong b^*$, by uniqueness of duals theirs is the fusion rule $\hat{1} \otimes \hat{1} = \bigoplus_{c \in \text{Irr}(\mathcal{C})} c \boxtimes c^*$, as is ours. □

In the next chapter we will illustrate how our model for permutation defects provides a natural way to construct \mathbb{Z}_2 -crossed braided extensions of bilayer topological order, the details of which will appear in [32]. The next examples give additional evidence and serve to demonstrate the permutation defect fusion ring and the algorithm to compute it.

5.3 Example: bilayer Fibonacci defect fusion

Recall the Fibonacci UMTC from Section 1.4, which has rank 2 and nontrivial fusion rule $\tau \otimes \tau = 1 \oplus \tau$.

Algebraic data for $(\text{Fib}^{\boxtimes 2})_{\mathbb{Z}/2\mathbb{Z}}^{\times}$ was first computed by computer assisted de-equivariantization of the UMTC $SU(2)_8$ in [25].

$$S_2 \curvearrowright \begin{array}{l} \text{Fib} \\ \text{Fib} \end{array} \longrightarrow (\text{Fib}^{\boxtimes 2})_{S_2}^{\times} = \text{Fib}^{\boxtimes 2} \oplus \mathcal{C}_{(12)}$$

Writing the bilayer anyons $a \boxtimes b =: ab$ and labeling defects by fixed points, we put

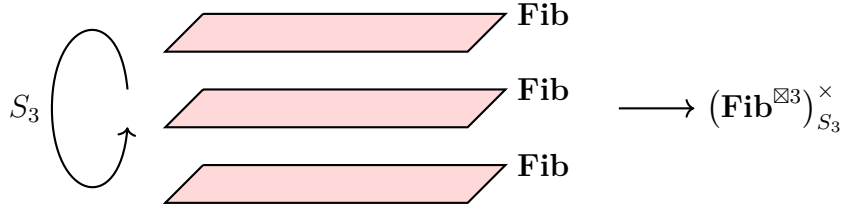
$$\text{Irr} \left((\text{Fib}^{\boxtimes 2})_{S_2}^{\times} \right) = \text{Irr} (\text{Fib}^{\boxtimes 2}) \cup \text{Irr} (\mathcal{C}_{(12)}) = \{11, 1\tau, \tau 1, \tau\tau, X_{11}, X_{\tau\tau}\}.$$

The fusion rules constructed in the previous section in the case $\mathcal{C} = \text{Fib}$ and $n = 2$ are listed in the table below.

\otimes	11	1 τ	τ 1	$\tau\tau$	X_{11}	$X_{\tau\tau}$
11	11	1 τ	τ 1	$\tau\tau$	X_{11}	$X_{\tau\tau}$
1 τ	1 τ	11 \oplus 1 τ	$\tau\tau$	$\tau 1 \oplus \tau\tau$	$X_{\tau\tau}$	$X_{11} \oplus X_{\tau\tau}$
τ 1	τ 1	$\tau\tau$	11 \oplus τ 1	1 τ \oplus $\tau\tau$	$X_{\tau\tau}$	$X_{11} \oplus X_{\tau\tau}$
$\tau\tau$	$\tau\tau$	$\tau 1 \oplus \tau\tau$	1 τ \oplus $\tau\tau$	11 \oplus 1 τ \oplus τ 1 \oplus $\tau\tau$	$X_{11} \oplus X_{\tau\tau}$	$X_{11} \oplus 2X_{\tau\tau}$
X_{11}	X_{11}	$X_{\tau\tau}$	$X_{\tau\tau}$	$X_{11} \oplus X_{\tau\tau}$	11 \oplus $\tau\tau$	1 τ \oplus τ 1 \oplus $\tau\tau$
$X_{\tau\tau}$	$X_{\tau\tau}$	$X_{11} \oplus X_{\tau\tau}$	$X_{11} \oplus X_{\tau\tau}$	$X_{11} \oplus 2X_{\tau\tau}$	1 τ \oplus τ 1 \oplus $\tau\tau$	11 \oplus 1 τ \oplus τ 1 \oplus $2\tau\tau$

Figure 5.1: Fusion table for bilayer Fibonacci anyons and defects.

5.4 Example: trilayer Fibonacci with S_3 permutation symmetry



There are $3! = 6$ graded components, written

$$(\mathbf{Fib}^{\boxtimes 3})_{S_3}^{\times} = \mathbf{Fib}^{\boxtimes 3} \oplus \mathcal{C}_{(12)} \oplus \mathcal{C}_{(23)} \oplus \mathcal{C}_{(13)} \oplus \mathcal{C}_{(123)} \oplus \mathcal{C}_{(132)}.$$

Suppressing the \boxtimes in the label set $\{1, \tau\}^3$ we label the defects in each sector \mathcal{C}_σ by the anyons fixed under the permutation of σ , thinking of anyons as trivial defects. We count a rank 24 fusion category with global quantum dimension

$$\mathcal{D}_{\mathbf{Fib}^{\boxtimes 3}} = \mathcal{D}_{\mathbf{Fib}}^3 = (2 + \phi)^{3/2} = \sqrt{15 + 20\phi}. \quad (5.19)$$

σ -sector	σ -defects	quantum dim.
\mathcal{C}_{id}	$\{111, 11\tau, 1\tau 1, 1\tau\tau, \tau 11, \tau 1\tau, \tau\tau 1, \tau\tau\tau\}$	$\{1, \phi, \phi, \phi^2, \phi, \phi^2, \phi^2, \phi^3\}$
$\mathcal{C}_{(12)}$	$\{X_{111}, X_{11\tau}, X_{\tau\tau 1}, X_{\tau\tau\tau}\}$	$\{\sqrt{2 + \phi}, \sqrt{3 + 4\phi}, \sqrt{3 + 4\phi}, \sqrt{7 + 11\phi}\}$
$\mathcal{C}_{(23)}$	$\{Y_{111}, Y_{\tau 11}, Y_{1\tau\tau}, Y_{\tau\tau\tau}\}$	$\{\sqrt{2 + \phi}, \sqrt{3 + 4\phi}, \sqrt{3 + 4\phi}, \sqrt{7 + 11\phi}\}$
$\mathcal{C}_{(13)}$	$\{Z_{111}, Z_{1\tau 1}, Z_{\tau 1\tau}, Z_{\tau\tau\tau}\}$	$\{\sqrt{2 + \phi}, \sqrt{3 + 4\phi}, \sqrt{3 + 4\phi}, \sqrt{7 + 11\phi}\}$
$\mathcal{C}_{(123)}$	$\{U_{111}, U_{\tau\tau\tau}\}$	$\{\sqrt{5 + 5\phi}, \sqrt{10 + 15\phi}\}$
$\mathcal{C}_{(132)}$	$\{V_{111}, V_{\tau\tau\tau}\}$	$\{\sqrt{5 + 5\phi}, \sqrt{10 + 15\phi}\}$

Table 5.2: Enumeration of simple objects in the invertible $\mathcal{C}^{\boxtimes 3}$ -bimodule categories \mathcal{C}_σ , which form the simple objects of a fusion category by [46].

The Fibonacci UMTC has no nontrivial abelian anyons, so $\mathcal{A} = 1$ and $H^3(S_3, \mathcal{A})$ is trivial. By the existence result of [46] and the classification of G -crossed braided

extensions of BFCs [39], there is a unique fusion ring shared among unitary S_3 -crossed extensions of $\text{Fib}^{\boxtimes 3}$, which was computed by hand and found to agree with the fusion rules defined in the previous section between anyons and bare defects.

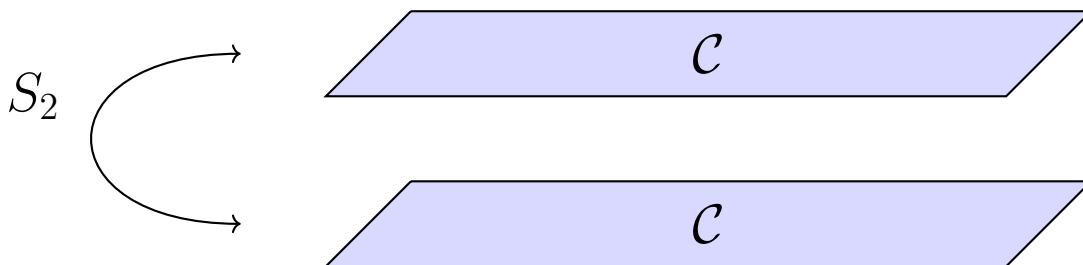
We list the fusion between anyons and bare defects in the next table.

By Lemma 6, the full fusion table for the S_3 -extension is determined by rows 1-3 and 8-10.

\otimes	X_{111}	Y_{111}	Z_{111}	U_{111}	V_{111}
11τ	$X_{11\tau}$	$Y_{1\tau\tau}$	$Z_{\tau 1\tau}$	$U_{\tau\tau\tau}$	$V_{\tau\tau\tau}$
$1\tau 1$	$X_{\tau\tau 1}$	$Y_{1\tau\tau}$	$Z_{1\tau 1}$	$U_{\tau\tau\tau}$	$V_{\tau\tau\tau}$
$\tau 11$	$X_{\tau\tau 1}$	$Y_{\tau 11}$	$Z_{\tau 1\tau}$	$U_{\tau\tau\tau}$	$V_{\tau\tau\tau}$
$1\tau\tau$	$X_{\tau\tau\tau}$	$Y_{111} \oplus Y_{1\tau\tau}$	$Z_{\tau\tau\tau}$	$U_{111} \oplus U_{\tau\tau\tau}$	$V_{111} \oplus V_{\tau\tau\tau}$
$\tau 1\tau$	$X_{\tau\tau\tau}$	$Y_{\tau\tau\tau}$	$Z_{111} \oplus Z_{\tau 1\tau}$	$U_{111} \oplus U_{\tau\tau\tau}$	$V_{111} \oplus V_{\tau\tau\tau}$
$\tau\tau 1$	$X_{111} \oplus X_{\tau\tau 1}$	$Y_{\tau\tau\tau}$	$Z_{\tau\tau\tau}$	$U_{111} \oplus U_{\tau\tau\tau}$	$V_{111} \oplus V_{\tau\tau\tau}$
$\tau\tau\tau$	$X_{11\tau} \oplus X_{\tau\tau\tau}$	$Y_{\tau 11} \oplus Y_{\tau\tau\tau}$	$Z_{1\tau 1} \oplus Z_{\tau\tau\tau}$	$U_{111} \oplus 2U_{\tau\tau\tau}$	$V_{111} \oplus 2V_{\tau\tau\tau}$
X_{111}	$111 \oplus \tau\tau 1$	U_{111}	V_{111}	$Y_{111} \oplus Y_{\tau\tau\tau}$	$Z_{111} \oplus Z_{\tau\tau\tau}$
Y_{111}	V_{111}	$111 \oplus 1\tau\tau$	U_{111}	$Z_{111} \oplus Z_{\tau\tau\tau}$	$X_{111} \oplus X_{\tau\tau\tau}$
Z_{111}	U_{111}	V_{111}	$111 \oplus \tau 1\tau$	$X_{111} \oplus X_{\tau\tau\tau}$	$Y_{111} \oplus Y_{\tau\tau\tau}$
U_{111}	$Z_{111} \oplus Z_{\tau\tau\tau}$	$X_{111} \oplus X_{\tau\tau\tau}$	$Y_{111} \oplus Y_{\tau\tau\tau}$	$2V_{111} \oplus V_{\tau\tau\tau}$	$111 \oplus \tau\tau 1 \oplus \tau 1\tau \oplus 1\tau\tau \oplus \tau\tau\tau$
V_{111}	$Y_{111} \oplus Y_{\tau\tau\tau}$	$Z_{111} \oplus Z_{\tau\tau\tau}$	$X_{111} \oplus X_{\tau\tau\tau}$	$111 \oplus \tau\tau 1 \oplus \tau 1\tau \oplus 1\tau\tau \oplus \tau\tau\tau$	$2U_{111} \oplus U_{\tau\tau\tau}$

Chapter 6

On the algebraic theory of bilayer symmetry defects



6.1 Introduction

Next we apply the model of permutation defects outlined in the previous chapter to construct data for the family of symmetry defect models that describe bilayer topological order enriched with layer-exchange symmetry. These SET phases are modeled by \mathbb{Z}_2 -extensions of Deligne products of UMTCs $\mathcal{C} \boxtimes \mathcal{C}$, where the categorical group action exchanges the factors in Deligne products of objects and morphisms.

In [33] we provide formulas for the family of natural isomorphisms giving the associators, G -crossed braiding, and G -action satisfying the coherence axioms of a GxBFC. We apply this construction to derive formulas for the skeletal data

$$\{N_Z^{XY}, [R_Z^{XY}]_{\mu\nu}, [F_Z^{WXY}]_{U,\alpha,\beta;V,\mu,\nu}, U_g(X, Y; Z), \eta_X(g, h)\}$$

in terms of the monolayer skeletal data $\{N_c^{ab}, [R_c^{ab}]_{\mu\nu}, [F_d^{abc}]_{n,\alpha,\beta;m,\mu,\nu}\}$.

6.2 Bilayer topological order $\mathcal{C} \boxtimes \mathcal{C}$ and layer-exchange symmetry

As before \mathcal{C} is a UMTC and we make no further assumptions about \mathcal{C} beyond that it satisfies the axioms of a UMTC. For simplicity we use the multiplicity-free notation for the algebraic data of \mathcal{C} , as it does not affect the scope of our discussion.¹

Let $\{N_c^{ab}, R_c^{ab}, [F_d^{abc}]_{ef}\}$ be a skeletonization of a UMTC \mathcal{C} . The Deligne product category $\mathcal{C} \boxtimes \mathcal{C}$ with objects $X \boxtimes Y$, $X, Y \in \text{Obj}(\mathcal{C})$ and morphisms

$$\text{Hom}_{\mathcal{C} \boxtimes \mathcal{C}}(X_1 \boxtimes X_2, Y_1 \boxtimes Y_2) \cong \text{Hom}_{\mathcal{C}}(X_1, Y_1) \otimes \text{Hom}_{\mathcal{C}}(X_2, Y_2)$$

is again a UMTC, where the associators and braidings of the product category are given by

$$\alpha_{a_1 \boxtimes a_2, b_1 \boxtimes b_2, c_1 \boxtimes c_2} = \alpha_{a_1, b_1, c_1} \otimes \alpha_{a_2, b_2, c_2} \quad (6.1)$$

$$c_{a_1 \boxtimes a_2, b_1 \boxtimes b_2} = c_{a_1, a_2} \otimes c_{b_1, b_2}. \quad (6.2)$$

Given a skeletonization of \mathcal{C} with respect to an ordering $\{a_1, a_2, \dots, a_r\}$ of $\text{Irr}(\mathcal{C})$, our convention for producing a skeletonization of $\mathcal{C} \boxtimes \mathcal{C}$ is with respect to the ordering $\{a_1 \boxtimes a_1, a_1 \boxtimes a_2, \dots, a_1 \boxtimes a_r, \dots, a_r \boxtimes a_{r-1}, a_r \boxtimes a_r\}$ of $\text{Irr}(\mathcal{C} \boxtimes \mathcal{C})$ is to take the tensor

¹Note however that the fusion in \mathcal{C} (and hence $\mathcal{C} \boxtimes \mathcal{C}$) being multiplicity-free does not prohibit the fusion in $(\mathcal{C} \boxtimes \mathcal{C})_{S_2}^\times$ from being multiplicity free. Take for example the Fibonacci defect fusion rule $\tau \otimes \tau \triangleright X_\tau = X_1 \oplus 2X_\tau$ and see the Fibonacci defect F -symbols at the end of the chapter.

product of the N -matrices, R -matrices, and F -matrices.

$$N_{c_1 \boxtimes c_2}^{a_1 \boxtimes a_2, b_1 \boxtimes b_2} = N_{c_1}^{a_1, b_1} \otimes N_{c_2}^{a_2, b_2} \quad (6.3)$$

$$R_{c_1 \boxtimes c_2}^{a_1 \boxtimes a_2, b_1 \boxtimes b_2} = R_{c_1}^{a_1, b_1} \otimes R_{c_2}^{a_2, b_2} \quad (6.4)$$

$$F_{d_1 \boxtimes d_2}^{a_1 \boxtimes a_2, b_1 \boxtimes b_2, c_1 \boxtimes c_2} = F_{d_1}^{a_1 b_1 c_1} \otimes F_{d_2}^{a_2 b_2 c_2} \quad (6.5)$$

6.2.1 Categorical layer-exchange symmetry

Let $\underline{\rho}$ be the monoidal functor

$$\underline{\rho}: \underline{S}_2 \longrightarrow \underline{\text{Aut}}_{\otimes}^{br}(\mathcal{C} \boxtimes \mathcal{C})$$

$$id \mapsto id : \mathcal{C} \boxtimes \mathcal{C} \rightarrow \mathcal{C} \boxtimes \mathcal{C}$$

$$(12) \mapsto \begin{aligned} T_{(12)} : \mathcal{C} \boxtimes \mathcal{C} &\rightarrow \mathcal{C} \boxtimes \mathcal{C} \\ X \boxtimes Y &\mapsto Y \boxtimes X \\ f_1 \boxtimes f_2 &\mapsto f_2 \boxtimes f_1 \end{aligned}$$

By the ENO G -crossed braided extension classification and Theorem 5.1.2, there are two distinct extensions $(\mathcal{C} \boxtimes \mathcal{C})_{S_2}^{\times}$ in the $H^3(S_2, U(1))$ torsor.

6.3 Single defect associators

In [33] we define a category $(\mathcal{C} \boxtimes \mathcal{C})_{S_2}^{\times}$ and show that it satisfies the definition of an S_2 -crossed braided fusion category.

In this chapter we will describe the idea of the construction and show that there is a natural way to construct extensions of $\mathcal{C} \boxtimes \mathcal{C}$ by considering $\mathcal{C}_{(12)}$ as a bimodule category

over $\mathcal{C} \boxtimes \mathcal{C}$ and so that will be the starting point for our presentation. We will prove some coherences when illuminating, but defer the full details to [33].

In terms of the basic algebraic data of SET order the structure of the invertible bimodule categories will give the fusion between anyons and defects and those F -symbols involving the two anyons and one defect.

The rank of $\mathcal{C}_{(12)}$ is equal to the number of fixed points in $\mathcal{C} \boxtimes \mathcal{C}$ under the bilayer exchange symmetry per Lemma 4.1, so there are r simple objects in $\mathcal{C}_{(12)}$. Departing from the notation of Chapter 5, instead of labeling these simple objects by the corresponding fixed points we adopt a labeling by the deconfinements.

$$\begin{aligned} \text{Irr}(\mathcal{C}_{(12)}) &= \{X_a \mid a \in \text{Irr}(\mathcal{C})\} \\ &:= \{X_{a \boxtimes a} \mid a \in \text{Irr}(\mathcal{C})\} \end{aligned} \tag{6.6}$$

Anyon-defect fusion and the notion of deconfinement

Recall that the left action of $\mathcal{C} \boxtimes \mathcal{C}$ on $\mathcal{C}_{(12)}$ on the level of objects is defined by the confinement map, see Definition 5.4.

$$\begin{aligned} a_1 \boxtimes a_2 \triangleright X_b &= X_{(a_1 \otimes a_2) \otimes b} \\ &:= \bigoplus_c N_c^{a_1 a_2 b} X_c. \end{aligned} \tag{6.7}$$

where we abuse notation for iterated fusion coefficients.

We recall the definition of deconfinement from the previous chapter in the $n = 2$ case.

Definition 6.1. *Let $X_b \in \text{Irr}(\mathcal{C}_{(12)})$, and suppose $a_1 \boxtimes a_2 \in \text{Irr}(\mathcal{C} \boxtimes \mathcal{C})$ satisfies*

$$a_1 \boxtimes a_2 \triangleright X_1 = X_b. \tag{6.8}$$

Then we say that $a_1 \boxtimes a_2$ is a (left) **deconfinement** of X_a .

In general a defect has many deconfinements. For example, whenever $b \in \text{Irr}(\mathcal{C})$ has a zero-mode $a \in \text{Irr}(\mathcal{C})$, i.e. $a \otimes b = b \otimes a = b$, one has $b \boxtimes a \triangleright X_1 = X_{b \otimes a} = X_b$ and similarly for $a \boxtimes b$.

Left module associators

The left-module associativity constraint

$$\alpha_{a_1 \boxtimes a_2, b_1 \boxtimes b_2, X_c} : ((a_1 \boxtimes a_2) \otimes (b_1 \boxtimes b_2)) \triangleright X_c \longrightarrow (a_1 \boxtimes a_2) \triangleright ((b_1 \boxtimes b_2) \triangleright X_c) \quad (6.9)$$

is defined by the following composition of associators and braidings in \mathcal{C} .

$$\begin{aligned} \alpha_{a_1 \boxtimes a_2, b_1 \boxtimes b_2, X_c} = & \alpha_{a_1, b_1, a_2 \otimes b_2} \otimes \text{id}_c \\ & \circ \text{id}_{a_1} \otimes \alpha_{b_1, a_2, b_2}^{-1} \otimes \text{id}_c \\ & \circ \text{id}_{a_1} \otimes C_{b_1, a_2} \otimes \text{id}_{b_2 \otimes c} \\ & \circ \text{id}_{a_1} \otimes \alpha_{a_2, b_1, b_2} \otimes \text{id}_c \\ & \circ \alpha_{a_1, a_2 \otimes (b_1 \otimes b_2), c} \\ & \circ \text{id}_{a_1} \otimes \alpha_{a_2, b_1 \otimes b_2, c} \\ & \circ \alpha_{a_1, a_2, (b_1 \otimes b_2) \otimes c}^{-1} \end{aligned} \quad (6.10)$$

We record a few observations about this composition of morphisms that help one understand the structure of the single-defect associators qualitatively.

Remark 6.1.

When re-associating a defect and two monolayer anyons in the same layer, e.g. X_c and either $a \boxtimes 1$ and $b \boxtimes 1$ or $1 \boxtimes a$ and $1 \boxtimes b$, the associator is simply given by the

monolayer associator of the anyons

$$\alpha_{a,b,c}$$

where c is the topological charge of the defect.

Physically, one can imagine stripping the topological charge $c \boxtimes 1$ or $1 \boxtimes c$ from the defect X_c and moving it into the layer with the anyons a and b , where they reassociate before re-confinement.

Lemma 6.1. *The action $(\triangleright, \alpha_{a_1 \boxtimes a_2, b_1 \boxtimes b_2, X_d})$ makes $\mathcal{C}_{(12)}$ into a left $\mathcal{C} \boxtimes \mathcal{C}$ module category.*

Proof. The pentagon diagram

$$\begin{array}{ccc}
 ((a_1 \boxtimes a_2 \otimes b_1 \boxtimes b_2) \otimes c_1 \boxtimes c_2) \triangleright X_d & \xrightarrow{\alpha_{a_1 \boxtimes b_1 \boxtimes a_2 \boxtimes b_2, c_1 \boxtimes c_2, X_d}} & (a_1 \boxtimes a_2 \otimes b_1 \boxtimes b_2) \otimes (c_1 \boxtimes c_2 \triangleright X_d) \\
 \downarrow \alpha_{a_1, b_1, c_1} \boxtimes \alpha_{a_2, b_2, c_2} \triangleright \text{id}_{X_d} & & \downarrow \\
 (a_1 \boxtimes a_2 \otimes (b_1 \boxtimes b_2 \otimes c_1 \boxtimes c_2)) \triangleright X_d & & a_1 \boxtimes a_2 \triangleright (b_1 \boxtimes b_2 \otimes (c_1 \boxtimes c_2 \triangleright X_d)) \\
 \downarrow \alpha_{a_1 \boxtimes a_2, b_1 \otimes c_1 \boxtimes b_2 \otimes c_2, X_d} & \nearrow \text{id}_{a_1 \boxtimes a_2} \triangleright \alpha_{b_1 \boxtimes b_2, c_1 \boxtimes c_2, X_d} & \\
 a_1 \boxtimes a_2 \otimes ((b_1 \boxtimes b_2 \otimes c_1 \otimes c_2) \triangleright X_d) & &
 \end{array}$$

becomes a diagram in \mathcal{C} :

$$\begin{array}{ccc}
 X_{((a_1 \otimes b_1) \otimes c_1) \otimes ((a_2 \otimes b_2) \otimes c_2)} \otimes d & \xrightarrow{\alpha_{a_1 \otimes b_1 \otimes a_2 \otimes b_2, c_1 \otimes c_2, X_d}} & X_{((a_1 \otimes b_1) \otimes (a_2 \otimes b_2)) \otimes ((c_1 \otimes c_2) \otimes d)} \\
 \downarrow \alpha_{a_1, b_1, c_1} \otimes \alpha_{a_2, b_2, c_2} \otimes \text{id}_d & & \downarrow \\
 X_{(a_1 \otimes (b_1 \otimes c_1)) \otimes (a_2 \otimes (b_2 \otimes c_2))} \otimes d & & X_{(a_1 \otimes a_2) \otimes ((b_1 \otimes b_2) \otimes ((c_1 \otimes c_2) \otimes d))} \\
 \downarrow \alpha_{a_1 \boxtimes a_2, b_1 \otimes c_1 \boxtimes b_2 \otimes c_2, X_d} & \nearrow \text{id}_{a_1 \otimes a_2} \otimes \alpha_{b_1 \boxtimes b_2, c_1 \boxtimes c_2, X_d} & \\
 X_{(a_1 \otimes a_2) \otimes ((b_1 \otimes c_1) \otimes (b_2 \otimes c_2))} \otimes d & &
 \end{array}$$

which commutes because any two paths between objects in \mathcal{C} composed of braidings and associators commutes by the braided coherence theorem 1.2. \square

Right module associators

We use the braiding in $\mathcal{C} \boxtimes \mathcal{C}$ and the left module structure $(\triangleright, \alpha_{\vec{a}, \vec{b}, X_c})$ to turn $\mathcal{C}_{(12)}$ into a bimodule category in the usual way, see for example [30]. The right action on objects is given by

$$\begin{aligned} X_a \triangleleft b_1 \boxtimes b_2 = b_1 \boxtimes b_2 \triangleright X_a &= X_{(b_1 \otimes b_2) \otimes a} \\ &:= \bigoplus_c N_c^{b_1 b_2 a} X_c. \end{aligned} \quad (6.11)$$

with right associativity structure

$$\alpha_{X_a, b_1 \boxtimes b_2, c_1 \boxtimes c_2} : (X_a \triangleleft b_1 \boxtimes b_2) \triangleleft c_1 \boxtimes c_2 \longrightarrow X_a \triangleleft (b_1 \boxtimes b_2 \otimes c_1 \boxtimes c_2) \quad (6.12)$$

given by postcomposing the left associator by the braiding of the two bilayer anyons $c_{c_1 \boxtimes c_2, b_1 \boxtimes b_2}$ in $\mathcal{C} \boxtimes \mathcal{C}$.

Here it is important to note that as a morphism of defects, $c_{c_1 \boxtimes c_2, b_1 \boxtimes b_2} \triangleright \text{id}_{X_a}$ is interpreted as a morphism in \mathcal{C} via

$$c_{c_1 \boxtimes c_2, b_1 \boxtimes b_2} \triangleright \text{id}_{X_a} := c_{c_1, b_1} \otimes c_{c_2, b_2} \otimes \text{id}_a. \quad (6.13)$$

Bimodule associators

Similarly, the middle module associativity structure is given by conjugating the braiding of the two anyons by the left associator:

$$\alpha_{a_1 \boxtimes a_2, X_b, c_1 \boxtimes c_2} : (a_1 \boxtimes a_2 \triangleright X_b) \triangleleft c_1 \boxtimes c_2 \longrightarrow a_1 \boxtimes a_2 \triangleright (X_b \triangleleft c_1 \boxtimes c_2) \quad (6.14)$$

Defining the right action to be equal to the left action and using the braiding of $\mathcal{C} \boxtimes \mathcal{C}$ to construct the middle and right associators guarantees that the remaining three of the four single-defect pentagons are satisfied. Alternatively, the explicit forms of the middle and right associators in terms of compositions of braidings and associators of \mathcal{C} satisfy braided coherence, and hence the pentagons commute.

6.3.1 Single-defect F -symbols

Given the standard skeletonization of $\mathcal{C} \boxtimes \mathcal{C}$, the formulas above for the single-defect associators can be used to produce the single-defect F -symbols. These are the entries of the F -matrices $[F_d^{abc}]$ for which only one of the external labels $a, b, c \in \text{Irr}(\mathcal{C}_{(12)})$. Since the fusion of anyons and defects must respect the S_2 grading, the total charge label d is some defect in $\text{Irr}(\mathcal{C}_{(12)})$ occurring in the fusion channel of a, b , and c . That is, F -symbols of the form

$$[F_{X_d}^{\vec{a}\vec{b}X_c}] \quad [F_{X_d}^{X_a,\vec{b},\vec{c}}] \quad [F_{X_d}^{\vec{a},X_b,\vec{c}}] \quad (6.15)$$

for all $\vec{a}, \vec{b}, \vec{c} \in \text{Irr}(\mathcal{C} \boxtimes \mathcal{C})$ and for all $a, b, c, d \in \text{Irr}(\mathcal{C})$ can be directly computed from the associators $\alpha_{\vec{a},\vec{b},X_c}$, $\alpha_{X_a,\vec{b},\vec{c}}$, and $\alpha_{\vec{a},X_b,\vec{c}}$ respectively.

Lemma 6.2. *1. Every defect is related to the bare defect by fusion with a monolayer deconfinement.*

2. The quantum dimensions of bilayer defects are given by

$$d_{X_1} = \mathcal{D}_{\mathcal{C}} \quad (6.16)$$

$$d_{X_a} = d_a \mathcal{D}_{\mathcal{C}} \quad (6.17)$$

Proof. Let X_a be the bilayer defect with charge label a . Then

$$X_a = a \boxtimes 1 \triangleright X_1 \quad (\text{also } X_a = 1 \boxtimes a \triangleright X_1).$$

This proves (1), and since quantum dimensions respect fusion rules, it follows that $d_{X_a} = d_a d_{X_1}$. To see the formula for quantum dimensions in (2), recall from Lemma 4.3 that $\mathcal{D}_{\mathcal{C}_{(12)}} = \mathcal{D}_{\mathcal{C} \boxtimes \mathcal{C}} = \mathcal{D}_{\mathcal{C}}^2$. Then we have

$$\mathcal{D}_{\mathcal{C}}^2 = \mathcal{D}_{\mathcal{C}_{(12)}} = \sqrt{\sum_{a \in \text{Irr}(\mathcal{C})} d_{X_a}^2} = \sqrt{\sum_{a \in \text{Irr}(\mathcal{C})} (d_a d_{X_1})^2} = \mathcal{D}_{\mathcal{C}} d_{X_1}. \quad (6.18)$$

Thus $d_{X_1} = \mathcal{D}_{\mathcal{C}}$ and by (1) $d_{X_a} = d_a \mathcal{D}_{\mathcal{C}}$. \square

The following is an immediate consequence of the formulas for the quantum dimensions of bilayer defects.

Corollary 2. *The category $(\mathcal{C} \boxtimes \mathcal{C})_{S_2}^{\times}$ is integral (weakly integral) if \mathcal{C} is integral (weakly integral).* \square

6.4 S_2 -crossed braiding of anyons and defects

Recall from Chapter 5 that a G -crossed braiding is a natural collection of isomorphisms

$$c_{X,Y} : X \otimes Y \longrightarrow T_g(Y) \otimes X$$

for all $X \in \text{Obj}(\mathcal{C}_g)$, $Y \in \text{Obj}(\mathcal{C}_G^{\times})$ satisfying various coherence axioms.

In this section we will define the isomorphisms $c_{X,Y}$ and their inverses when one of X and Y is a defect and the other an anyon.

Like with the single-defect associators, we will use confinement to define the S_2 crossed

braiding between anyons and defects, which will again be given by compositions of braiding and associators in \mathcal{C} .

Then we will argue that the S_2 -crossed braiding morphisms satisfy the subset of the G -crossed braided coherences that only involve the braiding between anyons and defects (as opposed to involving braiding between defects, which we defer to a later section).

Note that our convention for the braiding is the reverse to the one in Chapter 4.

Anyons braiding around defects (the trivial S_2 -braiding)

For $c_{a_1 \boxtimes a_2, X_b}$ since the first factor in the tensor product is in the trivial sector there is no action by $T_{(12)}$, while in the second case the braiding permutes the bilayer anyon by layer-exchange.

$$\begin{array}{ccc}
 \begin{array}{cc}
 X_b & a_1 \boxtimes a_2 \\
 \swarrow & \nearrow \\
 a_1 \boxtimes a_2 & X_b
 \end{array} & = & \begin{array}{ccc}
 a_1 \boxtimes a_2 \triangleright X_b = X_{(a_1 \otimes a_2) \otimes b} & & \\
 \uparrow & & \uparrow \\
 c_{a_1 \boxtimes a_2, X_b} := & \text{id}_{(a_1 \otimes a_2) \otimes b} & \\
 \downarrow & & \downarrow \\
 a_1 \boxtimes a_2 \triangleright X_b = X_{(a_1 \otimes a_2) \otimes b} & &
 \end{array}
 \end{array}$$

Therefore we define

$$c_{a_1 \boxtimes a_2, X_b} := \text{id}_{(a_1 \otimes a_2) \otimes b} \tag{6.19}$$

$$c_{X_a, b_1 \boxtimes b_2}^{-1} := \text{id}_{(b_1 \otimes b_2) \otimes a} \tag{6.20}$$

Defects braiding around anyons (the nontrivial S_2 -braiding)

The S_2 -crossed braiding

$$c_{X_a, b_1 \boxtimes b_2} : X_a \triangleleft b_1 \boxtimes b_2 \longrightarrow b_2 \boxtimes b_1 \triangleright X_a$$

and its inverse

$$c_{a_1 \boxtimes a_2, X_b}^{-1} : a_1 \boxtimes a_2 \triangleright X_b \longrightarrow X_b \triangleleft a_2 \boxtimes a_1$$

can be understood using the definition of the left and right action through the following picture, where we have chosen the convention that anyons get permuted by the symmetry action when they get passed over by a defect.

$$\begin{array}{ccc}
 \begin{array}{cc}
 b_2 \boxtimes b_1 & X_a \\
 \swarrow & \nearrow \\
 X_a & b_1 \boxtimes b_2
 \end{array} & = & \begin{array}{ccc}
 b_2 \boxtimes b_1 \triangleright X_a = X_{(b_2 \otimes b_1) \otimes a} & & \\
 \uparrow & & \uparrow \\
 c_{X_a, b_1 \boxtimes b_2} := & c_{b_1, b_2} \otimes \text{id}_a & \\
 \downarrow & & \downarrow \\
 b_1 \boxtimes b_2 \triangleright X_a = X_{(b_1 \otimes b_2) \otimes a} & &
 \end{array}
 \end{array}$$

We define

$$c_{X_a, b_1 \boxtimes b_2} := c_{b_1, b_2} \otimes \text{id}_a \quad (6.21)$$

$$c_{a_1 \boxtimes a_2, X_b}^{-1} := c_{a_1, a_2}^{-1} \otimes \text{id}_b \quad (6.22)$$

Lemma 6.3. *With the single defect associators and anyon-defect braiding defined above, the first S_2 -crossed hexagon is satisfied for $X_a \in \text{Irr}(\mathcal{C}_{(12)})$, $b_1 \boxtimes b_2, c_1 \boxtimes c_2 \in \text{Irr}(\mathcal{C} \boxtimes \mathcal{C})$.*

Proof. In case 1, the S_2 -hexagons only involve the single-defect associators and the braid-

ing between anyons and defects. Since in this case the tensorator $U_{(12)}$ of $T_{(12)}$ is trivial, the S_2 -crossed hexagon collapses to a true hexagon. At each vertex is a defect in $\mathcal{C}_{(12)}$ and each arrow is a composition of associators and/or braidings in \mathcal{C} . Thus the diagram commutes by braided coherence in \mathcal{C} .

In case 2, the S_2 -hexagons involve only the triple-defect associators and the braiding between anyons and defects. By the same argument above for case 1, the diagram commutes. \square

6.4.1 The S_2 -action on the defects

Lemma 6.4. *The isomorphism class of the bare defect $X_1 \in \text{Irr}(\mathcal{C}_{(12)})$ is fixed by the S_2 -action.*

Proof. Observe that a tensor autoequivalence T of $(\mathcal{C} \boxtimes \mathcal{C})_{S_2}^\times$ whose square is naturally isomorphic to the identity functor must satisfy either $T(X_a) \cong X_a$ or $T(X_a) \cong X_{a^*}$. \square

Corollary 3. *The isomorphism classes of all defects are fixed by the S_2 -action.*

Proof. Let $X_a \in \text{Irr}(\mathcal{C}_{(12)})$. Then by Lemma 6.4

$$T_{(12)}(X_a) \cong T_{(12)}(a \boxtimes 1) \otimes T_{(12)}(X_1) \cong 1 \boxtimes a \otimes X_1 = X_a.$$

\square

So far all we have done is leverage the fact that the single-defect associators and single-defect braiding can be deconfined into monolayer isomorphisms.

6.4.2 Braiding and associators for bare defects

In [33] we prove the following.

Proposition 6.1 (Bilayer bare defect data [33]). *Assuming the single-defect associators and braiding as above, we construct braiding and associators with the following skeletal data.*

$$[R^{X_1 X_1}] = T \quad (6.23)$$

$$[F_{X_1}^{X_1 X_1 X_1}] = S \quad (6.24)$$

$$U_{(\text{id})}(X_1, X_1; c \boxtimes c^*) = \Theta \quad (6.25)$$

$$\eta_{X_1}((12), (12)) = \Theta^* \quad (6.26)$$

where Θ is the invariant defined from a single layer \mathcal{C} .

As an example we give some partial algebraic data for bilayer defects in for the semion UMTC from Example 1.4.1.

Example 6.1 (Bilayer semion with layer-exchange defects).

Anyons and defects $\mathcal{L} = \{1 \boxtimes 1, 1 \boxtimes s, s \boxtimes 1, s \boxtimes s, X_1, X_2\}$

Fusion
 $(s \boxtimes 1) \otimes X_1 = (1 \boxtimes s) \otimes X_1 = X_s$
 $(s \boxtimes 1) \otimes X_s = (1 \boxtimes s) \otimes X_s = X_1$
 $(s \boxtimes s) \otimes X_1 = X_1, (s \boxtimes s) \otimes X_s = X_s$

Bare defect F -matrix $F_{X_1}^{X_1 X_1 X_1} = \frac{1}{\sqrt{2}} \begin{pmatrix} 1 & 1 \\ 1 & -1 \end{pmatrix}$

\mathbb{Z}_2 -crossed R -symbols

$$R_{1 \boxtimes 1}^{X_1, X_1} = 1, R_{s \boxtimes s}^{X_1, X_1} = i$$

$$R_{1 \boxtimes s}^{X_1, X_s} = 1, R_{s \boxtimes 1}^{X_1, X_s} = -i$$

$$R_{1 \boxtimes s}^{X_s, X_1} = i, R_{s \boxtimes 1}^{X_s, X_1} = 1$$

$$R_{1 \boxtimes 1}^{X_s, X_s} = i, R_{s \boxtimes s}^{X_s, X_s} = 1$$

Quantum dimensions $d_{X_1} = d_{X_s} = \sqrt{2}$

In the last part of this work we simply investigate some consequences of this result, deferring the full details of the algebraic theory of bilayer defects to [32]. The considerations we will make about bare defects are enough to appreciate the mathematical relationship between quantum symmetry and topology, and provide compelling evidence for this description without the categorification we give in [32].

There are several things worth pointing out. First of all, these pieces of data are invariants of \mathcal{C} , and hence independent of choice of skeletonization. Second, the fact that the S -matrix arises as an associator expresses a deep connection between modularity and extendability: here modularity is required for the extension-theory to be well-defined: if S is a singular matrix then the associators we constructed will not be isomorphisms.

6.4.3 Coherences

Lemma 6.5. *The S_2 -crossed hexagon equations are satisfied for three bare defects X_1 with total charge X_1 .*

Proof. We check the first, the other is similar.

$$\begin{array}{ccc}
 & (X_1 \otimes X_1) \otimes X_1 & \\
 \alpha_{X_1, X_1, X_1} \swarrow & & \searrow c_{X_1, X_1} \otimes \text{id}_{X_1} \\
 X_1 \otimes (X_1 \otimes X_1) & & (T_{(12)}(X_1) \otimes X_1) \otimes X_1 \\
 c_{X_1, X_1} \otimes \text{id}_{X_1} \downarrow & & \downarrow \alpha_{T_{(12)}(X_1), X_1, X_1} \\
 T_{(12)}(X_1 \otimes X_1) \otimes X_1 & & T_{(12)}(X_1) \otimes (X_1 \otimes X_1) \\
 (\mu_{(12)})_{X_1, X_1}^{-1} \otimes \text{id}_{X_1} \downarrow & & \downarrow \text{id}_{T_{(12)}(X_1)} \otimes c_{X_1, X_1} \\
 (T_{(12)}(X_1) \otimes T_{(12)}(X_1)) \otimes X_1 & \xrightarrow{\alpha_{T_{(12)}(X_1), T_{(12)}(X_1), X_1}} & T_{(12)}(X_1) \otimes (T_{(12)}(X_1) \otimes X_1)
 \end{array}$$

Fixing the total charge to be X_1 , the commutative diagram yields the matrix equation

$$[R^{X_1 X_1}]^{-1} [F^{X_1 X_1 X_1}] [R^{X_1 X_1}]^{-1} = [F^{X_1 X_1 X_1}] [U_{(12)}(X_1, X_1)] [R^{X_1 X_1}]^{-1} [F^{X_1 X_1 X_1}]. \quad (6.27)$$

It then remains to show this equation holds for the skeletal data we have constructed. Substituting in $[F^{X_1 X_1 X_1}] = S$, $[R^{X_1 X_1}]^{-1} = T^{-1}$, and $[U_{(12)}(X_1, X_1)] = \Theta I_n$, we have

$$S^{-1}T^{-1}ST^{-1}S^{-1} = \Theta T \tag{6.28}$$

$$\tag{6.29}$$

Now using the fact that $T^{\pm 1}C = T^{\pm 1}$ and $S^{\pm 1} = CS^{\mp 1} = S^{\mp 1}C$, we have

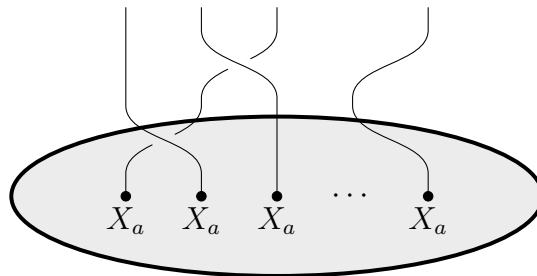
$$T^{-1}S^{-1}T^{-1}S^{-1}T^{-1}S^{-1} = \Theta C. \tag{6.30}$$

or $(ST)^{-3} = \Theta C$. Since $C = C^{-1}$, this equation holds due to the relations satisfied by the generators of the modular representation, see Chapter 1.

□

6.5 Topological quantum computing with bare defects and the modular representation

In the previous section we saw that every bilayer defect type X_a was fixed by the \mathbb{Z}_2 -action. Consequently there exist projective representations of \mathcal{B}_n on $\text{Hom}(1, X_a^{\otimes n})$ with the interpretation of quantum gates that can be generated by defect exchange.



$$\mathrm{Hom}(i, X_a \otimes X_a \otimes \cdots \otimes X_a) \cong V_i^{X_a^{\otimes n}}$$

We assume the result of Proposition 6.1, namely that the matrix entries of braiding and associator isomorphisms coming from bare defects satisfied

$$[R^{X_1 X_1}] = T \tag{6.31}$$

$$[F_{X_1}^{X_1 X_1 X_1}] = S \tag{6.32}$$

where T and S are the T -matrix and S -matrix of \mathcal{C} , the monolayer theory. We showed that these gave solutions to the relevant S_2 -crossed braided coherences: the two S_2 -crossed hexagons for the triple of objects (X_1, X_1, X_1) .

6.5.1 Bare defect qudit gates

The following theorem shows that bare defect exchange in $(\mathcal{C} \boxtimes \mathcal{C})_{S_2}^{\times}$ effects the same quantum logical operations as the modular transformations of the torus.

Theorem 6.1. *The unitary representation of \mathcal{B}_4 afforded by 4 bare defects $X_1 \in \mathrm{Irr}(\mathcal{C}_{(12)})$ is projectively equivalent to the representation of the mapping class group of the torus $SL(2, \mathbb{Z})$ generated by the S and T matrices of \mathcal{C} .*

Proof. As in Chapter 2 we will work with the (now projective) representation of \mathcal{B}_3 on $\mathrm{Hom}(X_1, X_1^{\otimes 3})$. Assuming the bare defects have the algebraic data as in the [equations above](#), the images of the \mathcal{B}_3 generators take the form

$$\rho(\sigma_1) = T \quad \text{and} \quad \rho(\sigma_2) = S^{-1}TS. \tag{6.33}$$

One can check that T and $S^{-1}TS$ indeed satisfy the braid relation using the modular

relations.

$$(ST)^3 = \Theta C, \quad S^2 = C, \quad C^2 = I_n, \quad \text{where } \Theta = \frac{1}{\mathcal{D}} \sum_{a \in \mathcal{C}} d_a^2 \theta_a \quad (6.34)$$

Then projectively the image of \mathcal{B}_3 is generated by the matrices T and $S^{-1}TS$, $\rho(B_3) \simeq \langle T, S^{-1}TS \rangle$.

Now recall that the modular representation is generated by S and T . We wish to show $\langle S, T \rangle \simeq \langle T, S^{-1}TS \rangle$.

Clearly $\langle T, S^{-1}TS \rangle \subset \langle T, S \rangle$, since $S^{-1}TS$ is a word in T and S . But we can also write S as a word in T and $S^{-1}TS$ up to an overall phase, for example by

$$S = \Theta T^{-1} (S^{-1}TS)^{-1} T^{-1}. \quad (6.35)$$

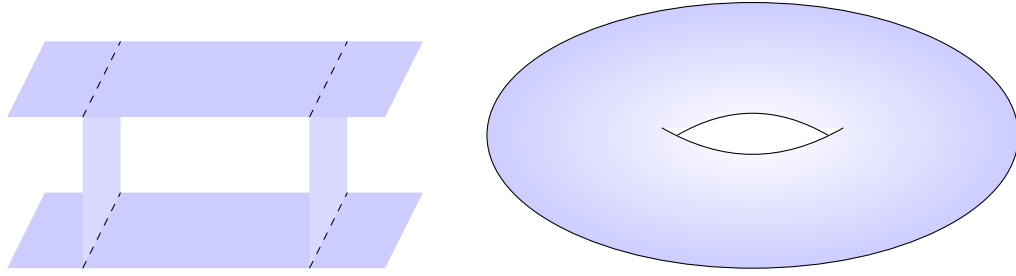
Thus $\langle T, S \rangle \subset \langle T, S^{-1}TS \rangle$, and it follows that the projective images of the representation in $U(n)$ are equal. \square

6.6 Conclusions

Recall from Section 1.3 that the projective image of the modular representation coming from an MTC is always finite. Thus we have the following as a physical corollary to Theorem 6.1.

Corollary 4. *The gates generated by bare defect exchange are never single-qudit universal.*

Our calculation corroborates the idea that bare defects effectively create genus.



In [32] we extend this result to prove a general relationship between the quantum systems of $2g + 2$ defects carrying charge label a and $2g + 2$ anyons of type a on a genus g surface.

Conjecture 4. *Braiding bilayer defects is not universal for TQC if braiding of the monolayer anyons is not universal for TQC.*

While braiding bare defects is not universal based on the theory outlined here, the sense in which they generate topology can be leveraged to realize universal gate sets when projective measurement is allowed [4]. This capacity makes bilayer symmetry defects worth consideration for experiments and devices despite their failure to generate universal quantum computation as nonabelian objects.

Bibliography

- [1] D. Aasen, E. Lake, K. Walker. *Fermion condensation and super pivotal categories*. [arXiv: 1709.01941](#). (2017).
- [2] F. A. Bais. J. K. Slingerland. *Condensate-induced transitions between topologically ordered phases*. Phys. Rev. B. Vol. 79, No.4:045316. (2009).
- [3] M. Barkeshli, P. Bonderson, M. Cheng, Z. Wang, *Symmetry, defects, and gauging of topological phases*. [arXiv:1410.4540](#). (2014).
- [4] M. Barkeshli, C. M. Jian, X. L. Qi, *Genons, twist defects, and projective non-Abelian braiding statistics*. Phys. Rev. B, Vol. 87, No. 045130. (2013).
- [5] T. Barmeier, C. Schweigert. *A geometric construction for permutation equivariant categories from modular functors*. Transformation Groups. Vol. 16, No. 2, Pgs. 287-337. (2011).
- [6] D. Barter, J. Bridgeman, C. Jones. *Domain walls in topological phases and the Brauer-Picard ring for $\text{Vec}(\mathbb{Z}/p\mathbb{Z})$* . C. Commun. Math. Phys. (2019).
- [7] D. Barter, J. Bridgeman, C. Jones. *Fusing Binary Interface Defects in Topological Phases: The $\text{Vec}(\mathbb{Z}/p\mathbb{Z})$ case*. [arXiv: 1810.09469](#)
- [8] B. Bartlett, C. L. Douglas, C. J. Schommer-Pries, J. Vicary. *Modular categories as representations of the 3-dimensional bordism 2-category*. [arXiv:1509.06811](#). (2015).
- [9] M. Bischoff. *Generalized Orbifold Construction for Conformal Nets*. Reviews in Mathematical Physics Vol. 29, No. 1. (2017).
- [10] M. Bischoff. *The rank of G -crossed braided extensions of modular tensor categories*. To appear in AMS Contemporary Mathematics Series.
- [11] W. Bloomquist. *Quantum representations of MCGs and their applications to quantum computing*. UCSB Ph.D. dissertation. (2019).
- [12] P. Bonderson. *Non-abelian anyons and interferometry*. Caltech Ph.D. Thesis. (2007). <https://thesis.library.caltech.edu/2447/2/thesis.pdf>.

- [13] P. Bonderson, M. Cheng, R. S. K. Mong, A. Tran. *Fermionic Topological Phases and Modular Transformations*. (In preparation.)
- [14] P. Bonderson, C. Delaney, C. Galindo, E. C. Rowell, A. Tran, Z. Wang. *On invariants of modular categories beyond modular data*. Journal of Pure and Applied Algebra. Vol. 223, No. 9. (2019).
- [15] P. Bonderson, M. Freedman, C. Nayak. *Measurement-Only Topological Quantum Computation*. Phys. Rev. Lett. Vol. 101, No. 010501. (2008).
- [16] P. Bruillard, C. Galindo, S. H. Ng, J. Y. Plavnik, E. C. Rowell, Z. Wang. *Classification of super-modular categories by rank*. Algebr. Represent. Theor. (2019).
- [17] P. Bruillard, S. H. Ng, E. C. Rowell, Z. Wang. *Rank-finiteness for modular categories*. J. Amer. Math. Soc. Vol. 29, Pgs. 857-881. (2016).
- [18] A. Bullivant, A. Kimball, P. Martin, E. Rowell. *Representations of the Necklace Braid Group: Topological and Combinatorial Approaches*. [arXiv: 1810.05152](https://arxiv.org/abs/1810.05152). (2018).
- [19] A. Bullivant, J. F. Martins, P. Martins. *From Aharonov-Bohm type effects in discrete (3+1)-dimensional higher gauge theory to representations of the loop braid group*. [arXiv:1807.09551](https://arxiv.org/abs/1807.09551). (2018).
- [20] S. Carpi, Y. Kawahigashi, R. Longo, M. Weiner. *From vertex operator algebras to conformal nets and back*. Memoirs of the American Mathematical Society, Vol. 254, No. 1213. (2018).
- [21] I. Cong, M. Cheng, Z. Wang. *On defects between gapped boundaries in two-dimensional topological phases of matter*. Phys. Rev. B. Vol. 96, No. 195129. (2017).
- [22] I. Cong, M. Cheng, Z. Wang. *Hamiltonian and algebraic theories of gapped boundaries in topological phases of matter*. Comm. Math. Phys. Vol. 355, No 2. (2017).
- [23] I. Cong, M. Cheng, Z. Wang. *Universal quantum computation with gapped boundaries*. Phys. Rev. Lett. Vol. 199, No. 170504. (2017).
- [24] M. Cheng, M. Zaletel, M. Barkeshli, A. Vishwanath, P. Bonderson. *Translational symmetry and microscopic constraints on symmetry-enriched topological phases: a view from the surface*. Phys. Rev. X. Vol. 6, No. 041068. (2016).
- [25] S. X. Cui, C. Galindo, J. Y. Plavnik, Z. Wang, *On gauging symmetry of topological phases*. Comms. in Math. Phys. Vol. 348, No. 3. (2016).
- [26] S. X. Cui, S. M. Hong, Z. Wang. *Universal quantum computation with weakly integral anyons*. Quantum Information Processing. Vol. 14. Pgs. 2697-2727. (2015).

- [27] S. X. Cui, M. Shokrian Zini, Z. Wang. *On generalized symmetries and structure of modular categories*. Science China Mathematics. Vol. 62, No. 3, Pgs. 417-446. (2019).
- [28] S. X. Cui, K. T. Tian, J. Vasquez, Z. Wang, H. M. Wong. *The Search For Leakage-free Entangling Fibonacci Braiding Gates*. [arXiv:1904.01731](https://arxiv.org/abs/1904.01731). (2019).
- [29] S. X. Cui, Z. Wang. *Universal quantum computation with metaplectic anyons*. J. Math. Phys. Vol. 56, No. 032202. (2015).
- [30] A. Davydov, D. Nikshych. *The Picard crossed module of a braided tensor category*. Algebra and Number Theory. Vol. 7, No. 6. (2013).
- [31] C. Delaney, E. C. Rowell, Z. Wang. *Local unitary representations of the braid group and their applications to quantum computing*. Rev. Colomb. Mat. Vol. 50, No. 2. (2016).
- [32] C. Delaney, E. Samperton. (In preparation.)
- [33] C. Delaney, E. Samperton. *Algebraic theory of bilayer symmetry defects*. (In preparation.)
- [34] C. Delaney, A. Tran. *A systematic search of knot and link invariants beyond modular data*. [arXiv:1806.02843](https://arxiv.org/abs/1806.02843). (2018).
- [35] C. Delaney, Z. Wang. *Symmetry defects and their application to topological quantum computing*. Accepted to AMS Contemporary Mathematics Series.
- [36] H. Doll, J. Hoste. *A tabulation of oriented links*. Math. of Computation. Vol. 57, Pgs. 747-761. (1991).
- [37] C. Edie-Michell, C. Jones, J. Plavnik. *Fusion rules for $\mathbb{Z}/2\mathbb{Z}$ -permutation gauging*. [arXiv:1804.01657](https://arxiv.org/abs/1804.01657). (2018).
- [38] P. Etinghof, S. Gelaki, D. Nikshych, V. Ostrik. *Tensor categories*. AMS. Mathematical surveys and monographs. Vol. 205. (2015).
- [39] P. Etinghof, D. Nikshych, V. Ostrik. *Quantum Topology*. Vol. 1, No. 209. (2010).
- [40] P. Etinghof, E. C. Rowell, S. Witherspoon. *Braid group representations from twisted quantum doubles of finite groups*. Pacific J. Math. Vol. 234, No. 1. (2008).
- [41] R. P. Feynman. *Simulating physics with computers*. International Journal of Theoretical Physics. Vol. 21, Nos. 6/7. (1982).
- [42] M. H. Freedman, A. Kitaev, Z. Wang. *Simulation of topological field theories by quantum computers*. Comm. Math. Phys. Vol. 227, No. 3, Pgs. 587-603. (2002).

- [43] M. H. Freedman, M. Larsen, Z. Wang. *A modular functor which is universal for quantum computation*. Comm. Math. Phys. Vol 227, No. 3, Pgs. 605–622. (2002).
- [44] D. Gaiotto, A. Kapustin. *Spin TQFTs and fermionic phases of matter*. Int. J. Mod. Phys. A. Vol. 31, No. 28-29. (2016).
- [45] C. Galindo. *On braided and ribbon unitary fusion categories* Vol. 57, No. 3. Pgs. 506-510. (2018).
- [46] T. Gannon, C. Jones. *Vanishing of categorical obstructions for permutation orbifolds*. Comm. Math. Phys. Vol. 369, No. 1. Pgs 245-259. (2019).
- [47] L. S. Georgiev. *Topological Quantum Computation with non-Abelian anyons in fractional quantum Hall states*. Quantum Systems in Physics, Chemistry, and Biology. Progress in Theoretical Chemistry and Physics. Vol. 30. (2017).
- [48] T. A. Gittings. *Minimum braids: a complete invariant of knots and links*. [arXiv:0401051](https://arxiv.org/abs/0401051). (2004).
- [49] D. L. Goldsmith. *Motion of links in the 3-sphere*. Bull. Amer. Math. Soc. Vol. 80, No. 1. (1974).
- [50] D. L. Goldsmith. *The theory of motion groups*. Michigan Math. J. Vol. 28, No. 1. (1981).
- [51] A. Gruen, S. Morrison. *Computing modular data for pointed fusion categories*. [arXiv:1808.05060](https://arxiv.org/abs/1808.05060)
- [52] P. Gustafson. *Finiteness of mapping class group representations from twisted Dijkgraaf-Witten theory*. Journal of Knot Theory and Its Ramifications. Vol. 27, No. 6: 1850043. (2018).
- [53] P. Gustafson, E. C. Rowell, Y. Ruan. *Metaplectic categories, gauging, and Property F*. [arXiv:1808.00698](https://arxiv.org/abs/1808.00698). (2018).
- [54] J. Haah. *Local stabilizer codes in three dimensions without string logical operators*. Phys. Rev. A. Vol. 83, No. 042330. (2011).
- [55] G. Hotz. *Eine Algebraisierung des Syntheseproblems von Schaltkreisen* EIK. Bd. 1, (185-205). Bd. 2, (209-231). (1965).
- [56] V. F. R. Jones. *Braid groups, Hecke algebras, and type II_1 factors*. Geometric methods in operator algebras. Pitman Res. Notes Math. Ser. 123, Pgs. 242-273. (1986).
- [57] A. Joyal, R. Street. *Braided monoidal categories*. Macquarie Mathematics Reports. No. 860081. (1986).

- [58] A. Joyal, R. Street. *The geometry of tensor calculus I*. Advances in Math. Vol. 88, No. 1, Pgs. 55-112. (1991).
- [59] A. Joyal, R. Street. *The geometry of tensor calculus II*. <http://www.math.mq.edu.au/street/GTCII.pdf>.
- [60] Z. Kadar, P. Martin, E. C. Rowell, Z. Wang. *Local representations of the loop braid group*. Glasgow Math. Journal. Vol. 59. (2017).
- [61] T. Karzig, C. Knapp, R. M. Lutchyn, P. Bonderson, M. B. Hastings, C. Nayak, J. Alicea, K. Flensberg, S. Plugge, Y. Oreg, C. M. Marcus, M. H. Freedman. *Scalable designs for quasiparticle-poisoning-protected topological quantum computation with Majorana zero modes*. Phys. Rev. B. Vol. 95, 235305. (2017).
- [62] Y. Kawahigashi. *A remark on gapped domain walls between topological phases*. Lett. Math. Phys. Vol. 105. (2015).
- [63] A. Kirillov Jr. *Modular categories and orbifold models II*. [arXiv:0110221](https://arxiv.org/abs/0110221). (2001).
- [64] A. Kitaev. *Anyons in an exactly solved model and beyond*. Annals of Physics. Vol. 321, No. 1. (2006).
- [65] A. Y. Kitaev, A. H. Shen, M. N. Vyalyi. *Classical and Quantum Computation*. Amer. Mathematical Society. (2002).
- [66] M. Mignard, P. Schauenburg. *Modular categories are not determined by their modular data*. [arXiv:1708.02796](https://arxiv.org/abs/1708.02796). (2017).
- [67] D. Naidu, E. C. Rowell. *A Finiteness Property for Braided Fusion Categories*. Algebras and Representation Theory. Vol. 14, No. 837. (2011).
- [68] M. A. Nielsen, I. L. Chuang. *Quantum Computation and Quantum Information: 10th Anniversary Edition*. Cambridge University Press. (2011).
- [69] nLab authors. *string diagram*. <https://ncatlab.org/nlab/show/string+diagram>.
- [70] A. G. Passegger. *Permutation actions on modular tensor categories of topological multilayer phases*. [arXiv:1804.08343](https://arxiv.org/abs/1804.08343). (2018).
- [71] J. Preskill. *Quantum Computing in the NISQ era and beyond*. Quantum. Vol. 79, No. 2. (2018).
- [72] M. Reiher, N. Wiebe, K. M. Svore, D. Wecker, M. Troyer. *Elucidating reaction mechanisms on quantum computers*. PNAS. Vol. 117. (2017).
- [73] J. Ricci. *Congruence subgroups from quantum representations of mapping class groups*. UCSB PhD Dissertation. (2018).

- [74] D. Ridout, S. Wood. *The Verlinde formula in logarithmic CFT*. Journal of Physics: Conference Series. Vol. 597, No. 1. (2014).
- [75] E. C. Rowell, R. Stong, Z. Wang. *On Classification of Modular Tensor Categories*. Comm. Math. Phys. Vol. 292, No. 2. Pgs. 342-389. (2009).
- [76] E. C. Rowell and Z. Wang. *Mathematics of topological quantum computing*. Bulletin of the American Mathematical Society. Vol. 55, No. 2. Pgs. 183-238. (2018).
- [77] E. C. Rowell, Z. Wang. *Degeneracy and non-abelian statistics*. Phys. Rev. A. Vol. 93. (2016).
- [78] N. Seiberg. In conversation.
- [79] V. Turaev. *Homotopy quantum field theory*, Appendix 5 by M. Müger. European Mathematical Society Tracts in Mathematics. Vol. 10. (2010).
- [80] D. Tambara, S. Yamagami. *Tensor categories with fusion rules of self-duality for finite abelian groups*. Journal of Algebra. Vol. 209, No. 2. (1998).
- [81] Z. Wang. *Topological quantum computation*. CBMS Regional Conference Series in Mathematics. Vol. 112, No. 201. (2010).
- [82] Z. Wang. *Beyond anyons*. Modern Physics Letters A. Vol. 33, No. 28. (2018).
- [83] D. J. Williamson, Z. Wang. *Hamiltonian models for topological phases of matter in three spatial dimensions*. Annals of Physics. Vol. 377. (2017).